

# **Kentucky Water Resources Research Institute Annual Technical Report FY 2017**

# Introduction

The 2017 Annual Technical Report for Kentucky consolidates reporting requirements for the Section 104(b) base grant award into a single document that includes: 1) a synopsis of each student research enhancement project that was conducted during the period, 2) citations for related publications, reports, and presentations, 3) a description of information transfer activities, 4) a summary of student support during the period, and 5) notable awards and achievements.

No funds were requested for general program administration activities. However, travel funds were provided to support the participation of the director and associate director in the annual meeting of the National Institutes for Water Resources in Washington, DC from February 25 - 28, 2018.

## Research Program Introduction

The activities supported by the Section 104(b) program funds and required matching are interwoven into the overall program of the Kentucky Water Resources Research Institute. Additional research, service, and technology transfer activities were funded through a variety of other sponsors. The Kentucky River Authority supported watershed management services in the Kentucky River basin and a small grant program to fund local grassroots watershed organizations. The National Institute of Environmental Health Services supported research translation activities through the Superfund Research Program and the development of ground water remediation processes for potential use at contaminated sites. Beam Suntory supported two summer intern students to conduct studies of water availability, quality, and use at the Kentucky distilleries.

The Institute's Committee on Research and Policy considered 15 student research proposals for support through 104(b) 2017 funding. Nine projects were selected. The projects were conducted at the University of Kentucky (5), University of Louisville (1), Eastern Kentucky University (1), and Western Kentucky University (2). The projects represented faculty and students from a variety of discipline areas including civil engineering, biosystems and agricultural engineering, geosciences, and plant and soil science. The goal of this approach is to support student-based efforts representing a variety of discipline areas at numerous educational institutions throughout the state to support broad research capacity related to water resources. It is critical that students are trained for the workforce in government, private industry, and academia. A total of 10 students participated in 2017 104(b) projects (2 PhD, 5 MS, 3 undergraduate students). One project, 2017KY270B, was conducted in conjunction Tanja Williamson of the USGS.

Three projects (2016KY254B, 2016KY260B, and 2016KY261B) were funded in FY2016 and were granted no-cost extensions. The reports indicate additional work accomplished since the FY2016 annual report. Three projects were granted no-cost extensions for FY2018 (2016KY254B, 2017KY266B, and 2017KY267B), and a final report will be provided in next year's annual report.

# Selenium removal by biological processes in water supplies

## Basic Information

<b>Title:</b>	Selenium removal by biological processes in water supplies
<b>Project Number:</b>	2016KY254B
<b>Start Date:</b>	3/1/2016
<b>End Date:</b>	7/31/2018
<b>Funding Source:</b>	104B
<b>Congressional District:</b>	KY 6th
<b>Research Category:</b>	Water Quality
<b>Focus Categories:</b>	Hydrogeochemistry, Toxic Substances, Water Quality
<b>Descriptors:</b>	None
<b>Principal Investigators:</b>	Yi-Tin Wang

## Publications

1. Ji, Yuxia, and Y.T. Wang, 2017, Selenium Reduction by Batch Cultures of Escherichia coli Strain EWB32213, ASCE Journal of Environmental Engineering, 143 (6).
2. Ji, Yuxia, and Y.T. Wang, 2016, Selenium Reduction in Batch Reactors, in Proceedings of the Water, Wastewater, Stormwater, and Watershed Symposium of the ASCE EWRI Conference, May 22-26, 2016, West Palm Beach, Florida, p. 175-180.
3. Ji, Yuxia, and Y.T. Wang, 2017 Selenium Reduction by a Co-Culture of Pantoea Vagans Strain EWB32213-2 and Shigella Fergusonii Strain TB42616, in Proceedings of the 2017 Kentucky Annual Water Resources Symposium, Kentucky Water Resources Research Institute, Lexington, KY, p. 35-36.
4. Ji, Yuxia, and Y.T. Wang, 2018, Selenium removal using activated alumina in a packed-bed reactor, poster presentation at the 2018 Kentucky Water Resources Annual Symposium, Lexington, KY.
5. Ji, Yuxia, and Y.T. Wang, 2018, Selenium reduction by a defined co-culture, in World Environmental and Water Resources Congress 2018: Protecting and Securing Water and the Environment for Future Generations, Environmental & Water Resources Institute, Minneapolis, MN. (In Preparation)



## Selenium Removal by Biological Processes in Water Supplies

### Problem and Research Objectives

Selenium occurs naturally and is an essential nutrient in small amounts. The oxidized forms, selenate (Se (VI)) and selenite (Se (IV)), are soluble and mobile and are found in well aerated conditions (Agency for Toxic Substances and Disease Registry 2003). In reducing environments, however, the elemental selenium (Se (0)) which is insoluble in water, and various selenides (-II) are the predominate species (WHO 2014). Anthropogenic sources of selenium are widespread including electronic and photography, glass manufacturing, pigments, additives for metal processing, copper refining operations, fossil fuel combustion, petroleum refining, and agricultural drainage waters in the Western United States (Fordyce 2013). In Eastern Kentucky, surface-mining operations in Appalachian coal regions have been identified as the major cause of selenium contamination in water and fish, due to the prevalence of selenium in overburden soils exposed during mining activities.

Selenium is toxic to aquatic life and can be harmful to human health (Letavayová, Vlčková, and Brozmanová 2006; Sun et al. 2014). Exposure to very high levels of selenium can cause dizziness, fatigue, irritation, collection of fluid in the lungs, and severe bronchitis. It was also reported that selenium release to the aquatic environments may potentially cause reproduction failure and mortality to aquatic birds as well as anemia and teratogenic deformities to fish (Janz et al. 2010; Lemly 2004; Spallholz and Hoffman 2002). Considering its inability to be absorbed by sediment and soil particles and capability of bioaccumulation, the adverse effects may be magnified and even deteriorated leading to significant threats to the ecosystem (Hamilton 2004). The U.S.EPA (2009) has established a chronic standard for selenium in freshwater at 5 µg/L and a maximum contaminant level for selenium in drinking water at 0.05 mg/L. The concentrations of different metals in sediments of a coal slurry pond were also measured in this study and has been shown in Table 1.

Table 1. Concentrations of different metals in sediments of a coal slurry pond in Harrodsburg, Kentucky.

<b>Metal</b>	<b>As</b>	<b>Cd</b>	<b>Cr</b>	<b>Cu</b>	<b>Mn</b>	<b>Ni</b>	<b>Pb</b>	<b>Se</b>
<b>Concentration, mg/L</b>	0.112477	<0.001	0.07678	0.004019	<0.003	<0.04	<0.01	0.46375

In this study, we evaluated the potential of biological processes as an efficient, cost-effective alternative for selenium reduction in water supplies. Laboratory experiments were conducted to assess the environmental factors affecting selenium reduction with a selenium-reducing strain isolated in our laboratory. Batch cultures were used to determine the effect of environmental factors such as temperature, pH, selenium concentration, and selenium co-contaminants on selenium reduction. Based on the batch results, the appropriate pH, and temperature were selected for study using a bench-scale, continuous-flow bioreactor.

The overall objective of the proposed study is to obtain a better understanding of selenium reduction in aqueous environment by microbial activities. The specific aims are:

1. To determine environment factors affecting microbial reduction of selenium.
2. To evaluate the toxicity of co-contaminants found in coal mining and processing operations on selenium reduction by microbial activities.
3. To develop kinetic expressions and a mathematical model for selenium reduction incorporating the above factors.
4. To evaluate selenium reduction and recovery potential in continuous-flow bioreactor systems.

## Methodology

This study was initiated with batch cultures of *Shigella fergusonii* strain TB42616 and *Pantoea vagans* strain EWB32213-2. These selenium-reducing strains were isolated in our laboratory from the aeration tank in the Town Branch Wastewater Treatment Plant in Lexington, Kentucky and from sediments of the slurry pond at the E.W.Brown Generating Station in Harrodsburg, KY, respectively. Batch cultures were used to evaluate the effect of the following variables on relative rates of Se(VI) and Se(IV) reduction: Concentrations of growth substrate, Se(VI), Se(IV), temperature, and pH. Glucose was used as the growth substrate. Se(VI) and Se(IV) concentrations were evaluated from 10 to 1000 mg/L and temperature was investigated from 10°C to 50° C while pH varied from 4 to 9.

Based on the batch results, the appropriate pH, and temperature were selected for study using a bench-scale, continuous-flow bioreactor. The bioreactor consists of 40 g activated alumina packed Pyrex glass column of 12 cm long with 2.5 cm i.d. operated in upflow mode (Figure 1).

## Principal Findings and Significance

*Batch co-culture experiment:* The effects of temperature and pH on Se(VI) reduction were first evaluated in pure cultures of selenium-reducing bacteria. The optimal temperature for selenium reduction by *Shigella fergusonii* strain TB42616 was observed at 40°C with around 92% reduction after 4 days. For *Pantoea vagans* strain EWB32213-2, selenium reduction rate increased from 20°C, peaked at 30°C, and decreased at higher temperature.

pH effects on both strains were investigated over a pH range of 4-9. For *Shigella fergusonii* strain TB42616, the highest selenium reduction rate was observed at pH 8 with an approximate reduction rate of 79% after 4 days. The selenium reduction rate by *Pantoea vagans* strain EWB32213-2 increased at pH lower than 7, peaked at pH 7 (87% after 4 days), and then remained rather stable (<10%) at higher pH. As a result, the optimal pH for *Pantoea vagans* strain EWB32213-2 was observed at pH 7. Thus, pH 8 was selected in the co-culture study as the difference of the selenium reduction rate between pH 7 and pH 8 was insignificant for *Pantoea vagans* strain EWB32213-2 but substantially different for *Shigella fergusonii* strain TB42616.

Four bacterial ratios 1:0.01, 1:0.1, 1:1 and 1:10 (*Shigella fergusonii* : *Pantoea vagans*) were selected to investigate the effect of culture composition on selenium reduction under initial Se(VI) concentration of 1100 mg/L. The results show that the bacterial ratio of 1:10 was the optimal

composition with both highest Se(VI) (90.9%) and total selenium (87.9%) reduction rate observed. As the ratio increased, no significant difference of Se(VI) reduction rate was observed at bacterial compositions above 1:1. However, the Se(IV) reduction rate decreased with the increasing bacterial composition rate due to the reduction in Se(IV)-reducing strain *Pantoea vagans* EWB32213-2.

The batch co-culture experiments were further conducted under optimal conditions with added initial Se(VI) concentration of 10 mg/L. Figure 2 shows the difference of selenium reduction by a pure culture of *Shigella fergusonii* strain TB42616 and a defined co-culture of *Pantoea vagans* strain EWB32213-2 and *Shigella fergusonii* strain TB42616. The result shows that the rate of Se(VI) reduction was similar to that observed in pure culture of *Shigella fergusonii* strain TB42616. However, significant difference was observed on Se(IV) reduction at a low initial Se(VI) concentration. Approximately 68.31%, 69.88%, 73.54% and 49.58% of Se(IV) accumulation was eliminated using the co-culture after 1, 2, 4 and 6 days, respectively. The effect of initial Se(VI) concentrations was also evaluated under a range of concentrations from 10-1000 mg/L. The result shows that selenium can be significantly reduced in the co-culture but not with the pure culture even at a high initial Se(VI) concentration. Approximately 87.2% selenium was completely reduced at an initial Se(VI) concentration of 1000 mg/L.

*Activated alumina packed reactor experiment:* Selenium adsorption onto activated alumina was first investigated in batch reactors supplemented with 20 mg/L Se(IV) or Se(VI) under a temperature of 30°C. An activated alumina weight span of 0.02-0.22 g (1-8 pellets) was selected to perform adsorption. The results shown in Figure 3 indicate that the adsorption capacity of Se(IV) was significantly higher than of Se(VI). The highest adsorption capacity of Se(VI) achieved in this study was observed at 0.85 mg/g compared with 7.41 mg/g as Se(IV) adsorption capacity. Additionally, the relative low adsorption capacity of Se(VI) may also attribute to the presence of high levels of bicarbonate (3 g/L) in the medium used for pH buffer since Se(VI) adsorption by activated alumina can be easily interfered by a number of anions including OH<sup>-</sup>, SO<sub>4</sub><sup>2-</sup>, HCO<sub>3</sub><sup>3-</sup>, etc.

Selenium removal was then investigated under a continuous flow condition using a packed-bed reactor with a hydraulic retention time of 3.1 days. Concentrations of Se(VI) and Se(IV) were fed at 50 mg/L, and a temperature of 30°C and a pH of 7 were applied. The results in Figure 4 shows that the adsorption of Se(VI) reached exhaustive phase much faster than of Se(IV) in the packed-bed reactors with no bacterial cells cultured. It was observed that Se(IV) adsorption did not reach the exhaustive phase after 42 days. As for Se(VI) adsorption, the exhaustive phase occurred after 14 days. Microbial reduction using *Shigella fergusonii* strain TB42616 was immobilized in the pack-bed bioreactor in this study for selenium removal in addition to the adsorption process. Figure 4 shows that around 19.7 mg/L of Se(VI) was detected in the effluents with feeding concentrations 50 mg/L after 42 days, indicating that Se(VI) has been significantly removed compared with 47.9 mg/L with no microbial cells added. No significant Se(IV) was observed in the effluent since the Se(IV) generated from biological Se(VI) reduction was absorbed by activated alumina. As a result, Se(IV) removal efficiency was also enhanced in this study.

Selenium removal in a real wastewater from the coal slurry pond in the Brown Generation Station in Harrodsburg, Kentucky, was also evaluated with the continuous-flow activated alumina bioreactor. Filtered coal slurry pond water supplemented with 10 mg/L of SE (VI) and glucose5les

was fed to the bioreactor. Figure 5 indicates that insignificant amount of Se(VI) and Se(IV) were detected in the effluent after one week into the study. The experiment will continue for several more weeks to evaluate the long-term performance of selenium removal of this activated alumina packed bioreactor.

Development of kinetic models for both pure and co-culture of Se(VI)-reduction bacteria for batch and continuous-flow bioreactors are ongoing.

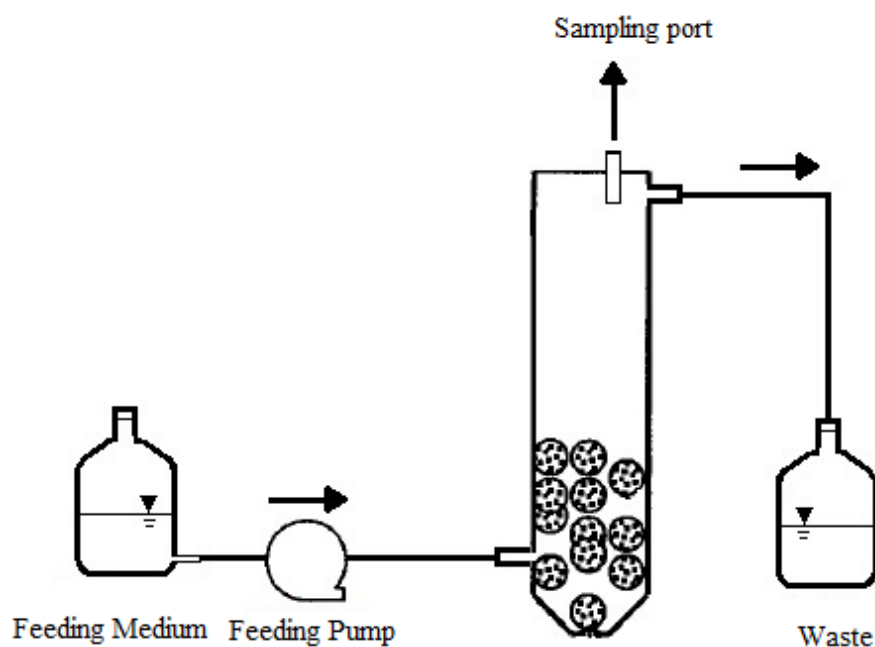


Figure 1. The configuration of the packed-bed reactor in this study.

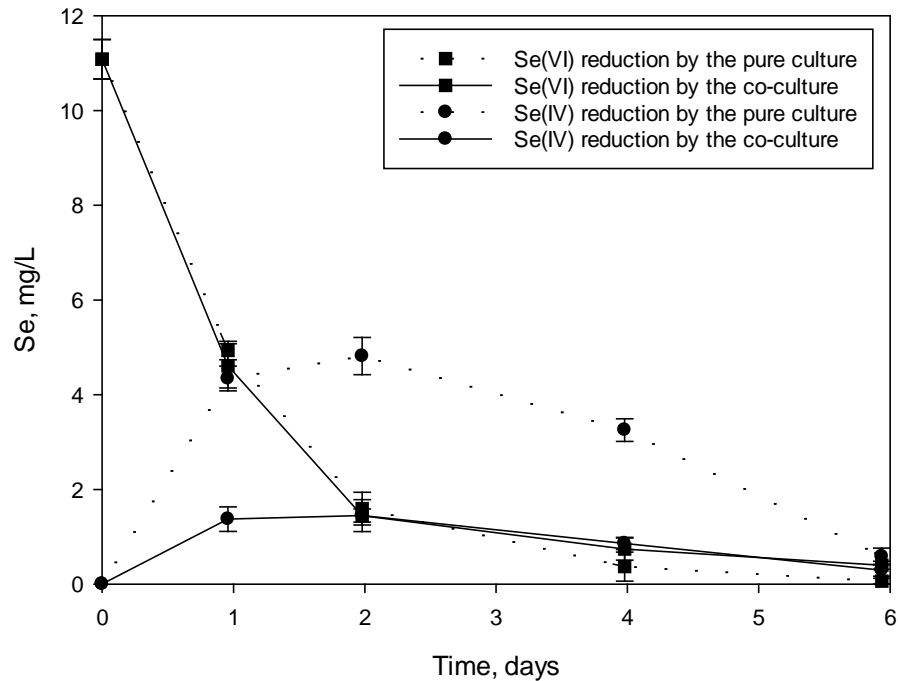


Figure 2. Selenium reduction by a pure culture of *Shigella fergusonii* strain TB42616 and a co-culture of *Shigella fergusonii* strain TB42616 and *Pantoea vagans* strain EWB32213-2 at initial Se(VI) concentration of 10 mg/L.

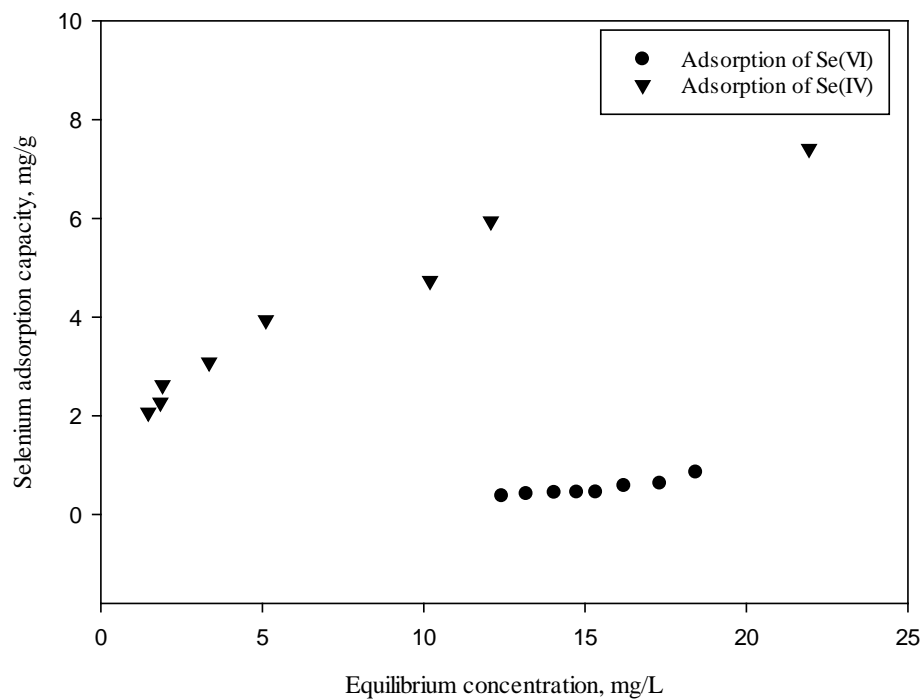


Figure 3. Adsorption isotherms of Se(VI) and Se(IV) onto activated alumina.

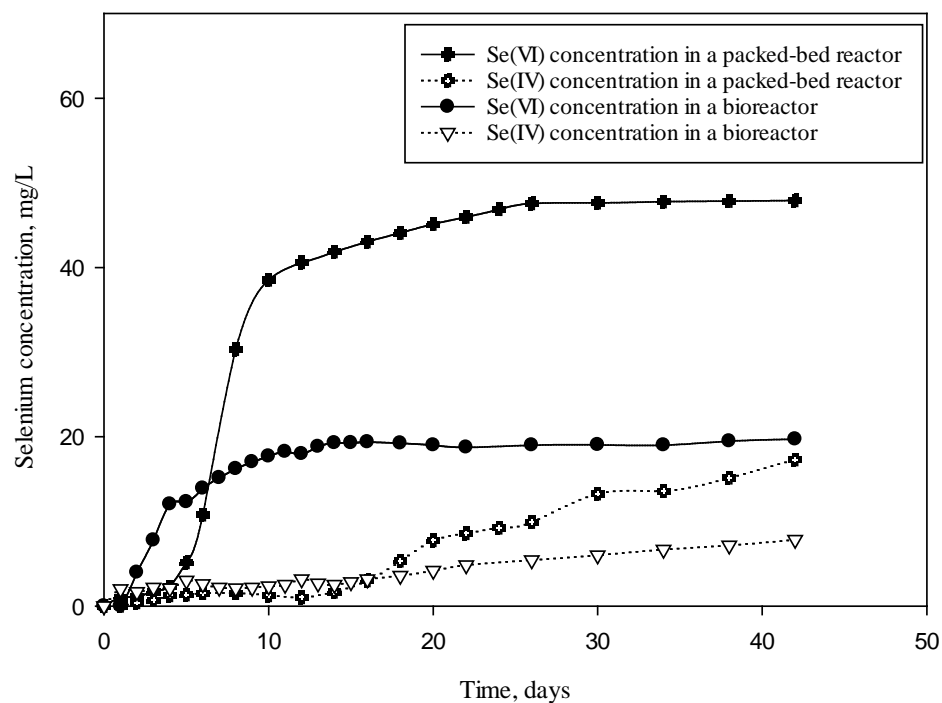


Figure 4. Effluent concentrations of Se(VI) and Se(IV) in a packed-bed reactor with 40 g activated alumina and a bioreactor packed with 40 g activated alumina and cultured with *Shigella fergusonii* strain TB42616.

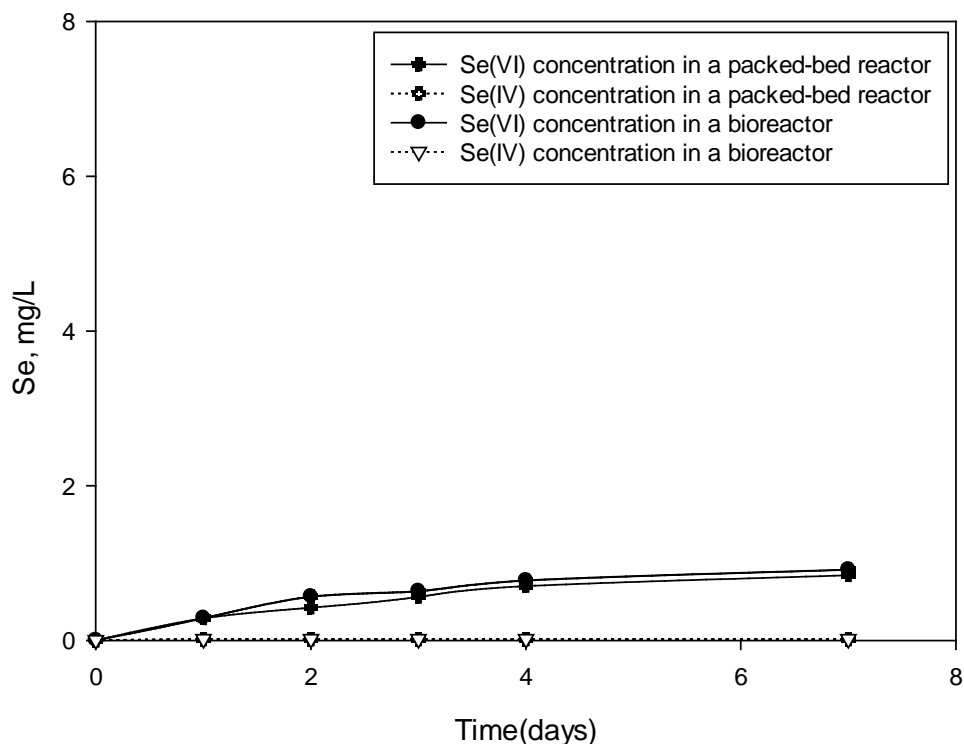


Figure 5. Effluent concentrations of Se(VI) and Se(IV) in a packed-bed reactor with 40 g activated alumina and a bioreactor fed with real wastewater.

## References

- Agency for Toxic Substances and Disease Registry. 2003. *Toxicological Profile for Selenium*. Atlanta, Georgia. <http://www.atsdr.cdc.gov/toxprofiles/tp92.pdf>.
- Fordyce, Fiona. 2013. "Selenium Deficiency and Toxicity in the Environment." In *Essentials of Medical Geology*, Dordrecht, Netherlands: Springer, 375–416.
- Hamilton, Steven J. 2004. "Review of Selenium Toxicity in the Aquatic Food Chain." *Sci. Total Environ.* 326(1–3): 1–31.
- Janz, David M. et al. 2010. "Selenium Toxicity to Aquatic Organisms." In *Ecological Assessment of Selenium in the Aquatic Environment*, Boca Raton, Florida: CRC Press, 141–210.
- Lemly, A. Dennis. 2004. "Aquatic Selenium Pollution Is a Global Environmental Safety Issue." *Ecotox. Environ. Safe.* 59(1): 44–56.
- Letavayová, Lucia, Viera Vlčková, and Jela Brozmanová. 2006. "Selenium: From Cancer Prevention to DNA Damage." *Toxicology* 227(1–2): 1–14.
- Spallholz, J. E., and David J. Hoffman. 2002. "Selenium Toxicity: Cause and Effects in Aquatic

Birds.” *Aquat. Toxicol.* 57(1–2): 27–37.

Sun, Hong-jie et al. 2014. “Arsenic and Selenium Toxicity and Their Interactive Effects in Humans.” *Environ. Int.* 69C: 148–158.

USEPA. 2009. “Table of Regulated Drinking Water Contaminants.” *National Primary Drinking Water regulations*. <http://www.epa.gov/your-drinking-water/table-regulated-drinking-water-contaminants>.

WHO. 2014. *Selenium in Drinking-Water*. Geneva, Switzerland.  
[http://www.who.int/water\\_sanitation\\_health/dwq/chemicals/selenium.pdf](http://www.who.int/water_sanitation_health/dwq/chemicals/selenium.pdf).



# The use of eDNA to detect bacterial genetic markers associated with fecal contamination in the Triplett Creek Watershed, Rowan County, Kentucky

## Basic Information

<b>Title:</b>	The use of eDNA to detect bacterial genetic markers associated with fecal contamination in the Triplett Creek Watershed, Rowan County, Kentucky
<b>Project Number:</b>	2016KY260B
<b>Start Date:</b>	3/1/2016
<b>End Date:</b>	2/28/2018
<b>Funding Source:</b>	104B
<b>Congressional District:</b>	KY 5th
<b>Research Category:</b>	Water Quality
<b>Focus Categories:</b>	Management and Planning, Water Quality, Wastewater
<b>Descriptors:</b>	None
<b>Principal Investigators:</b>	Geoff Gearner

## Publications

1. Brown, Rachel, Hannah Conley and Geoffrey Gearner, 2017, The Use of Environmental DNA to Detect Bacterial Molecular Markers in the Triplett Creek Watershed, Rowan County, Kentucky, in Proceedings of the 2017 Kentucky Water Resources Annual Symposium, Kentucky Water Resources Research Institute, Lexington, Kentucky, p. 77.
2. Conley, Hannah, Rachel Brown, and Geoffrey Gearner, 2017, The use of eDNA to detect bacterial molecular markers in the Triplett Creek Watershed, poster presentation at the Celebration of Student Scholarship, Morehead State University, Morehead, KY.
3. Conley, Hannah, Amina Anwar, and Geoffrey Gearner, 2018, Polymerase chain reaction detection of bacterial DNA markers in the Triplett Creek Watershed, poster presentation at the Celebration of Student Scholarship, Morehead State University, Morehead, KY.

# **The Use of eDNA to Detect Bacterial Genetic Markers Associated with Fecal Contamination in the Triplett Creek Watershed, Rowan County, Kentucky**

## **Project and Research Objectives**

The objective of the study is to develop and evaluate the use of bacterial genetic targets as markers of fecal contamination in the Triplett Creek Watershed for the purpose of identifying point and host sources of fecal pollution. Specifically, this project used quantitative polymerase chain reaction (qPCR) to evaluate DNA extracted from filtered water samples (heretofore referred to as environmental or eDNA) collected from long standing sampling sites in the Triplett Creek Watershed for the presence of genetic markers associated with fecal bacteria. Collected data could then be used to construct plume maps of human and/or cattle fecal-associated bacteria.

## **Methodology**

The workflow initially proposed for the project was as follows:

1. In the field, utilizing a peristaltic pump and 0.45- $\mu$ m pore size cellulose-nitrate filters in a flow through device, filter a minimum of 3-5 L of water from established sampling sites in the TCW.
2. Place filters in centrifuge tubes containing 95% ethanol for transport back to the lab.
3. In the lab, extract eDNA from the filters using Qiagen's DNeasy Tissue and Blood Kit, and Qiagen's QIAshredder Kit.
4. Post-extraction treatment of each sample by spin-column purification using the OneStep PCR Inhibitor Removal Kit (Zymo Research).
5. Assess the quality and yield of the extracted eDNA spectrophotometrically, store samples at -20°C.
6. Screen eDNA for the presence of specific antibiotic resistance genes (ARGs) and other bacterial markers by conventional polymerase chain reaction (PCR).
7. Analysis of PCR products by agarose gel electrophoresis.
8. Sequence (GenWiz) selected PCR products to confirm target gene.
9. Design qPCR primer/probes utilizing Primer Express software (v. 3.01; Applied Biosystems).
10. Utilize designed *TaqMan* primers/probes in qPCR reactions to detect and quantify target DNA sequences (see Tables 1 and 2 for DNA targets).
11. Data Analyses of qPCR products (qPCR product concentration to be determined using a serially diluted DNA standard and the resident software of the qPCR instrument).
12. Utilization of data to construct GIS map of study area to determine the point, and potentially host, source(s) of fecal contamination of the watershed.

For this project, we were to assess sampling sites in two Triplett Creek tributaries (Christy Creek and Island Fork) that were chronically contaminated with high *E. coli* counts; and sampling sites in a 6.5-mile section in the main stem of Triplett Creek between river miles 5.8 and 12.3 which is listed on the 2012 303(d) list as impaired by

the presence of fecal coliform bacteria. To avoid contaminating samples fresh disposable gloves were worn for each sampling, and all equipment was treated with DNA Away (Fisher Scientific) prior to filtering the water sample to remove any contaminating DNA.

Table 1. PCR primers utilized for the detection of *E. coli* and host-specific bacterial DNA sequences.

Gene	Bacterium	Primer	Sequence	Host Source
16S rRNA <sup>1</sup>	<i>Bacterioides-Prevotella</i>	HF183F Bac708R	5'-ATCATGATGTCACATGTCCG-3' 5'-CAATCGGAGTTCTTCGTG-3'	Human
16S rRNA <sup>2</sup>	<i>Bacterioides-Prevotella</i>	CF128F Bac708R	5'-CCAACYTTCCCGWTACTC-3' 5'-CAATCGGAGTTCTTCGTG-3'	Cattle
<i>esp</i> <sup>3</sup>	<i>Enterococcus faecium</i>	<i>espF</i> <i>espR</i>	5'- TATGAAAGCAACAGCACAAGTT-3' 5'-ACGTCGAAAGTTTCGATTTC-3'	Human
<i>uidA</i> <sup>4</sup>	<i>Escherichia coli</i>	<i>uidAF</i> <i>uidAR</i>	5'-ACGCGTGGTTACAGTCTTGCG-3' 5'- TGGTAATTACCGACGAAAACGGC-3	n.a.

Sources: 1 (Bernhard and King, 2000a; Carson, *et al.*, 2005); 2 (Bernhard and King, 2000b); 3 (Scott, *et al.*, 2005); 4 (Tantawiwat, *et al.*, 2005).

Table 2. Primers used to detect select antibiotic resistance genes.

ARG	Sequence	Annealing Temp	Amplicon Size
<i>TetW</i> <sup>1</sup>	FW: GAGAGCCTGCTATATGCCAGC	60°C	168 bp
	RV: GGGCGTATCCACAATGTTAAC		
<i>TetO</i> <sup>1</sup>	FW: ACGGARAGTTTATTGTATACC	50.3°C	171 bp
	RV: TGGCGTATCTATAATGTTGAC		
<i>ereA</i> <sup>1</sup>	FW: ATGACGTGGAGAACGACCAG	60°C	101 bp
	RV: CCGACAATTCGGGCGCCCTCAAT		

Sources: 1 (Aminov, *et al.*, 2001; Pei *et al.*, 2006 and 2007; Prudent, *et al.*, 2006; Storteboom, *et al.*, 2007)

Blanks of sterile distilled water was to be filtered in the field for every ten samples collected; and a duplicate sample was to be filtered for every ten samples collected. Sampling was to take place during the 2016 recreational season (May through October). At least one set of samples was to be collected immediately following a wet weather event (one or more inches of rainfall), and at least one set of samples was to be collected following a dry weather event (less than 0.1 inch of rain over a 7-day period). eDNA extraction and processing were to be conducted in laminar flow hoods located in the Microbiology Laboratory (Lappin Hall) on the Morehead State University campus, and according to the kit manufacturers' directions (Qiagen and Zymo Research). All eDNA samples were to be stored at -20°C until analysis. An Applied Biosystems' 7500 Fast Real Time PCR System was to be used for the qPCR analysis of the eDNA samples. All qPCR results were to be analyzed against a serially diluted DNA standard to determine absolute qPCR product concentration, utilizing the resident software of the qPCR instrument. All appropriate PCR and qPCR controls (non-target DNA, primer-only, target DNA only, *etc.*) were to be run alongside the experimental runs.

This methodology was followed with the exception of the following modifications:

1. We originally proposed using a peristaltic pump to filter water samples in the field at our sampling sites in the Triplett Creek Watershed. In consulting with others who work with eDNA, we decided to collect 3-liter samples in sample collection bottles, then transport the samples to the microbiology lab for filtration. This had the advantages of reducing the risk of sample contamination and cost savings of the project.
2. We found that yields were low when attempting to extract DNA directly from water samples. Although some positive PCR results were obtained, we decided to follow another approach (see Appendix 1). This resulted in much improved DNA yields.
3. Following DNA extraction, PCR was conducted utilizing primer sets for bacteria DNA (16S rRNA), *Escherichia coli*'s *uidA* gene, and a human specific enterococcal gene (*esp*). Additionally, DNA samples were screened by PCR for a variety of antibiotic resistance gene described in Table 3.

Table 3. Antibiotic Resistance Gene PCR Primer Sets Utilized.

Primer Name	Primer Sequence	Target
TetW-F TetW-R	5'-GAGAGCCTGCTATATGCCAG-3' 5'-GGGCGTATCCACAATGTTAAC-3'	tetracycline resistance gene
TetO-F TetO-R	5'-ACGGARAGTTTATTGTATACC-3' 5'-TGGCGTATCTATAATGTTGAC-3'	tetracycline resistance gene
SulI-F SulI-R	5'-CGCACCGGAAACATCGCTGCAC-3' 5'-TGAAGTTCCGCCGCAAGGCTCG-3'	sulfonamide resistance gene
SulII-F SulII-R	5'-TCCGGTGGAGGCCGGTATCTGG-3' 5'-CGGGAATGCCATCTGCCTTGAG-3'	sulfonamide resistance gene
ereA-F ereA-R	5'-ATGACGTGGAGAACGACCAG-3' 5'-CCGACAATTCGGGCGCCCTCAAT-3'	erythromycin resistance gene
msrA/B-F msrA/B-R	5'-CTGGAACGGTTGAAACGGATGGC-3' 5'-ACCACCACTCATACTGTTCGGTTG-3'	macrolide resistance gene
<i>bla</i> -CMY-F <i>bla</i> -CMY-R	5'-ATGATGAAAAAATCGTTATGCT-3' 5'-TTATTGCAGCTTTTCAAGAATGCG-3'	ESBL gene

## Principal Findings and Significance

- PCR Results for bacterial DNA markers.
  - **16S rRNA:**
    - Expected bp length: 550 bp
    - bands produced for sites TC 14.94, TC 19.94, IF 0.05, PB 0.42, LB 13.2, DC 0.27, EB 0.04, BB 0.23, NF 9.77, TC 12.27, TC 13.52. CC 0.37 (See Figure 1 below, a typical agarose gel result.)
    - Results: All samples were positive for bacterial 16S rRNA



Figure 1. Gel-red stained 1.25% agarose gel of

1	2	3	4	5	6	7	8	9	10	11	12	13	14
100bp ladder	TC 14.94	TC 19.94	IF 0.05	PB 0.42	LB 13.2	DC 0.27	EB 0.04	BB 0.23	NF 9.77	TC 12.27	TC 13.52	CC 0.37	X

- **esp:**
  - Expected amplicon bp length: 407 bp
  - Results: Four sampling sites, CC 0.37, BB 0.23, DC 0.27, and NF 9.77, were positive for the human-specific enterococcal *esp* gene.



Figure 2. Gel-red stained 1.25% agarose gel of *esp* PCR products.

1	2	3	4	5	6	7	8	9	10	11	12	13	14
x	100bp ladder	IF 0.05	TC 19.91	TC 14.99	PB 0.42	EB 0.04	CC 0.37	BB 0.23	DC 0.27	TC 12.27	NF 9.77	TC 13.52	LB 13.2

- **uidA:**
  - Expected amplicon bp length: 147 bp
  - Results: 11 of 12 samples sites were positive for the *Escherichia coli uidA* gene.
- PCR Results for antibiotic resistance genes.
  - **ereA:**
    - Expected amplican bp length: 101 bp
    - Results: 11 of 12 sample sites were positive for the *ereA* gene.
    -
  - **blac<sub>MY</sub>:**
    - Expected amplicon bp length: 1140 bp (*blac<sub>MY</sub>*)
    - Results: no bands were produced for either gene
  - **sulII, tetO:**
    - Expected amplicon bp lengths: 191 bp (*sulII*), 171 bp (*tetO*)
    - Results: All sample sites were positive for the *sulII* gene; while three sample sites were positive for the *tetO* gene.
  - **msrA, tetW:**
    - Expected amplicon bp lengths: 143 bp (*msrA*), 168 bp (*tetW*)

- Results: Data was inconclusive for the *msrA* gene as multiple PCR products were produced. Five sample sites, NF 9.77, IF 0.05, DC 0.27, CC 0.37 and BB 0.23, were positive for the *tetW* gene.

- **sulI:**

- expected bp length: 163 bp
- Results: All sample sites were positive for the *sulI* gene.

Of the twelve Triplett Creek Watershed sampling sites evaluated, all were positive for bacterial DNA, eleven of twelve sites were positive for *E. coli* DNA, and four of twelve sites were positive for human-specific enterococcal DNA. Various antibiotic resistance genes were detected in some of the twelve sampling sites. Previous work indicated that *E. coli* collected from these sites exhibited antibiotic resistance as assessed by the Kirby-Bauer method to tetracycline, erythromycin, various  $\beta$ -lactams, and sulfonamides. PCR results presented in this study support this observation. We found that the extraction of DNA directly from water samples resulted in low DNA yields. However, extracting DNA from enriched water-sample derived bacterial cultures dramatically improved DNA yield, which was sufficient to conduct PCR. More data will need to be collected to make a correlation to the presence of antibiotic resistance genes and *Escherichia coli* counts, as well as to determine if the presence of one or more antibiotic resistance genes can indicate that human and/or cattle feces is contaminating the watershed. Such data can inform the development of remediation strategies to improve the quality of the watershed.

Antibiotic resistant bacteria are routinely encountered in the Triplett Creek Watershed, which may indicate that human and/or cattle feces is polluting the watershed. We will continue with the work going forward.

## Appendix 1

### DNA EXTRACTION PROTOCOL

1. Filter 1 L of sample water through a 47-mm diameter Millipore membrane filter.
2. Place the filter into a labeled 50-mL conical tube containing 25 mL sterile PBS.
3. Agitate by Vortexing for 2 min.
4. Transfer 200  $\mu$ L of the suspension to a labeled 15-mL conical tube containing 10 mL of sterile tryptic soy broth (TSB) and incubate overnight at 37°C. Store the 50-mL conical tube containing the PBS and membrane filter at 4°C.
5. Invert the TSB culture tube several times to re-suspend the cells, then transfer 1 mL of the overnight TSB culture into a sterile, labeled 1.5-mL microcentrifuge tube. Store the 15-mL conical tube of the TSB culture at 4°C.
6. Pellet bacteria by centrifugation for 10 min at 5,000 x *g* (7,500 rpm).
7. Decant the supernatant, then suspend the bacterial pellet in 180  $\mu$ L of the lysozyme solution.
8. Incubate in a 37°C water bath for a minimum of 30 min.
9. Add 20  $\mu$ L proteinase K and 200  $\mu$ L Buffer AL. Vortex to mix.
10. Incubate at 56°C for 30 min and then for a further 15 min at 95°C.
11. Centrifuge for a few sec.
12. Add 200  $\mu$ L 100% ethanol to the sample, and mix by pulse-Vortex for 15 sec. After mixing, briefly centrifuge the 1.5-mL microcentrifuge tube to remove drops from inside the lid.  
NOTE: It is essential that the sample, Buffer AL, and ethanol are mixed thoroughly to yield a homogeneous solution. A white precipitate may form upon addition of ethanol. It is essential to apply all of the precipitate to the QIAamp Mini spin column.
13. Carefully apply the mixture from step 7 (including the precipitate) to the QIAamp Mini spin column (in a 2-mL collection tube) without wetting the rim. Close the cap, and centrifuge at 6,000 x *g* (8,000 rpm) for 1 min. Place the QIAamp Mini spin column in a clean 2-mL collection tube (provided), and discard the tube containing the filtrate.  
NOTE: Close each spin column tightly to avoid aerosol formation during centrifugation.



14. Carefully open the QIAamp Mini spin column and add 500  $\mu$ L Buffer AW1 without wetting the rim. Close the cap, and centrifuge at 6,000  $\times$  g (8,000 rpm) for 1 min. Place the QIAamp Mini spin column in a clean 2-mL collection tube, and discard the collection tube containing the filtrate.
15. Carefully open the QIAamp Mini spin column and add 500  $\mu$ L Buffer AW2 without wetting the rim. Close the cap and centrifuge at full speed (20,000  $\times$  g; 14,000 rpm) for 3 min.
16. Place the QIAamp Mini spin column in a new 2-mL collection tube, and discard the old collection tube with the filtrate. Centrifuge at full speed for 1 min.
17. Place the QIAamp Mini spin column in a clean, labeled 1.5-mL microcentrifuge tube, and discard the collection tube containing the filtrate. Carefully open the QIAamp Mini spin column and add 200  $\mu$ L Buffer AE. Incubate at room temperature for 1 min, and then centrifuge at 6,000  $\times$  g (8,000 rpm) for 1 min. This step elutes the DNA from the column into Buffer AE.
18. Carefully open the QIAamp Mini spin column and add an additional 200  $\mu$ L Buffer AE. Incubate at room temperature for 5 min, and then centrifuge at 6,000  $\times$  g (8,000 rpm) for 1 min. After this step, 400  $\mu$ L of DNA solution is present in the 1.5-mL microcentrifuge tube. (steps 5-18, Qiagen, 2010).
19. Assess the DNA solution spectrophotometrically to determine concentration and purity.
20. Store the DNA solution at -20°C until use.

# Climate change impacts on soil-water availability under different land management: forest and grasslands

## Basic Information

<b>Title:</b>	Climate change impacts on soil-water availability under different land management: forest and grasslands
<b>Project Number:</b>	2016KY261B
<b>Start Date:</b>	3/1/2016
<b>End Date:</b>	2/28/2018
<b>Funding Source:</b>	104B
<b>Congressional District:</b>	KY 1st & 2nd
<b>Research Category:</b>	Climate and Hydrologic Processes
<b>Focus Categories:</b>	Agriculture, Conservation, Geochemical Processes
<b>Descriptors:</b>	None
<b>Principal Investigators:</b>	Brad Lee

## Publications

1. Baker, Trinity J., T.N. Williamson, and Brad Lee, 2016, Comparing Simulated Soil Properties to Field Derived Values in Forested and Grassland Catenas of MLRA 120, in Proceedings of the 2016 Kentucky Water Resources Annual Symposium, Kentucky Water Resources Research Institute, Lexington, Kentucky, p. 29.
2. Williamson, Tanja N., Brad D. Lee, and Trinity J. Baker, 2017, Projections of 2050 Soil-Water Storage Under Differing Land Management, in Proceedings of the 2017 Kentucky Water Resources Symposium, Kentucky Water Resources Research Institute, Lexington, Kentucky, p. 53.
3. Baker, Trinity, 2017, MS Thesis, Soil Hydraulic Property Estimation Under Major Landuses in the Shawnee Hills, Department of Plant and Soil Science, College of Agriculture Food and Environment, University of Kentucky, Lexington, Kentucky, 371 p. [http://uknowledge.uky.edu/pss\\_etds/86](http://uknowledge.uky.edu/pss_etds/86)

# Climate Change Impacts on Soil-Water Availability under Different Land Management: Forest and Grasslands

## Problem and Research Objectives

The ability to model the effect of climate change on soil-water availability and agricultural production is dependent on reliable estimation of hydrologic soil properties under differing land management. Soil organic carbon (C) content has been linked to available water-holding capacity and hydraulic conductivity, however these hydrologic soil properties are also dependent on other soil factors, including particle-size distribution and bulk density (Rawls et al., 1983, 2003). The work presented here had two objectives: 1) Estimate hydrologic soil properties (field capacity, wilting point, and saturated hydraulic conductivity) for soils from NRCS's Rapid Assessment of U.S. Soil Carbon (RaCA) in MLRA 120 (figure 1) using both established equations and a Random-Forest (RF) model developed using the Shawnee Hills Loess Catenas Soil System pedons. 2) Incorporate these soil properties into a hydrologic model of soil-water storage under different RaCA land-management categories: forest, pasture, traditional agriculture (crop), and conservation agriculture. Soil-water storage simulated for a 12-yr historical period will be compared to that simulated using mid-century projections of temperature, precipitation, and potential evapotranspiration (PET).

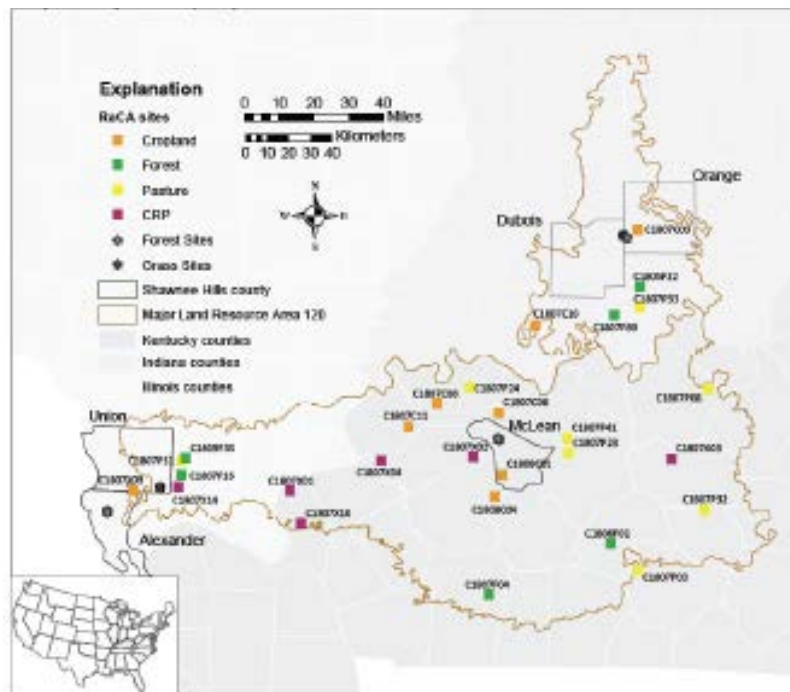


Figure 1. Location of model calibration sites (asterisks) and RaCA pedon description sites.

## Methodology

Soil hydrologic properties field capacity (FC), wilting point (WP), and saturated hydraulic conductivity (Ksat) were estimated for the RaCA pedons using three independent pedotransfer functions. Available water holding capacity (AWC) was determined by difference (FC – WP).

Physical property data available to use in the estimation included: bulk density (pb), organic carbon (OC) and sand, silt and clay proportions (PSA).  
 Pedotransfer functions included the PSA triangle (figure 2; NSSH Part 618.88 (Subpart B)), previously published equations that incorporated National Soil Survey pedon data (figure 3; Saxton and Rawls, 2006), and Random Forest models (figure 4) developed as part of this work.

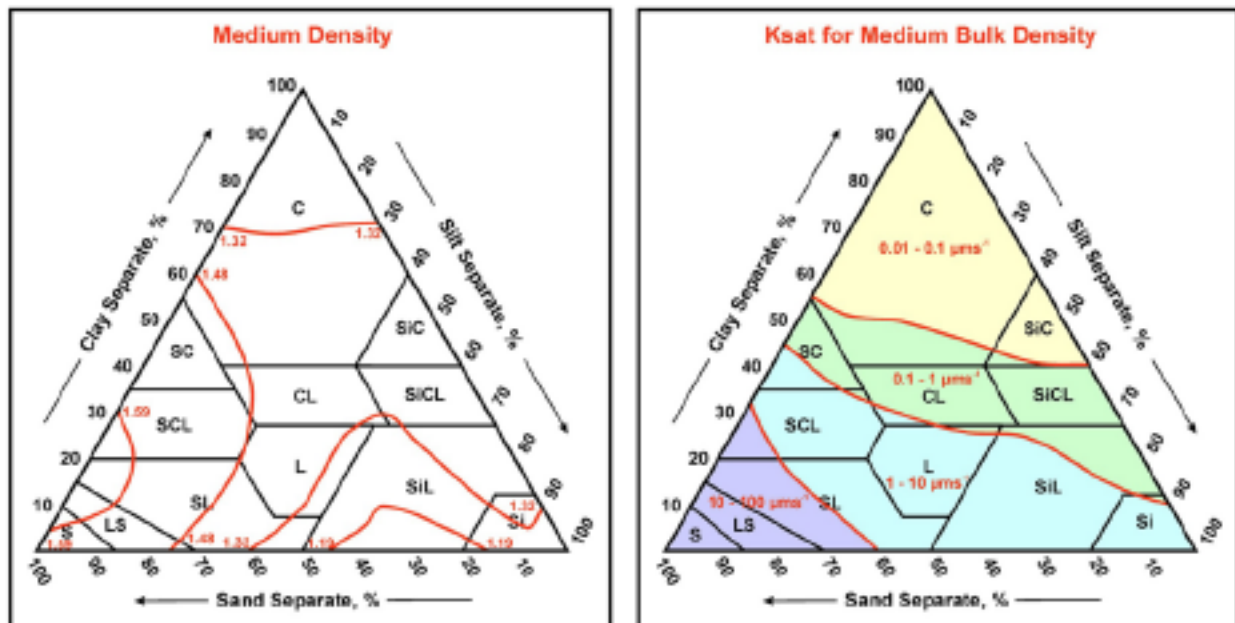


Figure 2. PSA triangle: working with NRCS (personal communication with Cathy Seybold, 2016), a scripted version of this NRCS method was produced and used to estimate Ksat for each horizon (image from NSSH Part 618.88 (Subpart B)).

$$\begin{aligned}
 \theta_{1500} & \quad \theta_{1500} = \theta_{1500r} + (0.14 \times \theta_{1500r} - 0.02) \\
 \theta_{1500r} & \quad \theta_{1500r} = -0.024S + 0.487C + 0.006OM \\
 & \quad \quad + 0.005(S \times OM) - 0.013(C \times OM) \\
 & \quad \quad + 0.068(S \times C) + 0.031 \\
 \theta_{33} & \quad \theta_{33} = \theta_{33r} + [1.283(\theta_{33r})^2 - 0.374(\theta_{33r}) - 0.015] \\
 \theta_{33r} & \quad \theta_{33r} = -0.251S + 0.195C + 0.011OM \\
 & \quad \quad + 0.006(S \times OM) - 0.027(C \times OM) \\
 & \quad \quad + 0.452(S \times C) + 0.299 \\
 \theta_{(S-33)} & \quad \theta_{(S-33)} = \theta_{(S-33)r} + (0.636\theta_{(S-33)r} - 0.107) \\
 \theta_{(S-33)r} & \quad \theta_{(S-33)r} = 0.278S + 0.034C + 0.022OM \\
 & \quad \quad - 0.018(S \times OM) - 0.027(C \times OM) \\
 & \quad \quad - 0.584(S \times C) + 0.078 \\
 \theta_S & \quad \theta_S = \theta_{33} + \theta_{(S-33)} - 0.097S + 0.043 \\
 K_S & \quad K_S = 1930(\theta_r - \theta_{33})^{(3-\lambda)}
 \end{aligned}$$

Figure 3. Saxton and Rawls (SR): These equations provide estimates for FC, WP and Ksat. These equations were originally developed using a national set of A-horizon samples. (Saxton and Rawls, 2006).

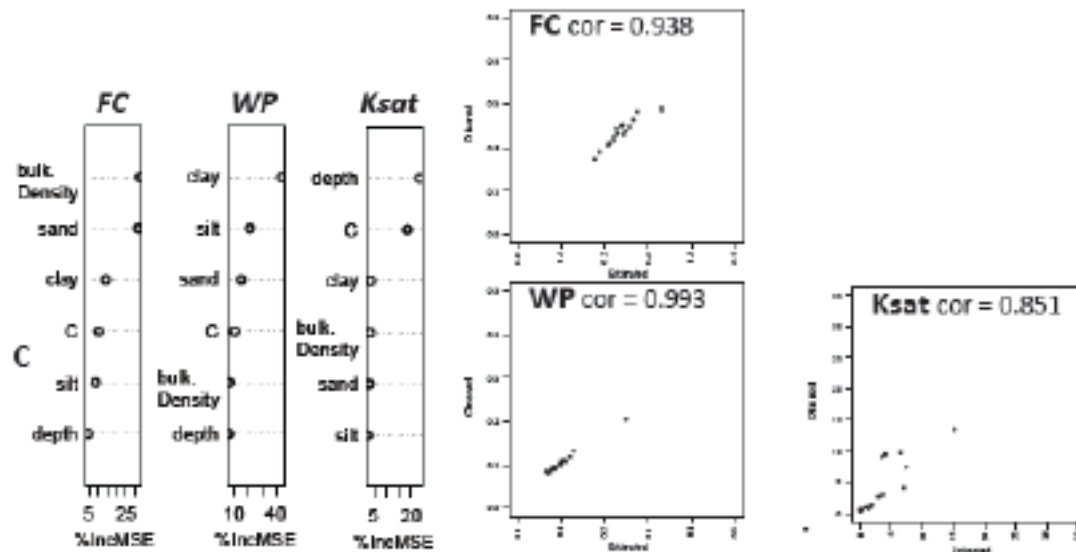


Figure 4. Random Forest (RF): 100 horizons, including both A and B horizons, were used to train RF models using Breiman and Cutler's Random Forest in R (2015). Each RF model was used to estimate hydrologic properties for horizons from two additional Shawnee Hills catenas. For the hydrologic modeling reported here, FC, WP, and Ksat were estimated using the RF model only. For reference, the importance of the independent variables in the RF model are shown for each estimated property (figure 4). The correlation of observed and estimated hydrologic properties for the Kentucky grass watershed used for the hydrologic modeling is shown to the right. Each correlation was significant ( $p\text{-value} < 1.5e-05$ ).

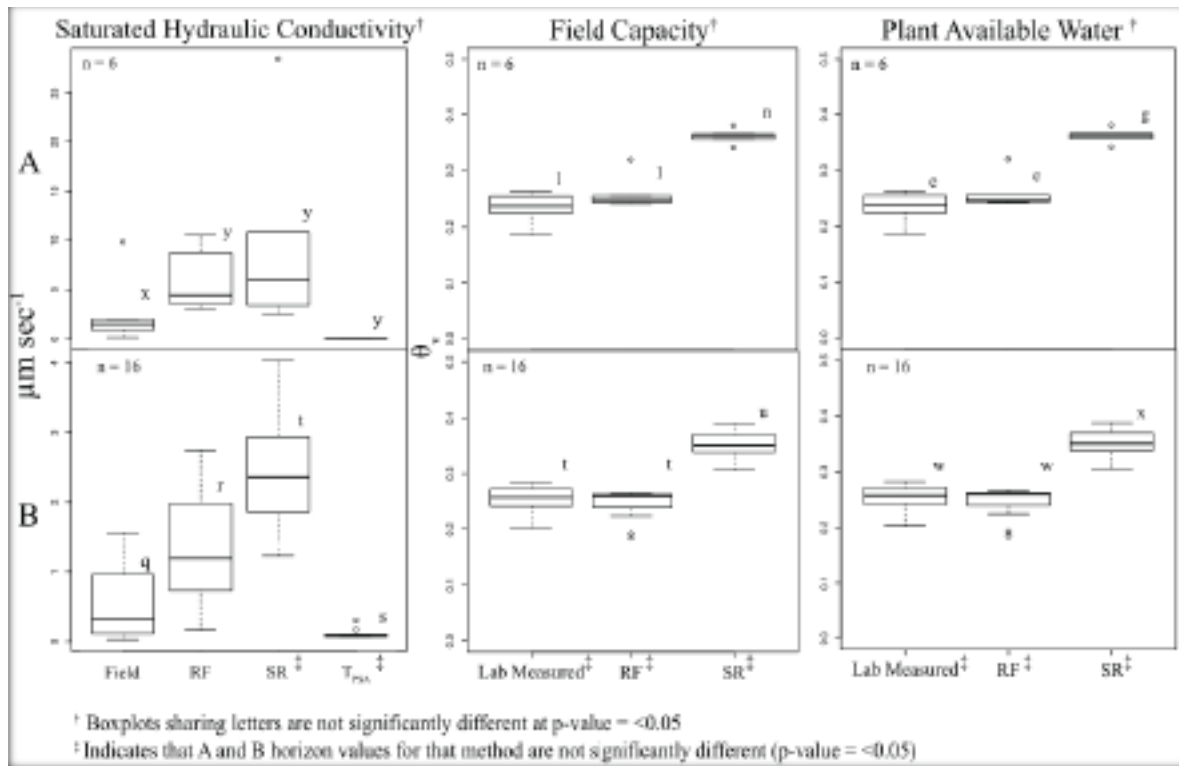


Figure 5. Comparison of hydrologic-property estimates to field-measured Ksat and laboratory-measured water contents.

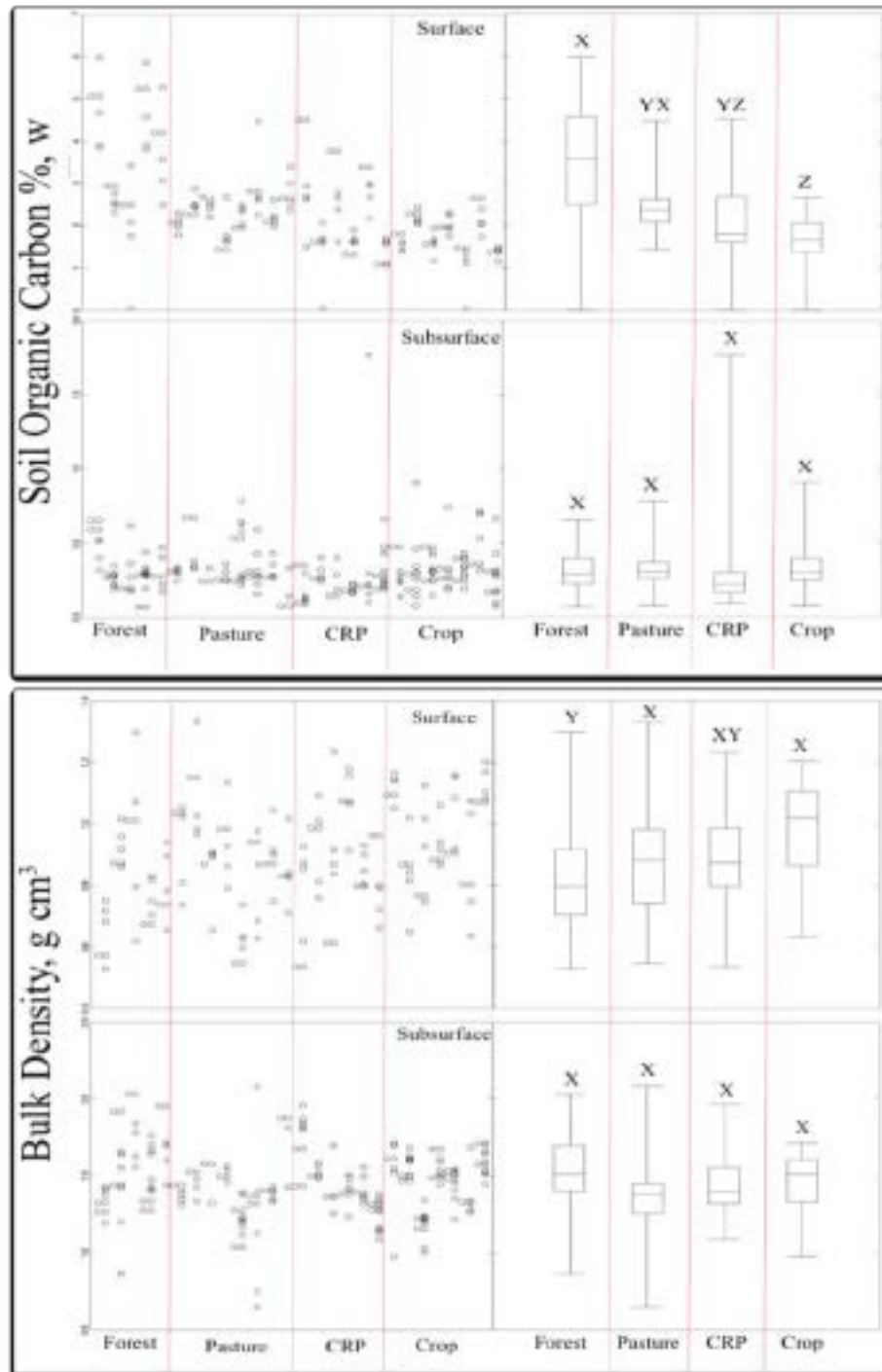


Figure 6. Physical Data for RaCA pedons - Soil organic Carbon (C) and Bulk Density (pd) are two physical properties used for estimation of hydrologic soil properties. A comparison of A- and B-horizon values among the four land-management approaches (Forest A n=25, B n=30; Pasture A n=40, B n=36; CRP A n=30, B n=36; Crop A n=35, B n=54) indicated that these properties only differed for the A horizon (Wilcoxon Rank Sum test). Consequently, only the A horizon was varied for the hydrologic model.

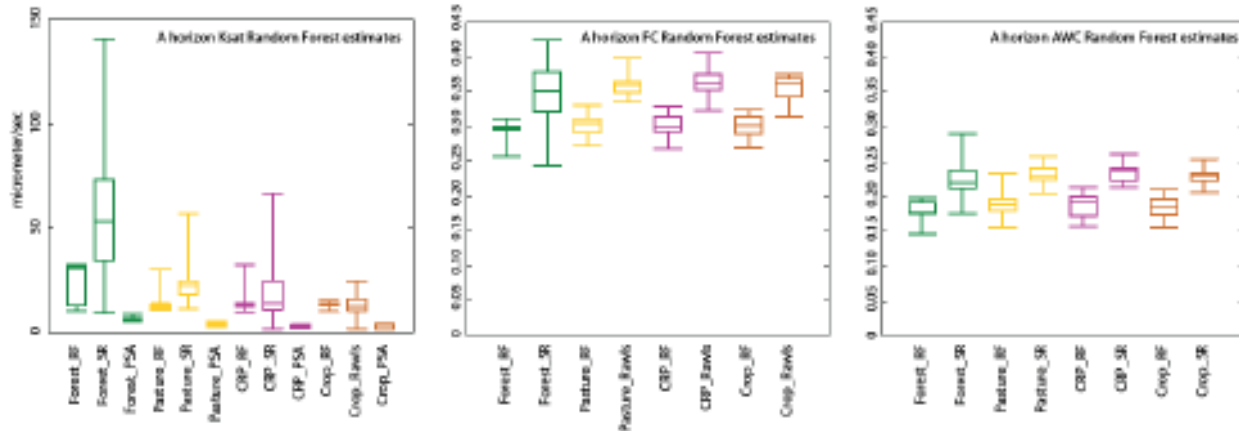


Figure. 7. Soil hydrologic properties estimates for RaCA A horizons. The same three pedotransfer methods were used to estimate (e) FCE, WPe, and Ksat for soils described under each of four land management types. In each case, there were significant differences among the estimations in all but one case (RF and SR Ksat for crop).

## Principal Findings and Significance

### SIMULATION OF STREAMFLOW AND SOIL WATER STORAGE

The median value for each land-management X hydrologic property combination was used to replace the A-horizon properties from the original field description of soils at the Kentucky grass watershed. These data were then used to simulate streamflow, actual evapotranspiration (AET), saturation deficit (empty pore space in 88.17 cm profile), and field-capacity deficit for a 0.045 km<sup>2</sup> basin previously described by Williamson and others (2014). Each simulation used the same temperature, precipitation, and PET time series, with hydrology simulated by TOPMODEL (Beven and Kirkby, 1979; Williamson and others 2014). A-horizon soil hydrologic properties were the only thing changed:

- The upper 15.7 cm were replaced with median values from the different RaCA land-management datasets, including Porosity (from pd measurements), FCE, AWCE, & Ksat.
- The remainder of the soil was left as originally described to 88.17 cm depth.

A new depth-weighted average was calculated for each soil property and used to calculate two TOPMODEL parameters that are derived from soils data - the conductivity multiplier and the scaling parameter. TOPMODEL was used as calibrated for original work.

Preliminary results reported here are 12-yr monthly averages for 2002-2013 and focus on spring and summer (April - October). The substitution of hydrologic property estimates for original field data resulted in a change in both streamflow and AET (compare black and gray bars in figure 8). AET is simulated by the model based on a combination of PET and plant available water. The differences in AET among these simulations is almost negligible, suggesting that the amount soil water available for plant use is adequate, regardless of land management. However, when the average monthly saturation deficit is compared (graphs on right in figure 8), differences related to land-management become more evident, with 50-100 mm more soil-water



stored under forested land relative to crop, pasture, and CRP. When only the pore space below field capacity is considered, the difference in soil-water storage shows the same pattern, with pasture and CRP soils having the largest deficit.

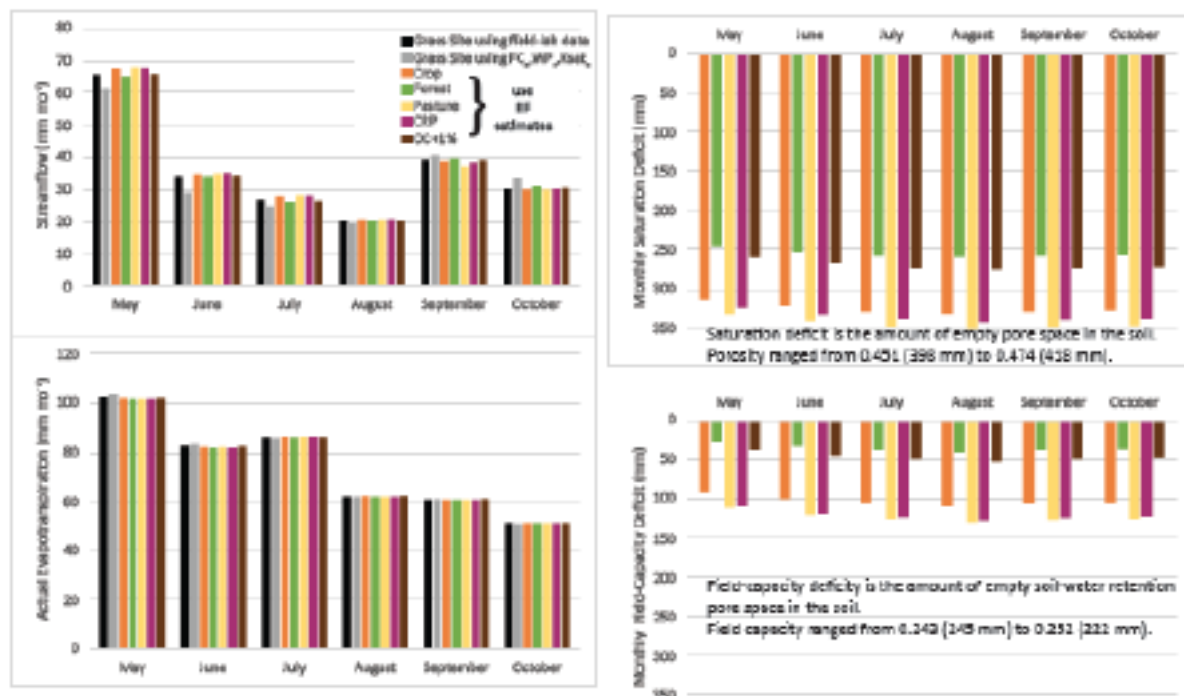


Figure. 8. Water Budget Components Simulated basin hydrology under different land covers.

## POTENTIAL EFFECTS OF SOIL-HEALTH MANAGEMENT

In order to simulate the potential effects of soil-health management, 1% C was added to that for the crop samples and new hydrologic soil properties calculated;  $\rho_d$  was not altered. Similar to the comparison of the four land-management types, there was minimal difference in streamflow or AET. However, this addition of 1% C resulted in soil-water storage that was more similar to that under forest than the original crop simulations. These results suggest that incorporation of additional soil carbon may make agricultural production more resilient to the increase in PET projected for the coming century (figures 9-11), when PET is estimated to increase by as much as 15 mm mo<sup>-1</sup> during the spring and summer. These soil-carbon additions might be from cover crops or conservation tillage.

## PROJECTED CLIMATE CHANGE

Monthly data from 21 global climate models (or general circulation models; GCMs) were downloaded from the Coupled Model Intercomparison Project (CMIP-5). Twenty-five year records for historical and mid-century, centered on 1995 and 2050, temperature (CMIP5 variable tas), precipitation (pr), as well as long (hfls) and short-wave (hfss) radiation, were aggregated and used to calculate normalized, monthly change-factors for temperature (T), precipitation (PPT), and potential evapotranspiration (PET) using a Priestley- Taylor (1972) change factor (Williamson and others, 2016).

Figure 9. An overall increase in mean daily temperature is projected for the site, with a mean annual change of  $+2.5^{\circ}\text{C}$  and a monthly range of  $+2.2^{\circ}\text{C}$  in March and  $+3.0^{\circ}\text{C}$  in September; mean annual Thist =  $13.6^{\circ}\text{C}$ .

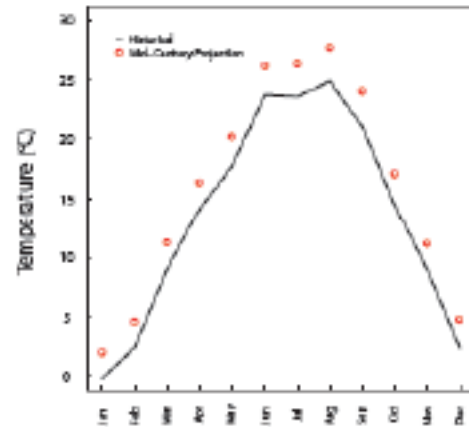


Figure 10. Similar to other areas of the country, precipitation is projected to increase in some months and decrease in others. The projected change is  $+76.2 \text{ mm yr}^{-1}$  relative to annual PPT<sub>hist</sub> =  $1312 \text{ mm yr}^{-1}$ , but is generally lower during the summer months.

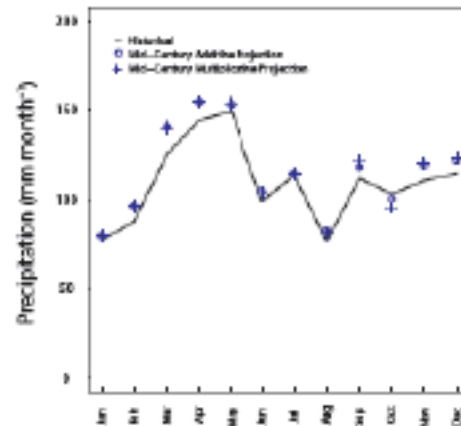
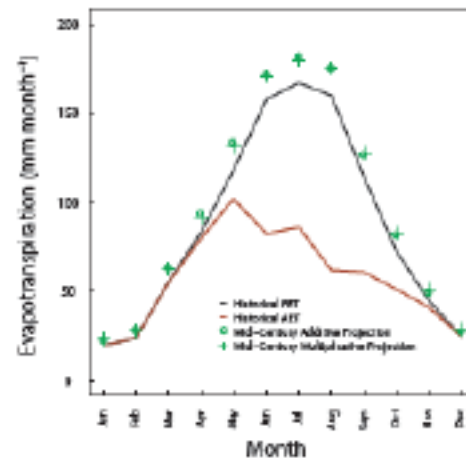


Figure 11. An overall increase in PET is projected, with an annual increase of  $112 \text{ mm yr}^{-1}$  relative to annual PET<sub>hist</sub> =  $1042 \text{ mm yr}^{-1}$ . This change reaches  $+15.2 \text{ mm}$  in May, when AET historically becomes water limited.



## References

- Beven KJ, Kirkby MJ (1979) A physically based, variable contributing area model of basin hydrology. *Hydrological Sciences Bulletin* 24:43-69 doi:10.1080/02626667909491834
- Breiman L, Cutler A, Liaw A, Wiener M (2015) random Forest - Breiman and Cutler's Random Forests for Classification and Regression, 4.6-12 edn. R-cran.
- Hamon WR (1963). Estimating Potential Evapotranspiration. *Trans. of the Am. Soc. of Civil Engineers* 128:324-337.
- Lu J, Sun G, McNulty SG, Amatya DM (2005). A comparison of six potential evapotranspiration methods for regional use in the southeastern United States. *JAWRA* 41:621-633. DOI: 10.1111/j.1752-1688.2005.tb03759.x.
- Priestley CHB, Taylor RJ (1972). On the Assessment of Surface Heat Flux and Evaporation Using Large-Scale Parameters. *Monthly Weather Review* 100:81-92. DOI: 10.1175/1520-0493(1972)100<0081:otaosh>2.3.co;2.
- Rawls, W., D. Brakensiek and N. Miller (1983). "Green-ampt Infiltration Parameters from Soils Data." *Journal of Hydraulic Engineering* 109(1): 62-70.
- Rawls, W. J., Y. A. Pachepsky, J. C. Ritchie, T. M. Sobecki and H. Bloodworth (2003). "Effect of soil organic carbon on soil water retention." *Geoderma* 116(1-2): 61-76.
- Saxton KE, Rawls WJ (2006) Soil Water Characteristic Estimates by Texture and Organic Matter for Hydrologic Solutions. *SSSAJ* 70:1569-1578 doi:10.2136/sssaj2005.0117
- Williamson TN, Lee BD, Schoeneberger PJ, McCauley WM, Indorante SJ, Owens PR (2014). Simulating Soil-Water Movement through Loess-Veneered Landscapes Using Nonconsilient Saturated Hydraulic Conductivity Measurements. *SSSAJ* 78:1320-1331. DOI: 10.2136/sssaj2014.01.0045.
- Williamson TN, Nystrom EA, Milly PCD (2016) Sensitivity of the projected hydroclimatic environment of the Delaware River basin to formulation of potential evapotranspiration *Clim. Ch.*:1-14 doi:10.1007/s10584-016-1782-2

# Temporal performance assessment of wastewater treatment plant by using multivariate statistical analysis

## Basic Information

<b>Title:</b>	Temporal performance assessment of wastewater treatment plant by using multivariate statistical analysis
<b>Project Number:</b>	2017KY264B
<b>Start Date:</b>	3/1/2017
<b>End Date:</b>	2/28/2018
<b>Funding Source:</b>	104B
<b>Congressional District:</b>	KY 4th
<b>Research Category:</b>	Water Quality
<b>Focus Categories:</b>	Wastewater, Water Quality, Nutrients
<b>Descriptors:</b>	None
<b>Principal Investigators:</b>	Tom Rockaway

## Publication

1. Rockaway, Thomas D. and Milad Ebrahimi, 2018, Temporal Performance Assessment of Wastewater Treatment Plants Using Multivariate Statistical Analysis in Proceedings of the 2018 Kentucky Water Resources Annual Symposium, Kentucky Water Resources Research Institute, University of Kentucky, Lexington, KY, p.7-8.

# **Temporal Performance Assessment of Wastewater Treatment Plants by Using Multivariate Statistical Analysis**

## **Problem and Research Objectives**

For wastewater treatment plants, many samples are obtained and tested to assess performance throughout the day. However, many of the analyzed samples may indicate conflicting results or trends whereby it is difficult to determine if the plant is performing as expected. The objective of this study is to create a framework where multiple variables are used to quantitatively assess the overall quality of wastewater treatment effluent with respect to intended applications. To develop the procedures, the study evaluated the performance of Floyds Fork Wastewater Treatment Plant in Louisville, KY and worked to address the following objectives.

- a. Identify the temporal characteristics of each monitored parameter
- b. Develop Wastewater Quality Index (WWQI) to quantitatively define wastewater quality
- c. Define the statistical interrelationships between different parameters and introduce a finite set of uncorrelated variables
- d. Develop multivariate statistical models to numerically express and forecast the significant quality parameters based on the measured historical process database

## **Methodology**

To comprehensively analyze the composition of wastewater and assess the treatment process performance, data from Louisville MSDs routine monitoring program were utilized. Collectively 9,180 samples were obtained from twelve quality and quantity variables between 2010 and 2016. The measured parameters include biochemical oxygen demand (BOD), total suspended solids (TSS), phosphorus (P), nitrogen (N), dissolved oxygen (DO), pH, mixed liquor volatile suspended solids (MLVSS) content in aeration tank, flow rate and the recycled activated sludge (RAS) rate.

Preliminary, descriptive statistics were used to identify the characteristics of each measured parameter in terms of central tendency, dispersion, and distribution. Thereupon, temporal fluctuation of each monitored parameter was studied. Investigating an individual water quality parameter's fluctuations can provide basic information. However, it is difficult to utilize a single parameter or one set of parameters to appropriately characterize the waste stream and comprehensively assess the treatment system efficiency. To overcome this challenging issues, two approaches were implemented:

- a. The Wastewater Quality Index (WWQI) was introduced to efficiently summarize the numerous monitored parameters into a single unit-less number
- b. Multivariate statistical analyses and exploratory data analyses were applied to provide a comprehensive methodology to temporally assess wastewater characteristics as well as process performance. The technique incorporated:
  - i. Principal component analyses (PCA): to investigate the interrelationships between a large group of variables, and to convert a large number of original correlated variables into a finite set of uncorrelated components.

- ii. Statistical modeling: to develop models that can predict important quality parameters based on input conditions. The modeling approach was carried out by combining three statistical methods including correlation, multivariate regression, and ANOVA analyses.

## Principal Findings and Significance

Descriptive Statistical Analysis: Performing the descriptive statistical analysis on 9200 measured quality and quantity samples for 2010 to 2016 discovered interesting understandings for the wastewater load and the treatment effectiveness, see Table 1 and Fig. 1.

**Table 1. Descriptive Statistics of the Influent (i) and Effluent (e) Parameters**

Variable	Unit	Discharge limit	Mean	Median	Standard error	Standard deviation	Variance	Kurtosis	Skewness	Range	Min	Max
Flow Rate	MGD		2.9	2.8	0.1	0.7	0.5	0.2	0.7	3.0	1.7	4.7
P <sub>i</sub>	mg/L		5.6	5.6	0.2	1.4	2.1	0.9	0.6	7.8	2.3	10.0
BOD <sub>i</sub>	mg/L		177.2	161.2	9.5	71.9	5174.5	5.1	1.6	447.7	40.2	487.9
TSS <sub>i</sub>	mg/L		361.2	351.8	15.4	115.9	13441.5	-0.3	-0.1	494.7	89.8	584.5
N <sub>i</sub>	mg/L		18.3	16.9	0.6	4.5	19.9	5.3	1.5	28.5	9.3	37.8
pH <sub>i</sub>	-		7.4	7.3	0.0	0.2	0.1	0.8	0.8	1.0	7.0	8.0
DO <sub>i</sub>	mg/L		4.2	4.1	0.1	1.0	1.1	0.0	0.2	5.2	1.6	6.7
P <sub>e</sub>	mg/L	0.5	0.3	0.3	0.0	0.1	0.0	-0.3	0.3	0.7	0.1	0.7
BOD <sub>e</sub>	mg/L	6	2.3	2.0	0.1	0.6	0.4	3.1	2.0	2.3	2.0	4.3
TSS <sub>e</sub>	mg/L	30	2.3	2.1	0.1	0.6	0.4	3.6	1.6	3.5	1.3	4.7
N <sub>e</sub>	mg/L	3	0.5	0.4	0.1	0.5	0.2	2.9	1.7	2.0	0.1	2.0
pH <sub>e</sub>	-	7-9	7.9	7.9	0.0	0.2	0.0	1.9	-0.3	1.2	7.2	8.4
DO <sub>e</sub>	mg/L	7	9.2	9.0	0.1	1.0	0.9	-0.6	0.7	3.4	8.0	11.3
MLVSS	mg/L		2050.1	1989.1	32.8	247.5	61271.2	0.5	0.9	1040.3	1661.0	2701.3
RAS	MGD		1.2	1.1	0.1	0.4	0.1	-0.4	0.5	1.6	0.6	2.2

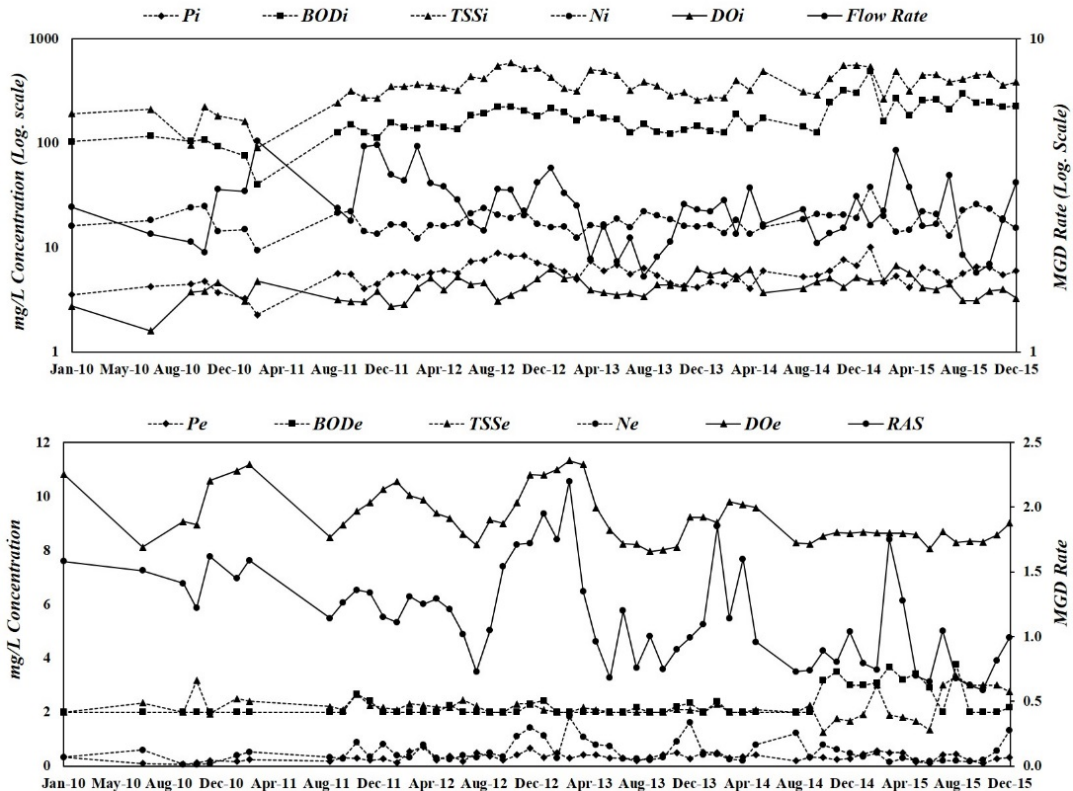


**Fig. 1. Temporal variation of influent (top) and effluent (bottom) parameters**

Evaluation of the above-mentioned Fig. and Table revealed that:

- Trends for influent BOD, TSS, N and P concentrations moved similarly for the entire period of study
- While, DO concentration moved in the opposite direction for similar period
- It can be inferred that while the availability of free oxygen within the influent load increased, contaminants level of incoming wastewater dropped
- This process was identified to be directly related to variation of inflow rate
- As a result: As inflow rate increased, availability of dissolved oxygen improved, and pollutants concentration decreased
- Regarding the treatment effectiveness: Variation of RAS affects effluent TSS and BOD concentrations
- Increase of RAS caused a raise of effluent TSS and decrease of effluent BOD for the entire period of study
- As a result, it can be inferred that availability of active microorganisms throughout the system significantly affects process performance

Analyzing monitoring program data comprised a complex matrix of physicochemical parameters which individually could not provide reliable temporal evaluation. Thus, Wastewater Quality Index was developed to summarize large amounts of monitored parameters into a simple term.

**Wastewater Quality Index:** To quantify the overall plant performance, the Wastewater Quality Index (WWQI) was developed. The WWQI for the Floyds Fork Water Treatment Plant was calculated based on the number, frequency, and amount of variables whose objectives were not met. Thus, based on the measured parameters and established water quality standards, the quality of influent and effluent wastewater was ranked from zero to 100. The higher values tend to indicate wastewater effluents are meeting design objectives and the plant is operating efficiently. For the Floyds Fork analysis, the WWQI was calculated based on the DO, BOD, TSS, N, P, and pH concentrations of the incoming and outgoing wastewater and the results are presented in Table 2 and Fig. 2. As a result, it was concluded that:

- Influent WWQI changed between 45 and 60, which indicated Water quality would be threatening to a receiving water
- Effluent WWQI changed between 96 and 100 which indicated Stream could be released to receiving waters with little threat of impairment
- Finally, it was concluded that treatment process improved wastewater quality by more than 51 percent

**Table 2. Wastewater Quality Category based on CCME WWQI.**

Quality range	WWQI	Water category
Excellent	95–100	Very close to natural or pristine levels
Good	80–94	Rarely depart from natural or desirable levels
Fair	65–79	Sometimes depart from natural or desirable levels
Marginal	45–64	Often depart from natural or desirable levels
Poor	0–44	Quality is almost always threatened or impaired

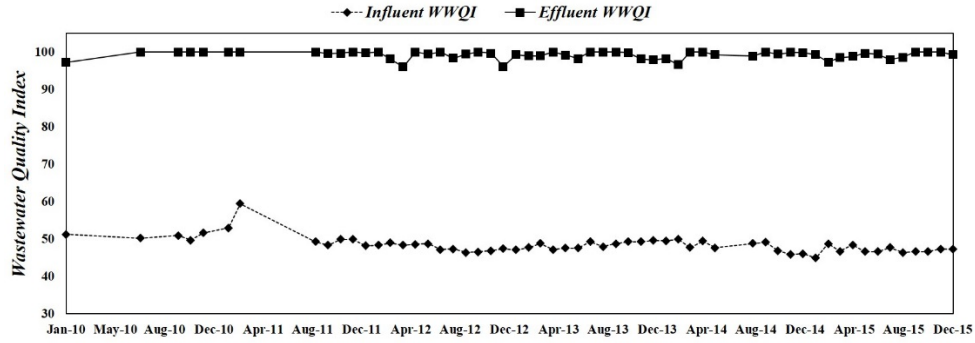


**Fig. 2. Influent and effluent WWQI variation**

To more comprehensively describe the overall characteristics of influent and effluent wastewater, the Principal Component Analysis (PCA) was applied.

**Principal Component Analysis:** Principal Component Analysis (PCA) is a technique to convert a large number of original variables into a set of uncorrelated components. Derived components represented information of the whole dataset with minimal loss of original information. For the Floyds Fork, the PCA was conducted and five components were extracted from fifteen parameters, see Table 3 and Fig. 3. The derived components include:

- PC1 which represented the Influent organic load
- PC2 which represented the Flow and Recycled rates
- PC3 which represented the Ion activity
- PC4 which represented the Effluent oxygen demand
- PC5 which represented the Nutrient removal efficiency

**Table 3. PCA's Rotated Component Matrix**

Attribute	Principal Component				
	PC1	PC2	PC3	PC4	PC5
Flow Rate		0.54			
P <sub>i</sub>	0.90				
BOD <sub>i</sub>	0.89				
TSS <sub>i</sub>	0.84				
N <sub>i</sub>	0.68				
pH <sub>i</sub>			0.91		
DO <sub>i</sub>	-0.63				
P <sub>e</sub>					0.61
BOD <sub>e</sub>				0.69	
TSS <sub>e</sub>					0.88
N <sub>e</sub>					0.61
pH <sub>e</sub>			0.88		
DO <sub>e</sub>				-0.84	
MLVSS		0.66			
RAS		0.78			
Eigenvalue	4.12	2.86	1.86	1.43	1.02
Initial Variance	27.45	19.08	12.40	9.51	6.80
Cumulative Variance	27.45	46.53	58.93	68.44	75.25



a. Rotation converged in 13 iterations

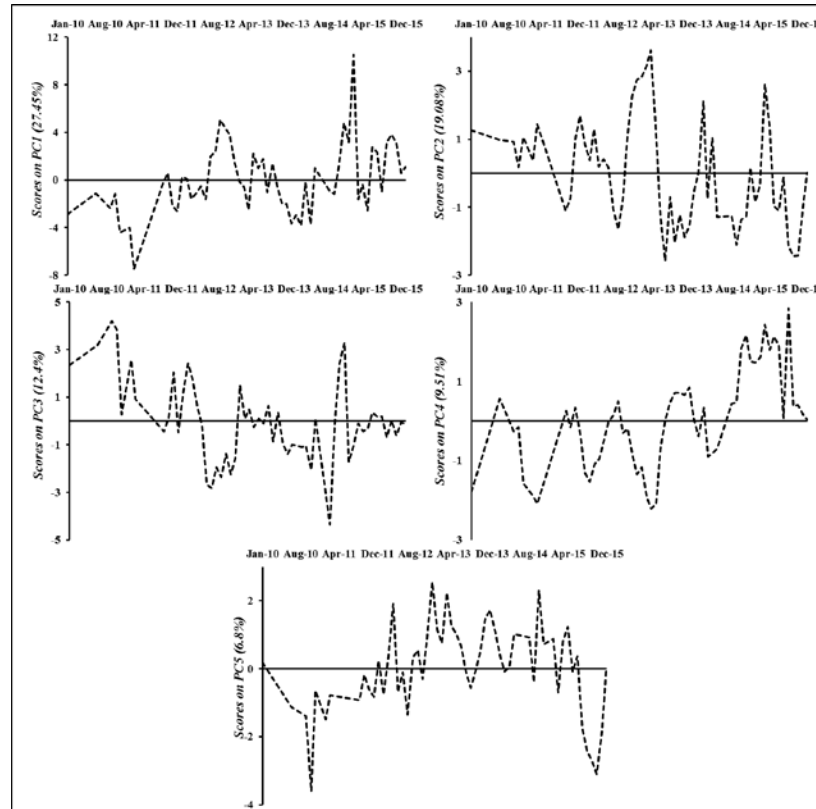


**Fig. 3. Temporal Variation of the Principal Components Scores**

Investigating the fluctuation of derived components within the study period indicated that:

- Positive scores for PC1 were observed for samples with negative scores on PC2 that means: More polluted incoming wastewater during seasons with lower flow rates
- Peak PC1 positive scores observed from 2013 that means: Overall increase of influent pollutant level from 2013
- PC5 fluctuations were considerably higher that means: Non-uniform nutrient removal performance over the study period
- Combined consideration of PC1 and PC5 indicated that more polluted influent led to less nutrient removal performance of the system
- Overall positive scores for PC4 for recent years indicated Less oxygen content and high oxygen demand of effluent wastewater

**Multivariate Statistical Modeling:** To provide a comprehensive data-basis for future studies on simulation and optimization, the multivariate statistical modeling was applied. As a result, six numerical forecasting models were developed for influent and effluent phosphorus, BOD, and WWQI, considering training dataset of 2010 - 2015 and validating dataset of 2016. The model preparation involved three steps including:

Step 1: Pearson product moment correlation analysis:

- Identifying predictor variables for each model
- Variables with correlation significance level of 0.01 were considered as predictors

Step 2: Stepwise Multivariate Regression Analysis:

- Multiple complex-terms of predictors and their interactions were considered
- Stepwise backward model generation were used with threshold p-value of 0.05
- Least statistically significant predictors with largest p-value were iteratively removed in each step

Step 3: ANOVA Test:

- To confirm and detect the optimum model from various developed models for each target parameter
- Admit/reject the null hypothesis of the  $p\text{-values} < \alpha = 0.05$

All six derived numerical expressions for the selected parameters were studied for quality identification see Table 4. Accuracy of developed models was evaluated in term of fitting with the training data for 2010 and 2015. Then, the predictive capability of each model was validated based on the results from the data monitoring program for 2016. The approach consisted of comparing the predicted values versus the measured values for training and testing datasets see Figs. 4 and 5.

**Table 4. Statistical Predictive Models for the Wastewater Quality Parameters**

Numerical Expression	R <sup>2</sup> %	RMSE		% Rel. error	
	Train data	Train data	Test data	Train data	Test data
<i>Influent Phosphorus Model</i> $= 2.71 + 8.5 \times 10^{-6} TSS_i^2$ $+ 3.9 \times 10^{-4} N_i \times TSS_i$ $- 1.4 \times 10^{-5} BOD_i \times TSS_i$	87	0.52	1.79	0.89	2.88
<i>Influent BOD Model</i> $= 126.95 + 45.93 P_i - 20.9 N_i$ $+ 0.42 N_i^2 + 0.001 TSS_i^2$ $- 0.16 P_i \times TSS_i + 0.03 N_i \times TSS_i$	83	29.26	85.36	1.53	3.21
<i>Influent WWQI Model</i> $= 68.84 - 0.057 TSS_i - 0.814 N_i$ $+ 4.5 \times 10^{-5} BOD_i^2 + 3.5 \times 10^{-5} TSS_i^2$ $+ 0.011 N_i^2 - 0.001 BOD_i \times N_i$ $+ 0.002 N_i \times TSS_i - 0.002 P_i \times BOD_i$	97	0.34	1.56	0.07	0.33
<i>Effluent Phosphorus Model</i> $= 1.274 - 2.2 RAS + 2.3 \times 10^{-5} BOD_i^2$ $- 4.3 \times 10^{-5} BOD_i \times TSS_i - 0.134 DO_i^2$ $- 1.09 RAS^2 + 0.004 BOD_i \times DO_i$ $+ 0.002 TSS_i \times RAS$ $+ 8.2 \times 10^{-8} BOD_i^3 \times RAS^2$ $+ 4.5 \times 10^{-11} TSS_i^4 + 0.006 DO_i^4$ $+ 0.085 RAS^4$ $- 2.4 \times 10^{-6} BOD_i^2 \times DO_i^2$ $+ 4.3 \times 10^{-6} TSS_i^2 \times RAS^2$ $- 3.6 \times 10^{-11} TSS_i^4 \times RAS$ $+ 3.5 \times 10^{-9} BOD_i^2 \times DO_i^5$ $- 9 \times 10^{-5} DO_i^6 - 0.004 BOD_i \times RAS^3$	71	0.32	0.27	9.01	8.34
<i>Effluent BOD Model</i> $= -0.174 + 0.023 TSS_i$ $+ 1.3 \times 10^{-4} BOD_i^2$ $- 2 \times 10^{-4} BOD_i \times TSS_i$ $+ 6.8 \times 10^{-10} BOD_i^2 \times TSS_i^2$ $- 1.3 \times 10^{-15} BOD_i^3 \times TSS_i^3$ $+ 0.015 DO_i^3 + 6.2 \times 10^{-6} TSS_i^2 \times RAS$ $+ 2.1 \times 10^{-6} BOD_i^2 \times DO_i^2$ $- 3.5 \times 10^{-4} DO_i^2 \times TSS_i$ $+ 1.7 \times 10^{-8} BOD_i^2 \times DO_i^5$ $- 2.7 \times 10^{-10} BOD_i^3 \times DO_i^4$ $- 5.6 \times 10^{-5} DO_i^6$ $- 3.7 \times 10^{-10} BOD_i^4 \times RAS^2$	82	0.21	0.86	0.88	2.84
<i>Effluent WWQI Model</i> $= 99.7 + 9 P_e - 3.16 N_e - 13.25 P_e^2$ $- 2.1 P_e \times TSS_e + 1.23 N_e \times TSS_e$	71	0.55	0.46	0.06	0.05

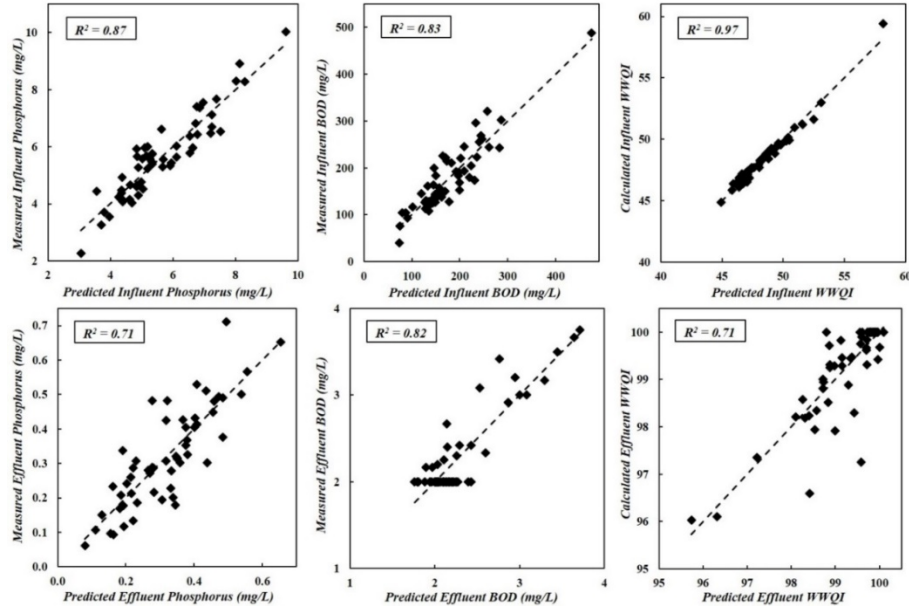


**Fig. 4. Verification of Predictive Models with Training Dataset (2010 – 2015)**

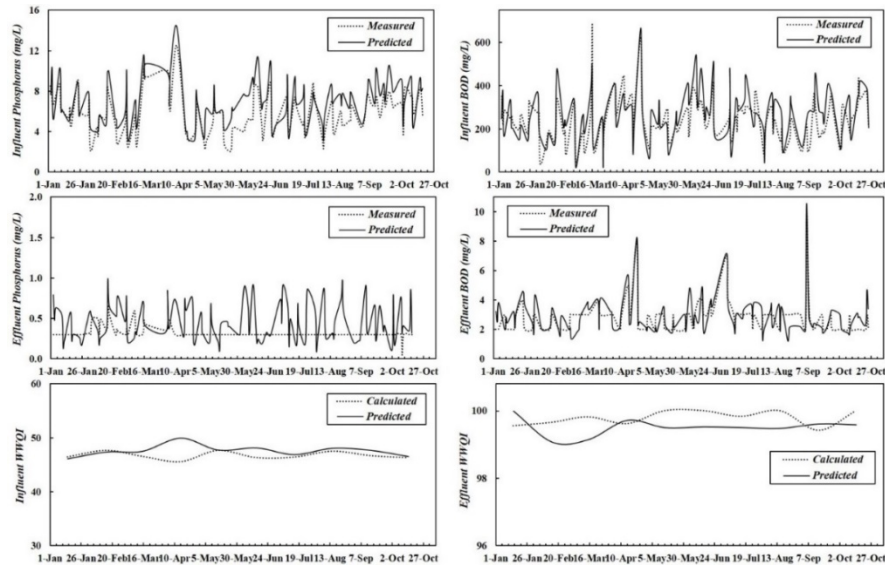


**Fig. 5. Validation of the Predictive Models with Testing Dataset (2016)**

The results confirmed strong accuracy, ranging from 71% to 97%, of the developed models in term of fitting with the training dataset. Also, all models showed minimum relative prediction errors for the training and testing dataset.

## Conclusion

The methods described in this research can be used to effectively manage water quality monitoring programs while reducing the number of quality parameters which must be routinely measured and also controlling the quality of sampling efforts and measurements. The proposed procedure can be summarized in the following steps:

- Calculate WWQI for influent and effluent streams
- Categorize flow conditions over the time
- Evaluate systems effectiveness by comparing influent and effluent indexes
- Conduct the PCA for historical dataset
- Evaluate temporal variation of influent and effluent organic loading, ion activities, oxygen demanding, and nutrient loading
- Determine interrelationship level between measured data using Correlation Analysis
- Identify the most highly correlated variables with target parameter
- Develop predictive models for target parameters
- Verify accuracy of models in terms of fitting with training and testing data

## References

Aguado, D., and Rosen, C. (2008). "Multivariate statistical monitoring of continuous wastewater treatment plants." *Engineering Applications of Artificial Intelligence*, 21(7), 1080-1091.

Alberto, W. D., del Pilar, D. a. M. a., Valeria, A. M. a., Fabiana, P. S., Cecilia, H. A., and de los Ángeles, B. M. a. (2001). "Pattern Recognition Techniques for the Evaluation of Spatial and Temporal Variations in Water Quality. A Case Study:: Suquia River Basin (Córdoba–Argentina)." *Water research*, 35(12), 2881-2894.

Apha, A. (2012). "WEF.(2012)." *Standard methods for the examination of water and wastewater*, 22.

Asadi, S., Vuppala, P., and Reddy, M. A. (2007). "Remote sensing and GIS techniques for evaluation of groundwater quality in municipal corporation of Hyderabad (Zone-V), India." *International journal of environmental research and public health*, 4(1), 45-52.

Avella, A., Görner, T., Yvon, J., Chappe, P., Guinot-Thomas, P., and de Donato, P. (2011). "A combined approach for a better understanding of wastewater treatment plants operation: Statistical analysis of monitoring database and sludge physico-chemical characterization." *Water research*, 45(3), 981-992.

Bayo, J., and López-Castellanos, J. (2016). "Principal factor and hierarchical cluster analyses for the performance assessment of an urban wastewater treatment plant in the Southeast of Spain." *Chemosphere*, 155, 152-162.

Bharti, N., and Katyal, D. (2011). "Water quality indices used for surface water vulnerability assessment." *International Journal of Environmental Sciences*, 2(1), 154.

Bordalo, A. A., Teixeira, R., and Wiebe, W. J. (2006). "A water quality index applied to an international shared river basin: the case of the Douro River." *Environmental management*, 38(6), 910-920.

Boyacioglu, H. (2007). "Development of a water quality index based on a European classification scheme." *Water Sa*, 33(1).

Bryant, C. W. (1995). "A simple method for analysis of the performance of aerated wastewater lagoons." *Water Science and Technology*, 31(12), 211-218.

CCME (2001). "Canadian water quality guidelines for the protection of aquatic life: CCME Water Quality Index." Canadian environmental quality guideline, Canadian Council of Ministers of the Environment, Winnipeg.

Chong, I.-G., and Jun, C.-H. (2005). "Performance of some variable selection methods when multicollinearity is present." *Chemometrics and Intelligent Laboratory Systems*, 78(1), 103-112.

Costa, J., Alves, M., and Ferreira, E. (2009). "Principal component analysis and quantitative image analysis to predict effects of toxics in anaerobic granular sludge." *Bioresource technology*, 100(3), 1180-1185.

De Rosemond, S., Duro, D. C., and Dubé, M. (2009). "Comparative analysis of regional water quality in Canada using the Water Quality Index." *Environmental monitoring and assessment*, 156(1-4), 223-240.

Durmusoglu, E., and Yilmaz, C. (2006). "Evaluation and temporal variation of raw and pre-treated leachate quality from an active solid waste landfill." *Water, Air, & Soil Pollution*, 171(1-4), 359-382.

Ebrahimi, M., Kazemi, H., Mirbagheri, S., and Rockaway, T. D. (2016). "An optimized biological approach for treatment of petroleum refinery wastewater." *Journal of Environmental Chemical Engineering*, 4(3), 3401-3408.

Ebrahimi, M., Kazemi, H., Mirbagheri, S. A., & Rockaway, T. D. (2017). Integrated Approach to Treatment of High-Strength Organic Wastewater by Using Anaerobic Rotating Biological Contactor. *Journal of Environmental Engineering*, 144(2), 04017102.

Goode, C., LeRoy, J., and Allen, D. (2007). "Multivariate statistical analysis of a high rate biofilm process treating kraft mill bleach plant effluent." *Water Science and Technology*, 55(6), 47-55.

Hurley, T., Sadiq, R., and Mazumder, A. (2012). "Adaptation and evaluation of the Canadian Council of Ministers of the Environment Water Quality Index (CCME WQI) for use as an effective tool to characterize drinking source water quality." *water research*, 46(11), 3544-3552.

Khambete, A., and Christian, R. (2014). "Statistical analysis to identify the main parameters to effecting WWQI of sewage treatment plant and predicting BOD." *Int. J. Research in Engineering and Technology (IJRET)*, 3(01), 186-195.

Khan, A. A., Paterson, R., and Khan, H. (2004). "Modification and Application of the Canadian Council of Ministers of the Environment Water Quality Index(CCME WQI) for the Communication of Drinking Water Quality Data in Newfoundland and Labrador." *Water Quality Research Journal of Canada*, 39(3), 285-293.

Kolluri, S. S., Esfahani, I. J., Garikiparthi, P. S. N., and Yoo, C. (2015). "Evaluation of multivariate statistical analyses for monitoring and prediction of processes in an seawater reverse osmosis desalination plant." *Korean Journal of Chemical Engineering*, 32(8), 1486-1497.

Lebart, L., Morineau, A., and F  nelon, J.-P. (1979). "Traitement des donn  es statistiques(m  thodes et programmes)."

Lee, D. S., Lee, M. W., Woo, S. H., Kim, Y.-J., and Park, J. M. (2006). "Multivariate online monitoring of a full-scale biological anaerobic filter process using kernel-based algorithms." *Industrial & engineering chemistry research*, 45(12), 4335-4344.

Lee, D. S., and Vanrolleghem, P. A. (2004). "Adaptive consensus principal component analysis for on-line batch process monitoring." *Environmental monitoring and assessment*, 92(1-3), 119-135.

Lefkir, A., Maachou, R., Bermad, A., and Khouider, A. (2015). "Factorization of physicochemical parameters of activated sludge process using the principal component analysis." *Desalination and Water Treatment*, 1-6.

Lumb, A., Halliwell, D., and Sharma, T. (2006). "Application of CCME Water Quality Index to monitor water quality: A case study of the Mackenzie River basin, Canada." *Environmental Monitoring and Assessment*, 113(1-3), 411-429.

Mackiewicz, A., and Ratajczak, W. (1993). "Principal components analysis (PCA)." *Computers and Geosciences*, 19, 303-342.

Mirbagheri, S. A., Ebrahimi, M., & Mohammadi, M. (2014). Optimization method for the treatment of Tehran petroleum refinery wastewater using activated sludge contact stabilization process. *Desalination and Water Treatment*, 52(1-3), 156-163.

Nagels, J., Davies-Colley, R., and Smith, D. (2001). "A water quality index for contact recreation in New Zealand." *Water Science and Technology*, 43(5), 285-292.

Ouali, A., Azri, C., Medhioub, K., and Ghrabi, A. (2009). "Descriptive and multivariable analysis of the physico-chemical and biological parameters of Sfax wastewater treatment plant." *Desalination*, 246(1), 496-505.

Ouyang, Y. (2005). "Evaluation of river water quality monitoring stations by principal component analysis." *Water research*, 39(12), 2621-2635.

Platikanov, S., Rodriguez-Mozaz, S., Huerta, B., Barceló, D., Cros, J., Batle, M., Poch, G., and Tauler, R. (2014). "Chemometrics quality assessment of wastewater treatment plant effluents using physicochemical parameters and UV absorption measurements." *Journal of environmental management*, 140, 33-44.

Rastogi, G. K., and Sinha, D. (2011). "A novel approach to water quality management through correlation study." *J. Environ. Res. Develop.*, 5 (4), 1029, 1035.

Reimann, C., Filzmoser, P., and Garrett, R. G. (2002). "Factor analysis applied to regional geochemical data: problems and possibilities." *Applied Geochemistry*, 17(3), 185-206.

Rosén, C., and Lennox, J. (2001). "Multivariate and multiscale monitoring of wastewater treatment operation." *Water research*, 35(14), 3402-3410.

Singh, K. P., Malik, A., Mohan, D., Sinha, S., and Singh, V. K. (2005). "Chemometric data analysis of pollutants in wastewater—a case study." *Analytica Chimica Acta*, 532(1), 15-25.

Sun, Y., Chen, Z., Wu, G., Wu, Q., Zhang, F., Niu, Z., and Hu, H.-Y. (2016). "Characteristics of water quality of municipal wastewater treatment plants in China: implications for resources utilization and management." *Journal of Cleaner Production*, 131, 1-9.

Tchobanoglous, G., and Burton, F. L. (1991). "Wastewater engineering." *Management*, 7, 1-4.

Timmerman, J. G., Beinart, E., Termeer, K., and Cofino, W. (2010). "Analyzing the data-rich-but-information-poor syndrome in Dutch water management in historical perspective." *Environmental management*, 45(5), 1231-1242.

Tomita, R. K., Park, S. W., and Sotomayor, O. A. (2002). "Analysis of activated sludge process using multivariate statistical tools—a PCA approach." *Chemical Engineering Journal*, 90(3), 283-290.

Wallace, J., Champagne, P., and Hall, G. (2016). "Multivariate statistical analysis of water chemistry conditions in three wastewater stabilization ponds with algae blooms and pH fluctuations." *Water research*, 96, 155-165.

Wanda, E. M., Mamba, B. B., and Msagati, T. A. (2015). "Determination of the water quality index ratings of water in the Mpumalanga and North West provinces, South Africa." *Physics and Chemistry of the Earth, Parts A/B/C*.



Zhang, Z., Tao, F., Du, J., Shi, P., Yu, D., Meng, Y., and Sun, Y. (2010). "Surface water quality and its control in a river with intensive human impacts—a case study of the Xiangjiang River, China." *Journal of environmental management*, 91(12), 2483-2490.

# The ecological importance of perched aquifers and their hydrological connectivity to ridge top ephemeral wetlands in Daniel Boone National Forest

## Basic Information

<b>Title:</b>	The ecological importance of perched aquifers and their hydrological connectivity to ridge top ephemeral wetlands in Daniel Boone National Forest
<b>Project Number:</b>	2017KY265B
<b>Start Date:</b>	3/1/2017
<b>End Date:</b>	2/28/2018
<b>Funding Source:</b>	104B
<b>Congressional District:</b>	KY 6th
<b>Research Category:</b>	Ground-water Flow and Transport
<b>Focus Categories:</b>	Ecology, Groundwater, Wetlands
<b>Descriptors:</b>	None
<b>Principal Investigators:</b>	Jonathan Malzone

## Publications

1. Stribling, Selsey, and Jonathan M. Malzone, 2018, Hydrogeological properties of natural and constructed wetlands in Kentucky's Daniel Boone National Forest, Poster Presentation at the Kentucky Water Resources Research Annual Symposium, Lexington, KY.
2. Sweet, Ethan, and Jonathan M. Malzone, 2018, The ecological importance of perched aquifers and their hydrological connectivity to ridgetop ephemeral wetlands in Daniel Boone National Forest, Poster Presentation at the Kentucky Water Resources Research Annual Symposium, Lexington, KY.
3. Malzone, Jonathan M., 2018, Geomorphic Controls of Groundwater Surface Water Interaction in Natural Ridge Top Vernal Pools. In Preparation. Anticipating submission to Ecohydrology in July 2018.
4. Malzone, Jonathan M. 2018, Comparing the hydrological function of natural and constructed ridgetop isolated wetlands in Proceedings of the 2018 Kentucky Water Resources Annual Symposium, Kentucky Water Resources Research Institute, Lexington, KY, p. 31.
5. Stribling, Selsey, and Jonathan M. Malzone, 2017, How does spatial heterogeneity influence groundwater flow on ridgetops in Kentucky's Daniel Boone National Forest? in Annual Meeting of Kentucky Academy of Science Meeting Abstracts Archive, Kentucky Academy of Science, Murray, KY.
6. Bell, Addison, and Jonathan M. Malzone, 2017, Modeling the groundwater storage and the groundwater recharge rate of an ephemeral wetland with Hydrus-1D, in Annual Meeting of Kentucky Academy of Science Meeting Abstracts Archive, Kentucky Academy of Science, Murray, KY.
7. Malzone, Jonathan M., 2017, Morphological Control of Seasonal and Sub-Seasonal Groundwater Flow in Geographically Isolated Wetlands, in Geological Society of America Abstracts with Programs, 49(6), Seattle, WA.

# **The Ecological Importance of Perched Aquifers and Their Hydrological Connectivity to Ridge Top Ephemeral Wetlands in Daniel Boone National Forest**

## **Problem and Research Objectives**

The overarching goal for this research is to quantify the ecological role of perched aquifers connected to ridge top ephemeral wetlands in the Daniel Boone National Forest, KY. The ecological role of perched aquifers includes sustaining water levels for aquatic life and supplying forest vegetation with a second source of water. Specific objectives included delineating the spatial/temporal extent of perched aquifers, quantifying the direction and magnitude of groundwater flow, and quantifying the evapotranspiration rates of groundwater. The overarching goal and specific objectives for this research have not changed at all and were successfully completed.

## **Methodology**

The research plan included:

- a. Constructing a well field of 30 wells at the DC2 wetland.
- b. Observing the water levels in each well over the cycle of aquifer recharge and depletion, 14 visits between March and October.
- c. Using GIS and surveying techniques to place the wells in a datum and create an aquifer map.
- d. Conducting slug tests to determine hydraulic conductivity.
- e. Use groundwater flow modeling to determine direction and magnitude of groundwater flow and recharge.
- f. Use a pressure transducer data of water level to determine evapotranspiration of groundwater.
- g. Compare flow rates and evapotranspiration to determine how much water local forest vegetation use and if groundwater flow drains or sustains surface water levels.

Aquifer Extent and Sustaining Water Levels: The extent of the perched aquifer was mapped by installing 30 groundwater wells and sampling them periodically between spring and fall of 2017. The hydraulic head of each well was calculated from a map made of the wetland surface using a total station (Figure 1). The aquifer surface was mapped using water level measurements and a spatial interpolation method in ArcGIS. The aquifer surface maps were then placed on the same scale and compared.

Water level measurements were also compiled into a groundwater flow model and a soil flow model. A groundwater flow model was set up in VisualAEM, an analytic element software method for solving Darcy's Law (Craig 2016). Boundary conditions of the model were defined by the known outflow and watershed boundaries. We used the calibration method to determine the groundwater recharge rate necessary to sustain the aquifer-pool complex in spring. Model calibration is a process that involves matching model output to actual data from a land surface map and field water level data. A soil water model was set up in HYDRUS-1D (Simunek et al. 2005) in order to determine how fast rainwater can infiltrate through the soil and recharge the

aquifer on the scale of minutes to days. This was a 1-dimensional model of a soil profile with inputs of precipitation and evapotranspiration. Precipitation data was gathered from a local weather station and the soil water evapotranspiration was estimated from a Penman-Monteith (Monteith 1965) model, which used weather station data available for the area (<http://kymesonet.org/>).

Supplying Forest Vegetation with a Second Source of Water: Evapotranspiration of groundwater (ET<sub>g</sub>) was calculated using the White method (White 1932) for 3 wells at the DC2 wetland. The White method involves measuring the daily cycle by which the water table is lowered during the daytime via plant transpiration and then recovers during the night when plants no longer transpire. Measurements of the daily drawdown and recovery cycle were used to calculate the total amount of water utilized by vegetation with roots tapping the aquifer (White 1932). The hourly measurements of water level needed to use this method were obtained via four Solinst water level. A transducer was located in wells A7, DC2-1, and AA (Figure 1). The fourth transducer measured the surface water level in DC2-C.

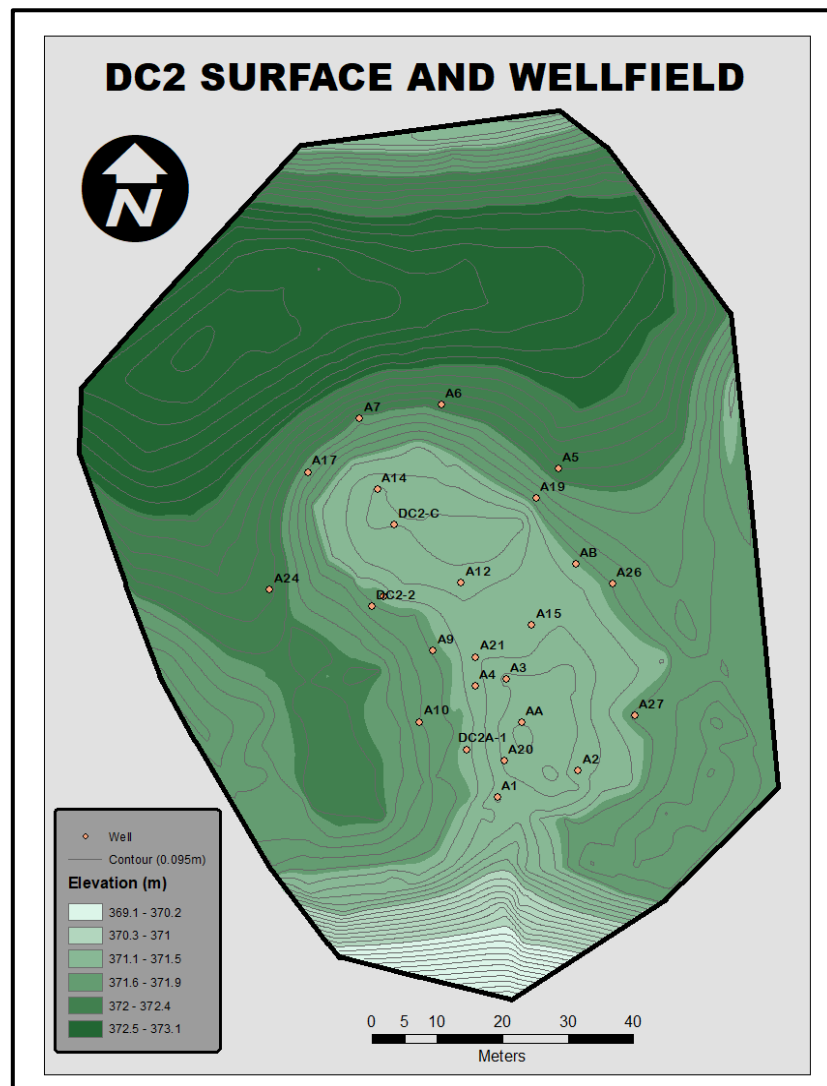


Figure 1: (Left) Final map of DC2 wetland with the well field marked as pink dots. (Above) Photo of student Ethan Sweet making the DC2 map with a total station.

## Principal Findings and Significance

Aquifer Extent and Sustaining Water Levels: The aquifer spatial extent was larger than expected. Previously it was thought that the wetland depression collected rainwater, which leaked into the subsurface. In this runoff-infiltration model of the wetlands, aquifers are thought to have water levels that fall off sharply away from the open water at the surface. Our results indicated that the spatial extent of the aquifer included almost the entire wetland watershed, 2500 m<sup>2</sup>, even as water levels were lowered into the dryer parts of the summer (Figure 2 and Figure 4).

The flow direction of the groundwater can also be interpreted from the aquifer surface maps. Our aquifer surface maps show that groundwater levels exceed the level of the surface water in the spring time (Figure 2). This means that a groundwater spring is created in the soil mounds surrounding the pool in the spring, which will sustain surface water levels in addition to runoff-infiltration. During late spring early summer the groundwater springs dry up and the wetland complex changes from a spring fed wetland to a runoff-infiltration wetland (Figure 2). This happens due to the increase in plant consumption of water as well as a decrease in rainfall.

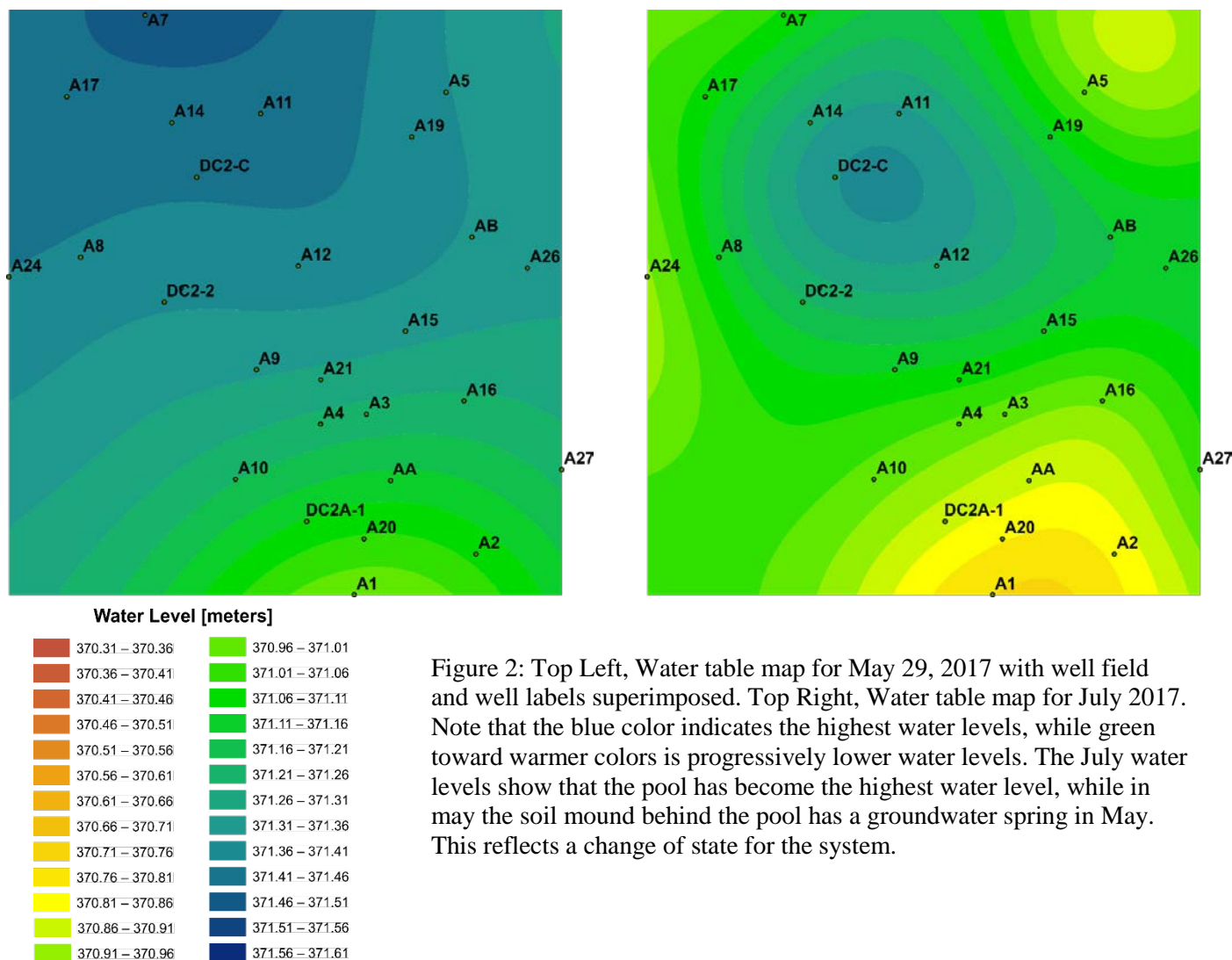


Figure 2: Top Left, Water table map for May 29, 2017 with well field and well labels superimposed. Top Right, Water table map for July 2017. Note that the blue color indicates the highest water levels, while green toward warmer colors is progressively lower water levels. The July water levels show that the pool has become the highest water level, while in May the soil mound behind the pool has a groundwater spring in May. This reflects a change of state for the system.

The final calibrated groundwater flow model indicated that spring groundwater recharge ranged between 0.001 and 0.0025 m/d. This is the groundwater recharge rate required to sustain the aquifer in spring. The groundwater flow model also shows the simulated water table surface for the entire wetland (Figure 3). The simulation shows that the wetland has groundwater flowing into and onto the other side of the open water (flow-through wetland).

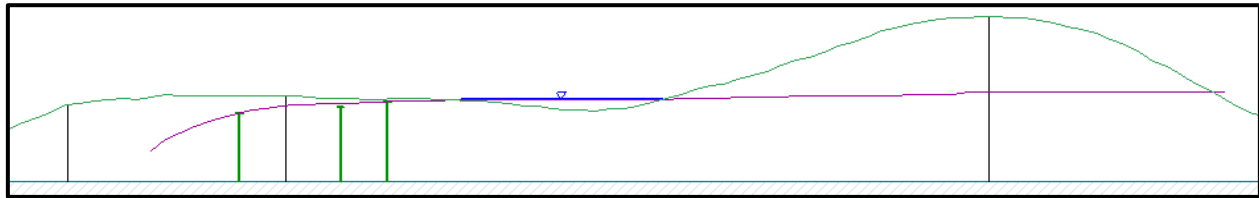


Figure 3: Final groundwater flow model of the DC2 wetland constructed in VisualAEM. This model produces a prediction of the water table surface based on boundary conditions set in the software. Conditions that must be set include known water levels in the wetlands, soil properties, and elevation. The blue surface is the wetland, the green surface is land elevation. The purple surface is the predicted water table surface, which can be fitted to our field measurement (green pegs). This simulation produced a 0.9  $R^2$  correlation with field data.

Supplying Forest Vegetation with a Second Source of Water: Between May 29 and June 12 the aquifer changes its state from a groundwater fed wetland to a runoff-infiltration type of wetland (Figure 2). The trigger for this change seems to be transpiration of groundwater by vegetation (ETg). The average water level of the wetland is stable for most of spring, but in the summer the average head drops 40cm in 13 days (Figure 4). This time also corresponds to when the first evapotranspiration signals appear in the water level sensors (Figure 5).

The evapotranspiration rate in the DC2 wetland is ~0.009 m/d, almost a full order of magnitude greater than the groundwater recharge rate (Figure 5). This value of evapotranspiration is not constant as it depends on temperature and the amount of sunlight, but all instances of measured ETg are higher than the maximum groundwater recharge rate. This means that the forest vegetation causes the wetland to change its hydrological function in the summer and controls the timing of when the wetland dries out.

The HYDRUS-1D model and water level sensor data show that groundwater recharge continues in the summer but it is more episodic. Rainfall between spring and summer changes patterns from longer slow rains to intense thunderstorms. Water levels rise rapidly during summer thunder showers and during this time the wetland and aquifer recover in as little as an hour. ETg by forest vegetation quickly consume this water in about 12 days. The HYDRUS model indicated that groundwater recharge during summer rain storms can exceed 0.003 m/d, essentially providing a mechanism by which the aquifers recover. Therefore, periods of high rainfall during the summer produce an extra water source for forest vegetation for ~12 days.

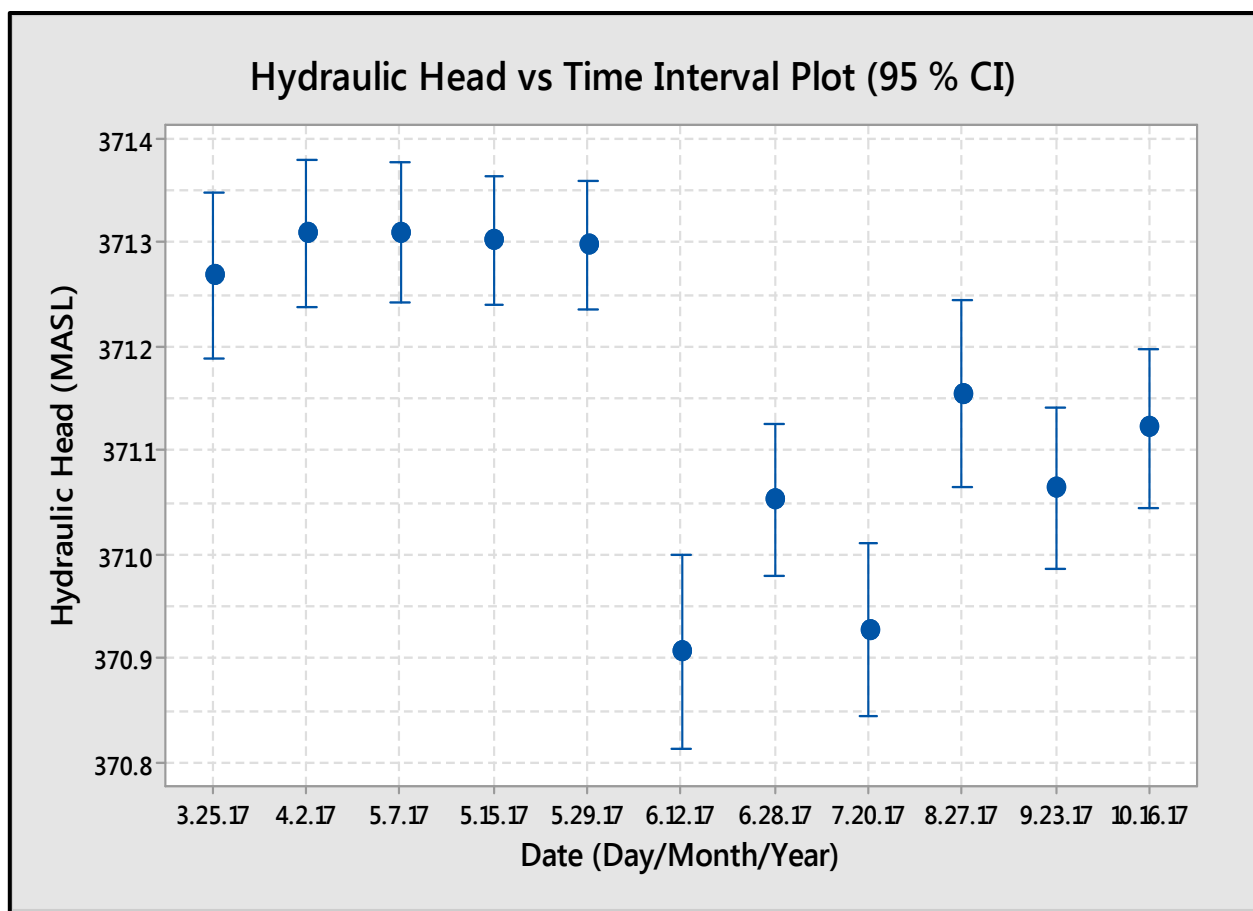


Figure 4: Plot of average water level for each day data was taken. Bars are 95% confidence intervals.

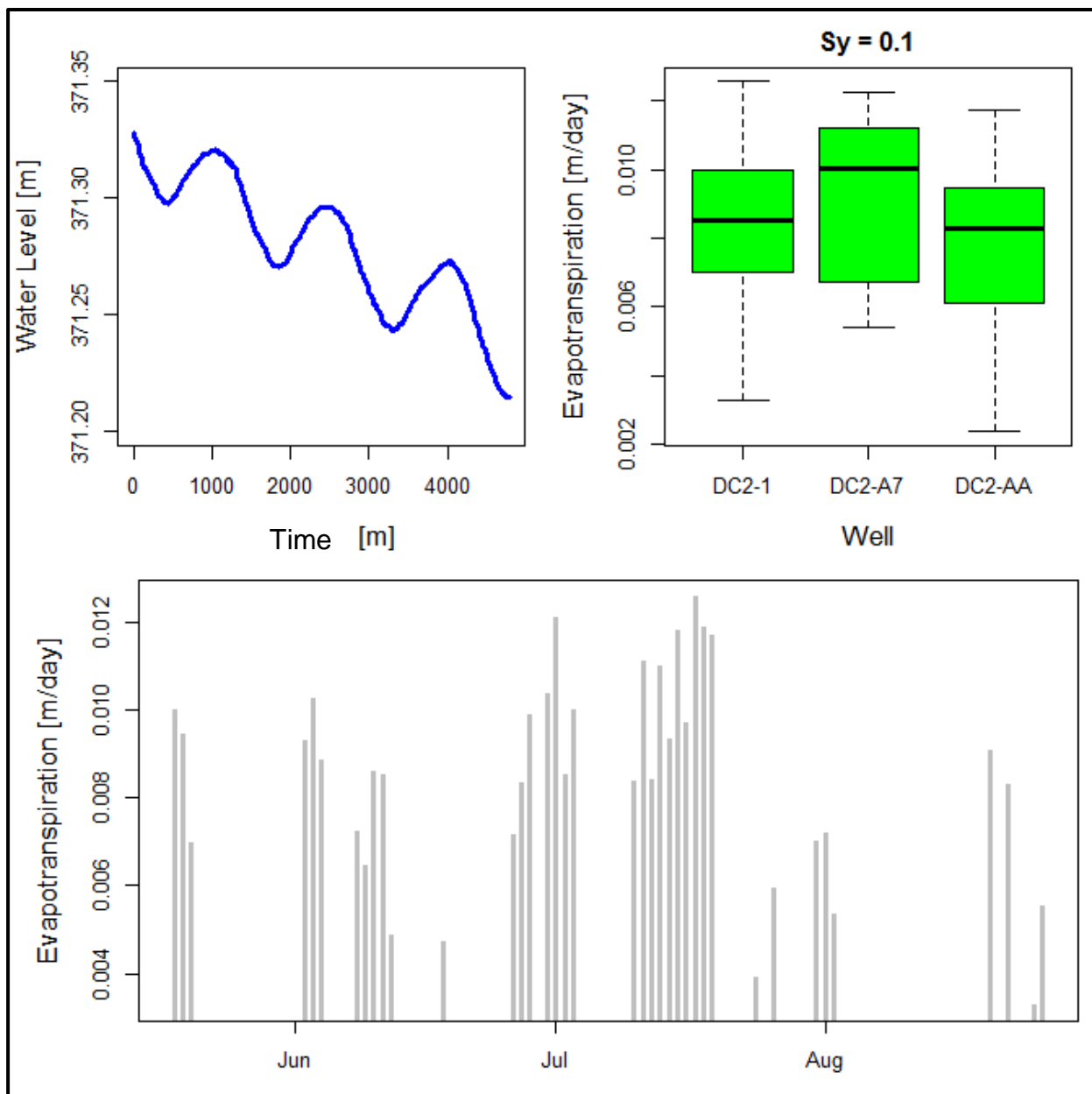


Figure 5: Top Left, raw hydrograph showing an evapotranspiration signal in the aquifer. Top Right, boxplots of ETg (evapotranspiration of groundwater) for the locations that had a water level sensor. Bottom, temporal plot of evapotranspiration. Sy is the specific yield. This is a parameter that is measured for the soil in order to calculate ETg.

The major conclusions from this work have shown that ridge top wetlands are associated with aquifers that control ecologically important variables such as surface water levels and forest vegetation water consumption. Specifically this research has shown a threshold relationship between groundwater recharge and evapotranspiration. In the winter and spring groundwater recharge is able to build up an extensive aquifer that creates a groundwater spring fed wetland. When spring rains end and trees consume groundwater to endure drought the system undergoes a change of state from a groundwater fed wetland to a runoff-infiltration wetland. This type of



wetland is maintained by heavy summer rainfalls, which produce smaller groundwater resources that vegetation use up in about 12 days if no further rainfall occurs. The aquifers are therefore providing the ecological benefits of surface water regulation (important for amphibian spawning) and drought resilience (extra water for vegetation).

Practically, this research has been important for improving wetland restoration and conservation practices for the United States Forest Service (USFS). All data from this research has been shared with the USFS in order to help create data driven management plans to conserve wetlands and to restore degraded systems. The role wetland hydrology may be playing in these remote wetlands systems was unquantified until this point and the occurrence and nature of the aquifers was unknown. For that reason restoration plans used a farm pond structure to restore wetlands, which involves packing impermeable clays in the wetland to hold water in a pond. Our research suggests that this practice will cut off ecological services and that wetlands need to be designed with groundwater resources in mind.

Scientifically, this research is important because it defines a threshold relationship between two types of wetland (groundwater fed and runoff-infiltration). The threshold for change between these two functional systems is not well understood and this study provides field data of the change. We hope to further develop this study in the future to determine the physical controls on which wetland type is manifested in different places. There are >500 ridge top wetlands in the Daniel Boone National Forest and all of them have been noted to dry out at different times. If this threshold behavior is better understood it may be possible to predict drought resilience of different systems or how the systems might change given extreme droughts.

## References

- Craig, J. R., 2018. VisualAEM software.  
<https://www.civil.uwaterloo.ca/jrcraig/visualaem/Downloads.html>
- Monteith, J.L., 1965. Evaporation and the environment. XIXth Symposia of the Society for Experimental Biology. In the State and Movement of Water in Living Organisms. University Press, Swansea, Cambridge, pp. 205–234
- Simunek, J., Van Genuchten, M. T., & Sejna, M. 2005. The HYDRUS-1D software package for simulating the one-dimensional movement of water, heat, and multiple solutes in variably-saturated media. *University of California-Riverside Research Reports*, 3, 1-240
- .White, W.N., 1932. A Method of Estimating Ground-water Supplies Based on Discharge by Plants and Evaporation from Soil: Results of Investigations in Escalante Valley, Utah. US Gov. Print. Off. 659.

# Application of pedotransfer function for estimating soil water permeability at field scale, western Kentucky: calibration and validation

## Basic Information

<b>Title:</b>	Application of pedotransfer function for estimating soil water permeability at field scale, western Kentucky: calibration and validation
<b>Project Number:</b>	2017KY266B
<b>Start Date:</b>	3/1/2017
<b>End Date:</b>	7/31/2018
<b>Funding Source:</b>	104B
<b>Congressional District:</b>	KY 1st
<b>Research Category:</b>	Ground-water Flow and Transport
<b>Focus Categories:</b>	Agriculture, Irrigation, Methods
<b>Descriptors:</b>	None
<b>Principal Investigators:</b>	Ole Wendroth

## Publications

1. Zhang, Xi, and Ole Wendroth, 2018, Spatial characterization of soil saturated and near-saturated hydraulic conductivity at the field scale, Poster Presentation at the 2018 Kentucky Water Resources Annual Symposium, Kentucky Water Resources Research Institute, Lexington, KY.
2. Zhang, Xi and Ole Wendroth, 2018, Spatial characterization of saturated hydraulic conductivity at the field scale with co-regionalization analysis. (In Preparation)
3. Zhang, Xi, Javier Reyes and Ole Wendroth, 2017, Field scale characterization of soil hydraulic conductivity and its implication for water movement in ASA, CSSA, SSSA Annual Meeting Abstracts, Tampa, FL.

# **Application of Pedo-transfer Functions for Estimating Soil Water Permeability at Field Scale, Western Kentucky: Calibration and Validation**

## **Problem and Research Objectives**

Saturated hydraulic conductivity ( $K_s$ ) is one of the pivotal parameters for assessing water transport in soil (Ghanbarian et al., 2017).  $K_s$  is also an essential input parameter for hydrological models and a matching point for the unsaturated hydraulic conductivity curve (Schaap and Leij, 2000). However,  $K_s$  is a heterogeneous parameter and exhibits high spatial variability (Nielsen et al., 1973). Due to the high spatial variability of  $K_s$ , soil water permeability varies and the need for irrigation differs between specific areas within the same field (Al-Karadsheh et al., 2002). Accurate characterization of the spatial pattern of  $K_s$  in a field is important for site-specific irrigation management. Large numbers of soil samples are generally required to accurately characterize  $K_s$  in a study area (Yao et al., 2015). For large areas, direct measurements are often arduous, time consuming and expensive (Li et al., 2007). To avoid these limitations, pedo-transfer functions (PTFs) have been developed to estimate  $K_s$  indirectly through more easily measurable soil properties that may already exist from soil surveys (Wösten et al., 2001). Although PTFs have been utilized for more than 30 years, there is very little information on where they can be applied and in many cases their performance is overoptimistically expected (McBratney et al., 2011). The performance of PTFs is influenced by the dataset that was used for compiling it, for its calibration and evaluation (Schaap and Leij, 1998). A PTF may perform well in the region or at the scale for which it was developed, however, its application in other regions or other scales does not always yield satisfactory results (Tietje and Hennings, 1996; Wagner et al., 2001). PTFs were usually developed over large regions (e.g., national, international or intercontinental scale) based on small sampling volumes and large sampling distances though. These PTFs are best suited for national or global modeling, but might be of little use for estimating water transport at smaller scales (e.g., field scale) (Lin et al., 1999). Agricultural management (e.g., irrigation) occurs at the field scale, therefore, the reliability of PTFs in predicting water permeability in a specific field needs to be critically evaluated.

The primary objectives of this project were to evaluate PTFs for estimating  $K_s$  at the field scale in a farmer's field in western Kentucky and to characterize the spatial pattern of  $K_s$  in the field by co-regionalization method.

## **Methodology**

This research was conducted in a no-till farmland (~30 ha) located in Caldwell County, Kentucky, United States (Fig. 1). Wheat/ double-crop soybean/ corn rotation is practiced in the particular field of this study.

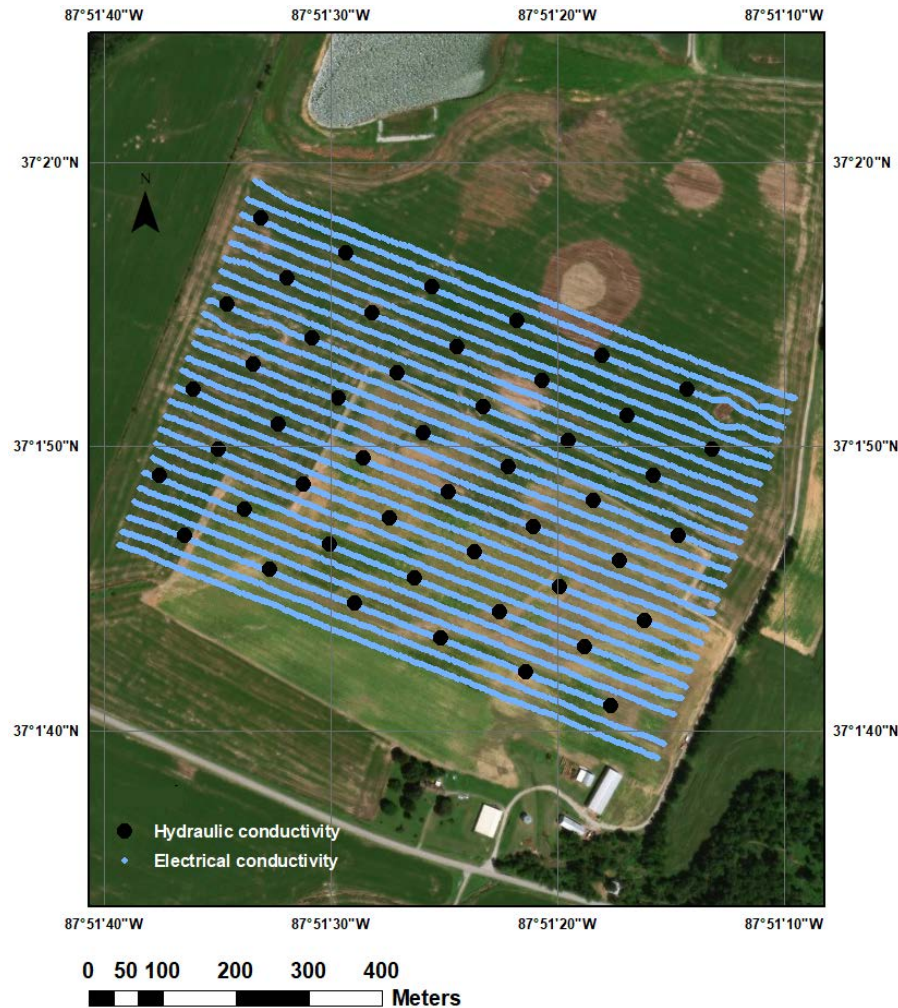


Fig. 1. Study area and sampling locations.

Undisturbed soil cores were sampled in a 100 m by 50 m grid of 48 locations from 7~13 cm depth by using cutting rings (diameter: 8.4 cm, height: 6 cm). Bulk soil samples were also collected from each point. Soil cores were used to measure saturated and near-saturated hydraulic conductivity, and bulk density. Disturbed soil samples were air-dried and passed through a 2-mm sieve for other soil physical property analyses. Soil apparent electrical conductivity at shallow depth (0–30 cm) was measured using a Veris 3150.

Soil texture was determined by the sieving and the pipette method (Gee and Or, 2002). Silty loam was determined as the predominant soil texture. The core method was used to measure bulk density ( $\rho_b$ ) (Grossman and Reinsch, 2002). Soil organic matter (SOM) was measured by the combustion method (Nelson and Sommers, 1982).

Saturated hydraulic conductivity ( $K_s$ ) was determined using a permeameter based on Darcy's law under constant and falling head conditions depending on the individual percolation rate of each sample (Klute and Dirksen, 1986). Hydraulic conductivity at potentials of -1 cm ( $K_{-1}$ ), -5 cm ( $K_{-5}$ )

and -10 cm ( $K_{-10}$ ) were measured with a self-developed double plate pressure-membrane apparatus with two tension plates at the upper and lower end of the soil core. The computation of  $K(h)$  is based on Buckingham-Darcy's law. Near-saturated hydraulic conductivity was used to study the influence of macro-pores on hydraulic conductivity.

Based on available soil data in this study, seven widely used PTFs (Cosby et al. 1984; Puckett et al. 1985; Saxton et al. 1986; Vereecken et al. 1990; Wösten 1997; Wösten et al. 1999; Schaap et al. 2001) were selected to assess their performance in estimating  $K_s$ . Two statistical parameters (root mean square error, RMSE and Nash-Sutcliffe efficiency, NSE) were considered as evaluation criteria.

$$\text{RMSE} = \sqrt{\frac{1}{n} \sum_{i=1}^n (m_i - p_i)^2}$$

$$\text{NSE} = 1 - \left[ \frac{\sum_{i=1}^n (m_i - p_i)^2}{\sum_{i=1}^n (m_i - \bar{m})^2} \right]$$

where  $n$  is the number of observations;  $m_i$  and  $p_i$  are the  $i^{\text{th}}$  measured and predicted values, respectively; and  $\bar{m}$  is mean of measured values. RMSE should be at minimum. NSE ranges from  $-\infty$  to 1 and should be close to 1.

Kriging and cokriging are widely used for spatial interpolation and has been successfully used in studying the spatial variation of soil hydraulic properties (Vauclin et al., 1983; Wang et al., 2013). Cokriging utilizes spatial information of two variables (one is the primary variable, the other is the ancillary variable) along with spatial cross-correlation between the two variables to estimate the undersampled variable (i.e., primary variable) at unobserved locations (Alemi et al., 1988). By properly choosing ancillary variables, cokriging has been proven to be superior to kriging in characterizing the spatial variability of  $K_s$  when  $K_s$  is only sparsely sampled in an area (Alemi et al., 1988; Ersahin, 2003; Basaran et al., 2011). Apparent electrical conductivity ( $EC_a$ ), which is influenced by a variety of soil properties (including texture, moisture, and salinity), is a simple, efficient and inexpensive measurement, and can be densely measured in large areas (Corwin and Lesch, 2005; Sudduth et al., 2005; Chaplot et al., 2010). Therefore,  $EC_a$  was considered as an ancillary variable and was used in cokriging to facilitate the estimation of  $K_s$  in this research.

To apply cokriging, parameters have to be identified that describe the spatial variance structure in semivariograms and cross semivariograms (Nielsen and Wendroth, 2003). In this study, experimental semivariograms and cross semivariograms were fitted to exponential and Gaussian models. The detailed procedures and equations used to perform cokriging are explained in Nielsen and Wendroth (2003). Both measured and Rosetta estimated data were used to characterize the spatial pattern of hydraulic conductivity in the field.

## Principal Findings and Significance\*

Evaluation of established pedo-transfer functions: Saturated hydraulic conductivity was calculated according to the selected PTFs and compared to  $K_s$  measured at the 48 locations in our field. Fig. 2 shows measured and predicted values for all models evaluated. All of the selected PTFs exhibited large differences between the measured and the calculated  $K_s$ . The predicted  $K_s$  exhibited less variability compared with our measured data. The predicted  $K_s$  values from the PTFs were weakly

related to measured  $K_s$  values based on high RMSE and low NSE values (Table 1). The results indicated that the prediction of  $K_s$  in this field using selected PTFs developed from large datasets appears to be inappropriate.

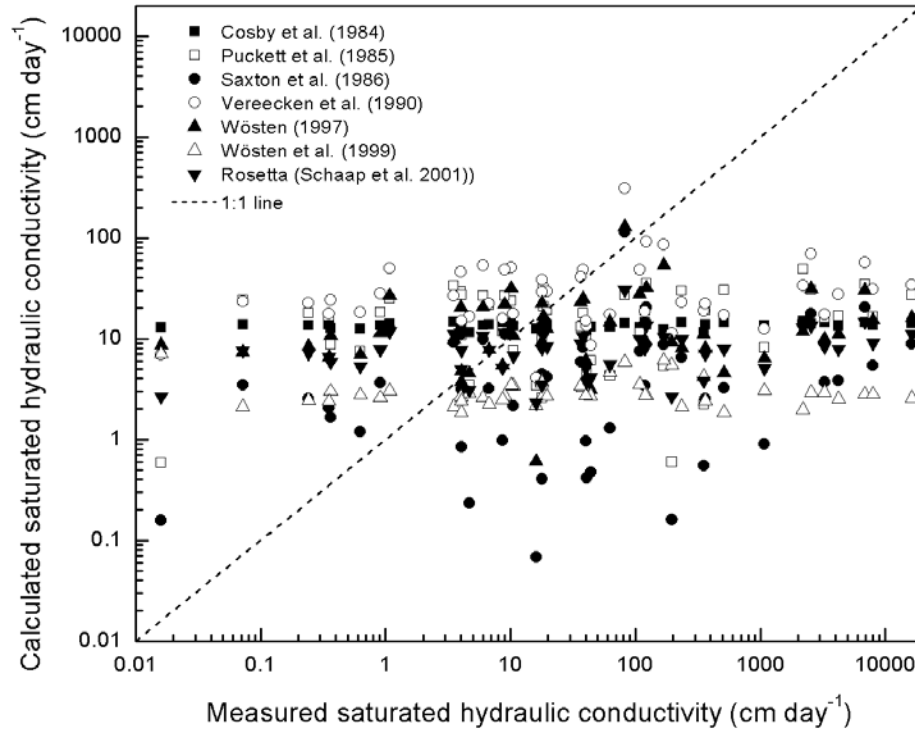


Fig.2. Measured and estimated saturated hydraulic conductivity for the seven models investigated.

Table 1 Performance of selected pedo-transfer functions in estimating soil saturated hydraulic conductivity

Pedo-transfer functions	RMSE $\log_{10}(\text{cm day}^{-1})$	NSE
Cosby et al. 1984	1.391	-0.067
Puckett et al. 1985	1.384	-0.056
Saxton et al. 1986	1.673	-0.542
Vereecken et al. 1990	1.317	0.044
Wösten 1997	1.391	-0.066
Wösten et al. 1999	1.702	-0.596
Rosetta (Schaap et al. 2001) (sand, silt, clay and $\rho_b$ )	1.445	-0.150

Spatial variability of hydraulic conductivity: Fitted semivariograms and cross semivariogram models for both measured and estimated hydraulic conductivity were used in cokriging to generate hydraulic conductivity patterns. Measured  $K_s$  showed strong spatial variability as a result of macro-pores effect. However, PTF estimated  $K_s$  showed less spatial variability and similar to the spatial patterns of near saturated hydraulic conductivity. This result indicated that spatial variability of  $K_s$  cannot be fully captured by PTFs.

In summary, all selected PTFs exhibited unsatisfactory predictions of  $K_s$  because they were derived for a larger variety of soil types, making them less sensitive to the particular soil structural conditions at our site. The co-regionalization analysis indicated that the  $K_s$  map based on PTFs estimates should be evaluated carefully and handled with caution. According to the  $K_s$  map using measured data,  $K_s$  showed high spatial heterogeneity, which means water management strategies should be adapted to different zones within the field.

\*All results from this project are currently under consideration for publication in a peer reviewed journal. For this reason, the results are of preliminary character and only briefly stated in this report. The complete final report with detailed results and discussion, as well as relevant figures will be submitted to the Kentucky Water Resources Research Institute after the acceptance of our manuscript.

## **Acknowledgements**

We thank the farmer Trevor Gilkey for allowing us to conduct this research in his field. We appreciate Riley J. Walton and Javier Reyes for their help in the field. We thank Diane Hunter in the Division of Regulatory Services for her help in soil analysis. We gratefully acknowledge the support of this project by United States Geological Survey and Kentucky Water Resources Research Institute 104-B Student Research Enhancement Program, as well as support from the SB-271 Water Quality program from the College of Agriculture Food & Environment and from the Department of Plant & Soil Sciences. The Co-PI (O.W.) thanks for support through the USDA National Institute of Food and Agriculture, Multistate Project KY006093.

## **References**

Al-Karadsheh, E., H. Sourell and R. Krause. 2002. Precision irrigation: New strategy irrigation water management. In: Conference on International Agricultural Research for Development, Witzenhausen, Germany. October 9-11, 2002. p. 1-7.

Alemi, M.H., M.R. Shahriari and D.R. Nielsen. 1988. Kriging and cokriging of soil water properties. *Soil Technol.* 1: 117-132.

Basaran, M., G. Erpul, A.U. Ozcan, D.S. Saygin, M. Kibar, I. Bayramin, et al. 2011. Spatial information of soil hydraulic conductivity and performance of cokriging over kriging in a semi arid basin scale. *Environ. Earth Sci.* 63: 827-838.

Chaplot, V., S. Lorentz, P. Podwojewski and G. Jewitt. 2010. Digital mapping of A-horizon thickness using the correlation between various soil properties and soil apparent electrical

resistivity. *Geoderma* 157: 154-164.

Corwin, D.L. and S.M. Lesch. 2005. Characterizing soil spatial variability with apparent soil electrical conductivity I. Survey protocols. *Comput. Electron. Agr.* 46: 103-133.

Cosby, B.J., G.M. Hornberger, R.B. Clapp and T.R. Ginn. 1984. A statistical exploration of the relationships of soil moisture characteristics to the physical properties of soils. *Water Resour. Res.* 20: 682-690.

Ersahin, S. 2003. Comparing ordinary kriging and cokriging to estimate infiltration rate. *Soil Sci. Soc. Am. J.* 67: 1848-1855.

Gee, G.W., and D. Or. 2002. Particle-size analysis. In: J. H. Dane and C. G. Topp, editors, *Methods of soil analysis. Part 4. Physical methods. SSSA Book Ser. 5.4.* SSSA, Madison, WI. p. 255-293.

Ghanbarian, B., V. Taslimitehrani and Y.A. Pachepsky. 2017. Accuracy of sample dimension dependent pedotransfer functions in estimation of soil saturated hydraulic conductivity. *Catena* 149(Part 1): 374-380.

Grossman, R.B., and T.G. Reinsch. 2002. Bulk density and linear extensibility. In: J. H. Dane and C. G. Topp, editors, *Methods of soil analysis. Part 4. Physical methods. SSSA Book Ser. 5.4.* SSSA, Madison, WI. p. 201-228.

Klute, A., and C. Dirksen. 1986. Hydraulic conductivity and diffusivity: Laboratory methods. In: A. Klute, editor, *Methods of soil analysis: Part 1. Physical and mineralogical methods. 2nd ed.* SSSA Book Ser. 5.1. ASA and SSSA, Madison, WI. p. 687-734.

Li, Y., D. Chen, R.E. White, A. Zhu and J. Zhang. 2007. Estimating soil hydraulic properties of Fengqiu County soils in the North China Plain using pedo-transfer functions. *Geoderma* 138: 261-271.

Lin, H.S., K.J. McInnes, L.P. Wilding and C.T. Hallmark. 1999. Effects of soil morphology on hydraulic properties II. Hydraulic pedotransfer functions. *Soil Sci. Soc. Am. J.* 63: 955-961.

McBratney, A.B., B. Minasny and G. Tranter. 2011. Necessary meta-data for pedotransfer functions. *Geoderma* 160: 627-629.

Nelson, D.W., and L.E. Sommers. 1982. Total carbon, organic carbon, and organic matter. In: A. L. Page, editor, *Methods of soil analysis. Part 2. Chemical and microbiological properties. 2nd ed.* Agron. Monogr. 9.2. ASA and SSSA, Madison, WI. p. 539-579.

Nielsen, D., J. Biggar and K. Erh. 1973. Spatial variability of field-measured soil-water properties. *Hilgardia* 42: 215-259.



Nielsen, D.R. and O. Wendroth. 2003. Spatial and temporal statistics: Sampling field soils and their vegetation. Catena Verlag, Reiskirchen, Germany.

Puckett, W.E., J.H. Dane and B.F. Hajek. 1985. Physical and mineralogical data to determine soil hydraulic properties. Soil Sci. Soc. Am. J. 49: 831-836.

Saxton, K.E., W.J. Rawls, J.S. Romberger and R.I. Papendick. 1986. Estimating generalized soil water characteristics from texture. Soil Sci. Soc. Am. J. 50: 1031-1036.

Schaap, M.G., and F.J. Leij. 1998. Database-related accuracy and uncertainty of pedotransfer functions. Soil Sci. 163: 765-779.

Schaap, M.G., and F.J. Leij. 2000. Improved prediction of unsaturated hydraulic conductivity with the Mualem-van Genuchten model. Soil Sci. Soc. Am. J. 64: 843-851.

Schaap, M.G., F.J. Leij and M.T. van Genuchten. 2001. ROSETTA: a computer program for estimating soil hydraulic parameters with hierarchical pedotransfer functions. J. Hydrol. 251: 163-176.

Sudduth, K.A., N.R. Kitchen, W.J. Wiebold, W.D. Batchelor, G.A. Bollero, D.G. Bullock, et al. 2005. Relating apparent electrical conductivity to soil properties across the north-central USA. Comput. Electron. Agr. 46: 263-283.

Tietje, O., and V. Hennings. 1996. Accuracy of the saturated hydraulic conductivity prediction by pedo-transfer functions compared to the variability within FAO textural classes. Geoderma 69: 71-84.

Vauclin, M., S.R. Vieira, G. Vachaud and D.R. Nielsen. 1983. The use of cokriging with limited field soil observations. Soil Sci. Soc. Am. J. 47: 175-184.

Vereecken, H., J. Maes and J. Feyen. 1990. Estimating unsaturated hydraulic conductivity from easily measured soil properties. Soil Sci. 149: 1-12.

Wagner, B., V.R. Tarnawski, V. Hennings, U. Müller, G. Wessolek and R. Plagge. 2001. Evaluation of pedo-transfer functions for unsaturated soil hydraulic conductivity using an independent data set. Geoderma 102: 275-297.

Wang, Y., M.A. Shao, Z. Liu and R. Horton. 2013. Regional-scale variation and distribution patterns of soil saturated hydraulic conductivities in surface and subsurface layers in the loessial soils of China. J. Hydrol. 487: 13-23.

Wösten, J.H.M. 1997. Pedotransfer functions to evaluate soil quality. Dev. Soil Sci. 25: 221-245.

Wösten, J.H.M., A. Lilly, A. Nemes and C. Le Bas. 1999. Development and use of a database of

hydraulic properties of European soils. *Geoderma* 90: 169-185.

Wösten, J.H.M., Y.A. Pachepsky and W.J. Rawls. 2001. Pedotransfer functions: Bridging the gap between available basic soil data and missing soil hydraulic characteristics. *J. Hydrol.* 251: 123-150.

Yao, R.J., J.S. Yang, D.H. Wu, F.R. Li, P. Gao and X.P. Wang. 2015. Evaluation of pedotransfer functions for estimating saturated hydraulic conductivity in coastal salt-affected mud farmland. *J. Soils Sediments* 15: 902-916.

# Effects of stream restoration on pollutant load reductions in an urban watershed

## Basic Information

<b>Title:</b>	Effects of stream restoration on pollutant load reductions in an urban watershed
<b>Project Number:</b>	2017KY267B
<b>Start Date:</b>	3/1/2017
<b>End Date:</b>	7/31/2018
<b>Funding Source:</b>	104B
<b>Congressional District:</b>	KY 6th
<b>Research Category:</b>	Water Quality
<b>Focus Categories:</b>	Water Quality, Non Point Pollution, Nutrients
<b>Descriptors:</b>	None
<b>Principal Investigators:</b>	Carmen Agouridis

## Publication

1. Austen, Sam and Carmen Agouridis, 2018, Effects of Stream Restoration on Pollutant Load Reductions in an Urban Watershed, in Proceedings of the 2018 Kentucky Water Resources Annual Symposium, Kentucky Water Resources Research Institute, Lexington, Kentucky, p. 27.

# Effects of Stream Restoration on Pollutant Load Reductions in an Urban Watershed

## Problem and Research Objectives

Streams draining urban lands consistently suffer from “urban stream syndrome” (Walsh et al., 2005), which is characterized by flashy hydrology, elevated concentrations of nutrients and contaminants, altered morphology, decreased amounts of organic matter, and poor biotic richness. Urban streams are often incised, over widened, lack bed complexity, have small hyporheic zones, have narrow floodplain corridors bordered by structures and utilities, and lack woody material. Restoring urban streams is a challenging endeavor, particularly when restoration goals include water quality and habitat improvements, the top two components of the Stream Functions Pyramid (Harman et al., 2012). Notable water quality impairments in many urban streams include elevated nutrient, sediment, and pathogen concentrations (Walsh et al., 2005). Of particular concern is nitrogen (N) and phosphorus (P) as these two constituents, in excess levels, promote eutrophication. In the U.S., eutrophication is one of the leading water quality impairments (Sharpley et al., 2003). Stormwater best management practices focus on reducing pollutant loads from upland sources, but do not address pollutant removal in the stream itself. Restoring the hyporheic zone, particularly through the addition of woody material in the floodplain, could promote retention and processing of instream pollutants (Valett et al., 1996). In 2013, a nearly 950 ft of an unnamed headwater tributary (UT) to the South Elkhorn Creek at the Montessori Middle School of Kentucky (MMSK) was restored using regenerative design techniques whereby a floodplain-wetland complex was created. The restoration resulted in a wide, wetland-like floodplain, comprised of a rock base that was overtopped with a filtration media (approximately 30% woodchips and 70% topsoil). This combination of regenerative design and woody material addition to floodplain soils, may improve the quality of downstream receiving waters indicating such stream restoration efforts may serve as a viable TMDL.

The purpose of this work is to determine the effectiveness of using regenerative design techniques coupled with a designed filter media to improve water quality of urban streams. Specific objectives of the project are to: 1) determine the effect of the MMSK stream restoration project on hydrology, 2) determine the ability of the MMSK stream restoration project to improve water quality, and 3) educate water managers, design professionals, and other stakeholders on strategies to restore urban streams and improve water quality. Installation of hydrologic equipment and initial water quality sampling (not part of the funding request) will occur during the fall of 2016. Data collection and analysis will continue through winter of 2017 with publication and presentation of results to occur during spring and summer of 2018.

## Methodology

The stream restoration site is located at the MMSK in Lexington, KY (Figure 1). The UT to South Elkhorn was restored in 2013 via the Lexington-Fayette Urban County Government (LFUCG) Stormwater Incentive Grant Program. Prior to restoration, the University of Louisville (U of L) Stream Institute monitored the hydrology (storm and base flows) and water quality ( $\text{PO}_4\text{-P}$ ,  $\text{NO}_3\text{+NO}_2\text{-N}$ ,  $\text{NH}_3\text{-N}$ , BOD, pH, EC, and DO) at three locations on the stream (see Figure 1) for a one-year period (Parola et al., 2013). These data were provided to the PIs by the U of L Stream Institute.

The upstream and downstream extents of the project are equipped with trapezoidal flumes, which will be equipped with stage height recorders (HOBO water level loggers) for continuous discharge measurements. Floodplain cross-sections, at the upstream and downstream weirs, were surveyed to develop stage-discharge relationships when flood stage exceeds weir capacity. Three well transects, each consisting of six wells were installed along the project reach to evaluate water levels and constituent concentrations within the restored floodplain (Figure 2). Water levels within the wells are measured bi-weekly. During equipment installation, it was noted that two pipes, 24-inch and 42-inch diameters, discharged into the project reach. Discharge in both pipes is measured using ISCO 4250 flow meters (one per pipe). Bi-weekly grab samples are collected from the three locations along the stream (upstream, downstream, and middle) and the wells and analyzed for PO<sub>4</sub>-P, NO<sub>3</sub>-N/NO<sub>2</sub>-N, NH<sub>3</sub>-N, Cl<sup>-</sup>, SO<sub>4</sub>, TOC, DOC, *E.coli* (stream only), TSS, and turbidity using standard methods (APHA, 1992). Bi-weekly, *in situ* measurements of pH, EC, DO, and temperature (measured using a YSI 556 multiprobe system) are taken at the three stream sample locations and at each well. A rain gauge was installed at the project site to provide precipitation data.

Comparisons between upstream, middle, and downstream hydrology and water quality will be conducted using a second-order autoregressive model (PROC AUTOREG). The autoregressive model is useful in instances where the present value depends on preceding values, such as in the case of accumulating streamflow (Hann, 1977). Significantly different hydrograph parameters will be further evaluated using a linear mixed model (PROC MIXED). Statistical analyses will be conducted following consultation with the College of Agriculture, Food and Environment Graduate Statistical Consultant.

### **Principal Findings and Significance**

Data collection is actively ongoing and in-depth hydrologic and water quality analyses have not been completed. Preliminary results indicate that the upstream inflow is larger than the downstream outflow, though the level of significance has not been determined (Figure 3). These findings suggest that the wetland-like stream and its associated floodplain and enhance hyporheic zone store baseflow and stormwater. Evapotranspiration is also visually notable as baseflow levels, at the downstream portion of the project, are lower than the upstream segment during the growing season suggesting the thick vegetation is influencing hydrology at the site. Data indicates that the two large culverts are only active during large storm events meaning the more frequent, smaller events are addressed by the restoration design.

Presently, water samples from 16 of 22 sampling events have been collected and analyzed. A visual examination of preliminary results indicate that constituent concentrations for PO<sub>4</sub>-P, NO<sub>3</sub>-N/NO<sub>2</sub>-N, and NH<sub>3</sub>-N are decreasing within the hyporheic zone, in the downstream direction.

### **Status Information**

Data collection is actively on-going and is on-schedule. Data collection is expected to conclude summer of 2018. Preliminary data analyses (hydrology and water quality) continue to be

performed, and final data analysis will occur late summer of 2018 following the end of the sampling period. The start of the project was delayed due to receipt of funding. The goals of the stream restoration project as well as this project have been presented to the students at MMSK as well as practitioners at the Kentucky Water Resources Research Institute Symposium.

### **Plan for Project Completion**

The graduate student (Austen) will continue to collect data through early summer of 2018 (1-year sampling cycle). Well locations will be surveyed to allow for the production of water depth and water quality contour maps. Data analyses will be completed summer of 2018. Completion of one M.S. thesis and a manuscript draft will occur summer of 2018. Preliminary results of this project will be presented to stream restoration and water resources professionals through extension workshops and related publications. Preliminary results were already presented at the KWRRI annual conference.



Figure 1: Red circles indicate the location of the flumes (upstream and downstream extent) and stream grab samples. Red lines indicate approximate locations where well transects (six wells per transect, three on each side of the stream) were installed. The rain gauge (blue cloud) was installed near the MMSK building.





Figure 2: Well transects allow for sampling of hyporheic zone waters. Each transect consists of six well, three on each side of the restored stream.



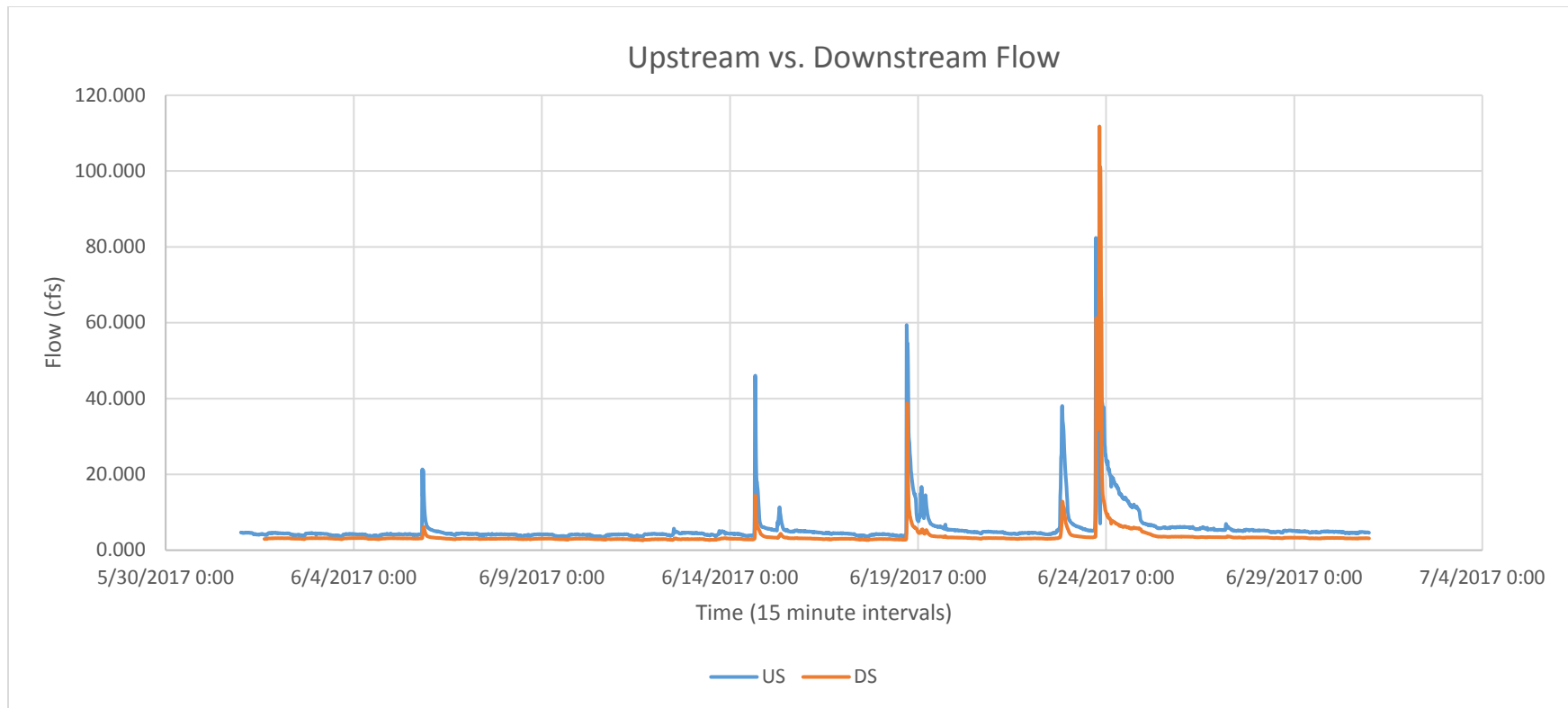


Figure 3. Upstream and downstream hydrographs for June 2017. Except when the two, large culverts are active, as seen around June 24<sup>th</sup>, downstream volumes and peaks are less than upstream values.

## References

- Alexander, R.B., R.A. Smith, G.E. Schwarz, E.W. Boyer, J.V. Nolan, and J.W. Brakebill. 2008. Differences in phosphorus and nitrogen delivery to the Gulf of Mexico from the Mississippi River Basin. *Environment. Science and Technology*. 42: 822-830.
- American Public Health Association. 1992. *Standard Methods for the Examination of Water and Wastewater*, 18<sup>th</sup> Ed.: Washington, D.C., American Public Health Association.
- Greenan, C.M., T.B. Moorman, T.B. Parkin, T.C. Kaspar, and D.B. Jaynes. 2009. Denitrification in wood chip bioreactors at different water flows. *Journal of Environmental Quality* 38: 1164-1671.
- Hann, C.T. 1977. *Statistical methods in hydrology*. Iowa State University Press, Ames, IA.
- Harman, W., R. Starr, M. Carter, K. Tweedy, M. Clemmons, K. Suggs, and C. Miller. 2012. A function-based framework for stream assessment and restoration projects. U.S. Environmental Protection Agency, Office of Wetlands, Oceans, and Watersheds, Washington, D.C.
- Parola, A.C., M.A. Croasdaile, R.M. Nagisetty, and J.W. Park. 2013. Stream water quality at Montessori Middle School of Kentucky. University of Louisville, Stream Institute, Louisville, KY.
- Robertson, W.D., L.C. Merkley. 2009. In-stream bioreactor for agricultural nitrate treatment. *Journal of Environmental Quality* 38: 230-237.
- Schipper, L.A., W.D. Robertson, A.J. Gold, D.B. Jaynes, and S.C. Cameron. 2010. Denitrifying bioreactors-An approach for reducing nitrate loads to receiving waters. *Ecological Engineering* 36:1532-1543.
- Sharpley, A.N., J.L. Weld, D.B. Beegle, P.J.A. Kleinman, W.J. Gburek, P.A. Moore, Jr. and G. Mullins. 2003. Development of phosphorus indices for nutrient management planning strategies in the United States. *Journal of Soil and Water Conservation* 58: 137-152.
- Valett, H.M., J.A. Morrice, C.N. Dahm, and M.E. Campana. 1996. Parent lithology, surface-groundwater exchange, and nitrate retention in headwater streams. *Limnol. Oceanogr.* 41: 333-345.
- Walsh, C.J., A.H. Roy, J.W. Feminella, P.D. Cottingham, P.M. Groffman, and R.P. Morgan. 2005. The Urban Stream Syndrome: Current Knowledge and the Search for a Cure. *Journal of the North American Benthological Society* 24(3): 706-723.

# Using anthropogenic compounds in sewage to create new fecal source and fecal age indicators for use in protecting and improving water quality in Kentucky watersheds

## Basic Information

<b>Title:</b>	Using anthropogenic compounds in sewage to create new fecal source and fecal age indicators for use in protecting and improving water quality in Kentucky watersheds
<b>Project Number:</b>	2017KY268B
<b>Start Date:</b>	3/1/2017
<b>End Date:</b>	2/28/2018
<b>Funding Source:</b>	104B
<b>Congressional District:</b>	KY 6th
<b>Research Category:</b>	Water Quality
<b>Focus Categories:</b>	Wastewater, Methods, Water Quality
<b>Descriptors:</b>	None
<b>Principal Investigators:</b>	Gail Montgomery Brion

## Publications

1. Hall, Ashley and Gail Brion, 2016, Using Anthropogenic Compounds in Sewage to Create New Fecal Source and Age Indicators, poster presentation at the 2016 Sustainability Forum, Tracy Farmer Institute for Sustainability and the Environment, Lexington, KY.
2. Hall, Ashley, Laira Kelley, and Gail Brion, 2018, Using Anthropogenic Compounds in Sewage to Create New Fecal Source and Age Indicators, poster presentation at the 2018 Kentucky Water Resources Annual Symposium, Kentucky Water Resources Research Institute, Lexington, KY.
3. Hall, Ashley, Laira Kelley, and Gail Brion, 2018, Using Anthropogenic Compounds in Sewage to Create New Fecal Source and Age Indicators, poster presentation at the University of Kentucky Undergraduate Research Symposium, Lexington, KY.
4. Hall, Ashley and Gail Brion, 2017, Using Anthropogenic Compounds in Sewage to Create New Fecal Source and Age Indicators, in AWWA Annual Conference and Exposition Proceedings, American Water Works Association, Philadelphia, PA.

# **Using Anthropogenic Compounds in Sewage to Create New Fecal Source and Age Indicators**

## **Problem and Research Objectives**

Surface waters are susceptible to many forms of contamination. Of those, the most concerning is that of untreated human fecal matter. This can enter the environment through sewer line leaks and overflows as well as old septage systems. When these impaired waterways lie within watersheds used as a drinking water source, the importance of a reliable, timely, and accurate way to determine point sources of contamination is undeniable. While there are many methods that are able to identify human fecal contamination, they are not without their shortcomings. Biological methods take time and can be costly. Chemical methods can become ubiquitous in the environment and become unable to determine fresh from aged human impact. Even more, no single indicator can determine the source, load, and age within the environment. Previous studies suggest that Personal Care Products (PCPs) can be used as fecal indicators (Oppenheimer *et al*, 2011). This study set out to investigate the use of pharmaceuticals and artificial sweeteners present in raw sewage to pinpoint sewage leaks in the environment through a ratio of a biodegradable and persistent compound.

## **Methodology**

Samples were collected from wastewater treatment plants (WWTP) and surface waters in the Lexington area. Samples were extracted and analyzed for the presence and concentration of acetaminophen and sucralose using LC-MS/MS (Loos *et al*, 2008). Samples were taken at the influent, final clarifying, and effluent stages of the WWTP. Laboratory scale decay studies were performed with spiked WWTP influent and spiked surface waters to observe the behavior of these compounds over time. Samples were collected in surface waters up and down stream for suspected hot spots and to monitor for the concentrations of sucralose and acetaminophen as well as the ratio of the two.

## **Principal Findings and Significance**

To determine the presence of sucralose and acetaminophen in sewage, samples were taken from the influent (INF), final clarifying (FCT), and post chlorination effluent (PCE) from two WWTP, Town Branch (TB) and West Hickman (WH). Results suggest that sucralose persists through the treatment process while acetaminophen is effectively removed, indicating that acetaminophen in the environment implies untreated human sewage is present. The ratio of acetaminophen to sucralose was also observed and T-confidence intervals show that there is no significant difference in the ratio between WWTP, indicating that a ratio between two PCPs, specifically acetaminophen and sucralose, can be used between sewer-sheds, at least locally.

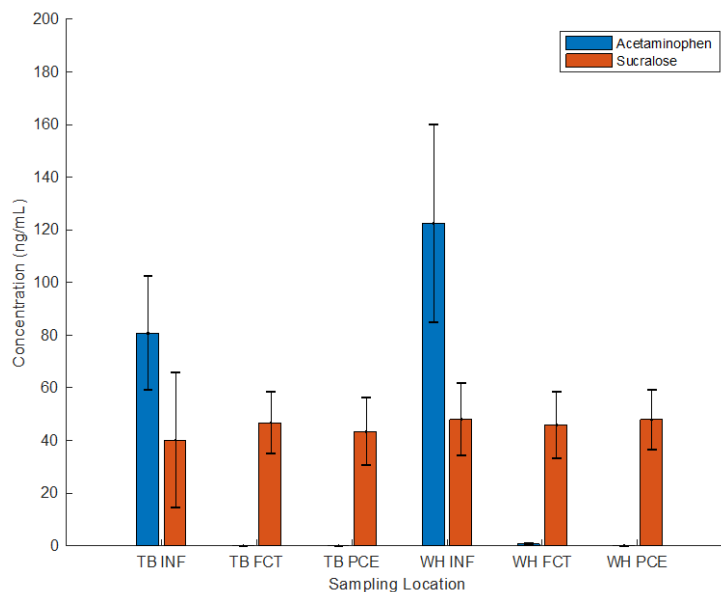


Figure 1: Concentrations of sucralose and acetaminophen during WWTP (n=15 for TB and n=11 for WH)

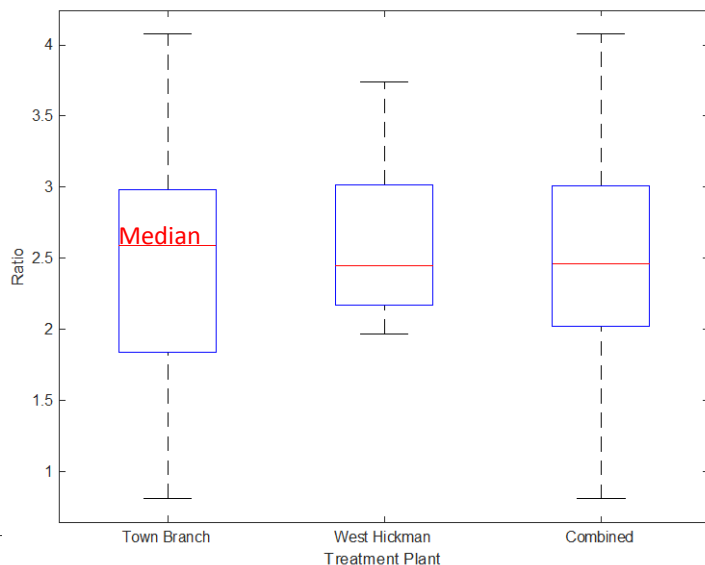


Figure 2: Ratio of acetaminophen to sucralose in WWTP influent (n=15 for TB, n=11 for WH, n=26 Combined)

Laboratory scale studies were conducted with spiked WWTP influent and spiked surface waters to observe the behavior of sucralose and acetaminophen in a simulated environment. Both the influent and surface water studies were conducted in the dark at 21°C and 4°C. Results show that the rate of degradation of acetaminophen, and subsequently the ratio of acetaminophen to sucralose decrease with temperature.

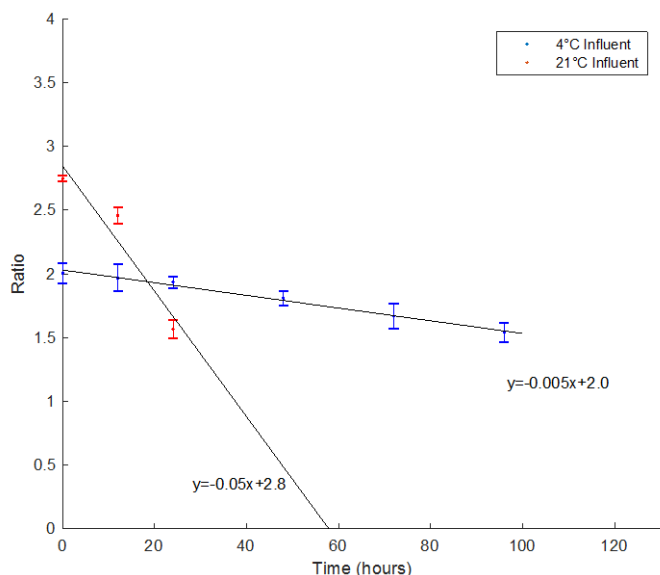


Figure 3: Laboratory scale decay study of acetaminophen to sucralose ratio in spiked WWTP influent.

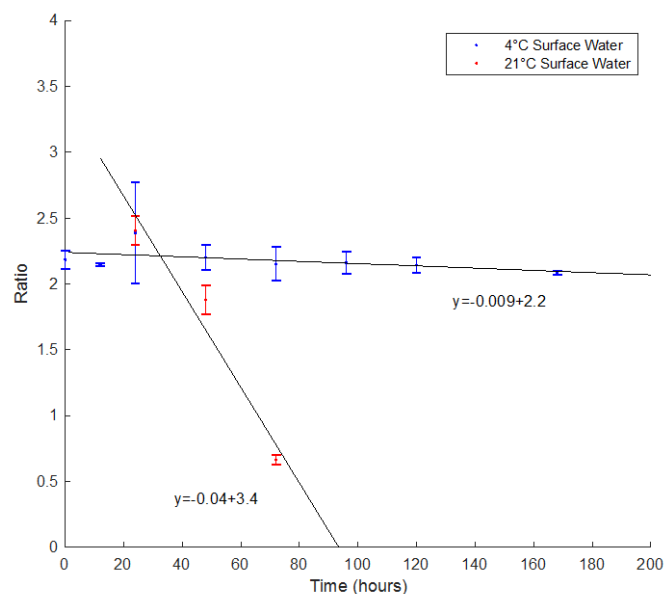


Figure 4: Laboratory scale decay study of acetaminophen to sucralose ratio in spiked surface water from McConnell Springs

Tap water samples were collected in 13 different municipalities in Central Kentucky to determine the persistence of acetaminophen and sucralose through tap water treatment. Sucralose was detectable in every sample while acetaminophen was detected in 2 of the 13 samples. This further indicates that sucralose is persistent while acetaminophen is not.

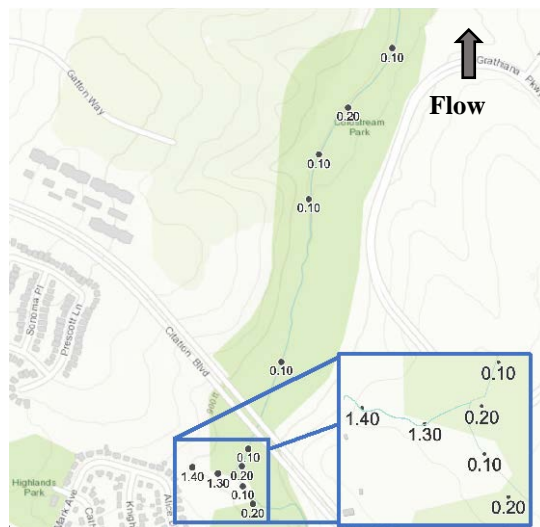


Figure 5: Ratios of acetaminophen to sucralose along Cane Run creek in Lexington, KY

Finally, a known impaired water was monitored near a suspected leak. A magnitude difference (from 1 to 0.2) in ratios of acetaminophen to sucralose between the tributary and main channel of Cane Run (flowing NE) indicates that there is fresh sewage entering the stream. The decrease in the ratio of acetaminophen to sucralose downstream indicates that this indicator can be related to the age and presence of human sewage.

## References

- Loos, R., Gawlik, B., Boettcher, K., Locoro, G., Contini, S., Bidoglio, G. (2008). Sucralose screening in european surface waters using solid-phase extraction-liquid-chromatography-triple-quadrupole mass spectrometry method. *Journal Chromatography A* 1126-1131
- Oppenheimer, J., Eaton, A., Badruzzaman, M., Haghani, A. W, Jacangelo, J. G. (2011) Occurrence and suitability of sucralose as an indicator compound of wastewater loading to surface waters in urbanized regions. *Water Research*. 45: 4019-4027.

## Predictive hydrologic and hazard modeling of injection well density and usage in urban karst aquifers

### Basic Information

<b>Title:</b>	Predictive hydrologic and hazard modeling of injection well density and usage in urban karst aquifers
<b>Project Number:</b>	2017KY269B
<b>Start Date:</b>	3/1/2017
<b>End Date:</b>	2/28/2018
<b>Funding Source:</b>	104B
<b>Congressional District:</b>	KY 2nd
<b>Research Category:</b>	Ground-water Flow and Transport
<b>Focus Categories:</b>	Floods, Groundwater, Models
<b>Descriptors:</b>	None
<b>Principal Investigators:</b>	Jason Polk

### Publications

1. Shelley, James and Jason Polk, 2018, Modeling and Evaluating the Influences of Class V Injection Wells on Urban Karst Hydrology in Annual Meeting of Kentucky Academy of Science Meeting Abstracts Archive, Kentucky Academy of Science, Murray, KY.
2. Shelley, James, Jason Polk, and Matt Powell, 2018, Modeling and Evaluating the Influences of Class V Injection Wells on Urban Karst Hydrology, poster presentation at the 2018 Kentucky Water Resources Annual Symposium, Kentucky Water Resources Research Institute, Lexington, Kentucky.

# **Predictive Hydrologic and Hazard Modeling of Injection Well Density and Usage in Urban Karst Aquifers**

## **Problems and Research Objectives**

Flooding is one of the most common and economically impactful natural hazards that occur in the United States (FEMA 2012). The National Flood Insurance Program (NFIP) estimates that the average total per year for flood insurance claims from 2003 to 2012 was approximately four billion dollars (NFIP 2016). In addition to these reactive expenses, the United States (U.S.) government spends billions of dollars each year to respond, assess, and mitigate geohazards. Flooding in karst environments does not represent a large portion of the aforementioned flood cost, but it does cause significant monetary damage. Nevertheless, most damages resulting from karst flooding could be assuaged or circumvented with the promulgation of reasonable, practical regulations and the implementation of proper flood controls. The importance of sustainable management in karst environments cannot be overstated, given that more than 20% of the world's land surface is underlain by karst geology (Veni et al. 2001). In most environments, flooding is a function of the precipitation infiltration/runoff relationship. Likewise, flooding in a karst environment is the result of a similar relationship, but is influenced by many more variables; moreover, to adequately characterize flooding in a karst terrain, it is necessary to understand how subsurface fluid flow in a heterogeneous medium responds to surface influences.

The majority of urban karst areas (UKAs) are prone to groundwater flooding due the high permeability and diffusivity of the underlying aquifer. Unfortunately, very few studies examine the influence of subsurface function on surface flooding in karst areas (Zhou 2007). Additionally, there are relatively few studies examining urban karst flooding through a modeling approach. Evidence supporting the previous statement is affirmed through examining the City of Bowling Green's (CoBG) history of flooding and urban karst issues. The CoBG is one of the most extensively studied karst environments in the United States (Nedvidek 2014); however, there are very few studies in the area that attempt to quantitatively evaluate flooding mechanisms based on aquifer properties and urban development. The CoBG is a representative example of the aforementioned hydrological problems that can plague karst environments. The CoBG is arguably the largest city in the United States built entirely upon a sinkhole plain (Crawford et. al. 1987). Over the last thirty years, the CoBG population has almost doubled, and the land area has grown by approximately 16 kilometers (Nedvidek 2014). During this period, stormwater quantity management has not significantly changed and the CoBG still uses many of the same flood controls, which primarily include Class V Injection Wells. Neglecting several studies by Crawford (1982) that identified that the overuse and poor siting of Injection Wells may be contributing to localized flooding and sinkhole collapse in the area. Furthermore, sustainable development necessitates proactive management, and without an understanding of the system, it is impossible to maintain the health of the environment during urban expansion; therefore, it is important to model system behavior and evaluate the development criteria to understand the impacts and influences of urbanization on karst hydrology.

The primary objective of this research is to examine Class V Injection Wells in the CoBG to determine how Injection Well siting, design, and performance influence urban karst hydrology. It is believed that satisfying the primary objective will improve flood hazard mapping in karst



terrains and enable the creation of a methodology for adequate design and siting procedures for Class V Injection Wells in UKAs. Herein, I have proposed to examine the impacts of stormwater injection wells under variable precipitation and hydrologic conditions, with research objectives to:

1. Characterize the volume of recharge entering the wells in a defined urban karst basin.
2. Determine at high-resolution the seasonal and storm influences on well volume inputs/outputs.
3. Measure the discharge of the drainage basin's final output.
4. Develop a model to quantify the impact of injection wells on recharge, responsiveness, and flooding in the system based on their siting and characterization.

## **Methodology**

The study area was restricted to a 5 km<sup>2</sup> groundwater basin located within the City limits. A Class V Injection Well inventory was conducted and 100 wells were identified within the study basin. Out of the 100 wells, viable wells without obstruction served as the population from which monitoring sites were selected. For statistical purposes, 30 wells in the basin were randomly selected for data logger outfitting. Once the injection well sites were chosen, a HOB0 Water Level Logger was placed in each well to monitor water level fluctuations during storm events and seasonally at 1-minute intervals. Additionally, water level loggers were installed at a local lake and river within the basin. The aforementioned sites are believed to act as groundwater regulators. To adequately assess the aquifer's response to storm events and flood conditions in the study area basin, it was necessary to measure several meteorological parameters. The following input parameters were measured for further data manipulation and analysis: precipitation, temperature, relative humidity, and barometric pressure. All data loggers used in this study recorded data continuously at a one-minute resolution. The data loggers were downloaded and processed on a weekly basis as a part of a precautionary maintenance schedule to prevent data loss. The one-minute resolution was chosen to capture the storm events fully and to satisfy the sensitivity of the data analysis. A HOB0 RX 3000 remote monitoring station was outfitted with several data loggers to monitor weather within the basin continuously. The RX 3000 platform was chosen because it allows multiple data loggers to be linked to one system. Additionally, the monitoring station allows downloading of the data being recorded without disturbance or interruption. A HOB0 tipping bucket rain gauge, smart barometric pressure sensor, and U23 Temperature/Relative Humidity data loggers were attached to the monitoring station to measure precipitation, barometric pressure, temperature, and relative humidity. After accounting for the inputs for the groundwater basin it was necessary to determine the output of the basin. The delineated groundwater basin has one primary outlet; a spring referred to as New Spring. Discharge measurements were made at New Spring using the velocity-area method. A stage-discharge rating curve (Figure 1), was constructed by curve fitting the recorded discharge and staff gauge measurements to a power function.

$$Q = Cx^{\beta}$$

(1)

Where,

Q = Stream Discharge

C and  $\beta$  = Rating Curve Constants

x = Stream Stage

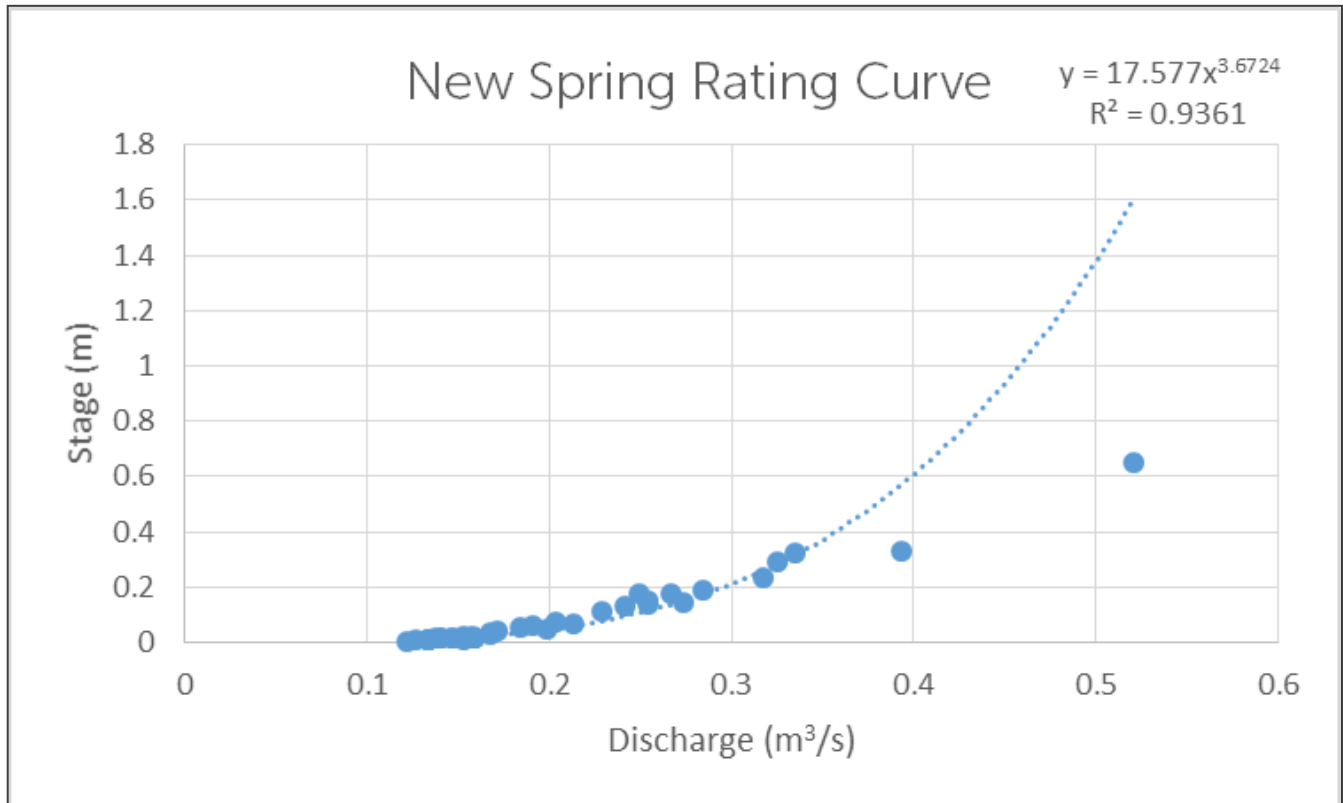


Figure 2.0: New Spring Stream Discharge Rating Curve

Each observed storm event was classified based on generated Frequency Curves (Figures 2.1, and 2.2). The Intensity-Duration Frequency (IDF), and Depth-Duration Frequency (DDF) curves were created using data from the National Oceanic and Atmospheric Administration's (NOAA) Hydrometeorological Design Studies Center Precipitation Frequency Data Server (HDSC-PFDS). To create the IDF Curves an empirical relationship was used.

$$i = \frac{A}{t + B} \quad (2)$$

Where,

i = Precipitation Intensity (in/hr)

t = Precipitation Duration (hr)

A, B = Calculated Constants

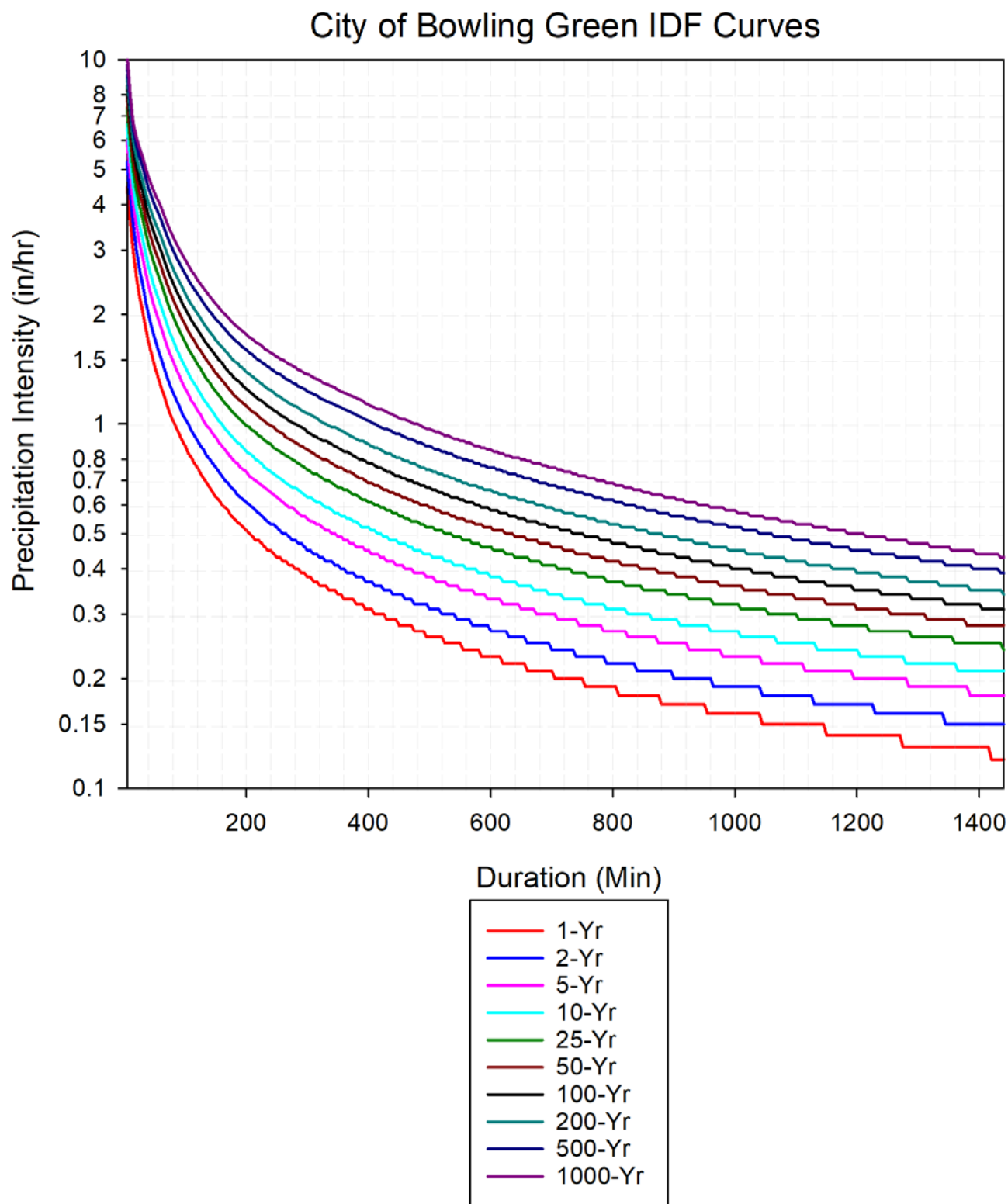


Figure 2.1: Intensity-Duration-Frequency Curves for the City of Bowling Green

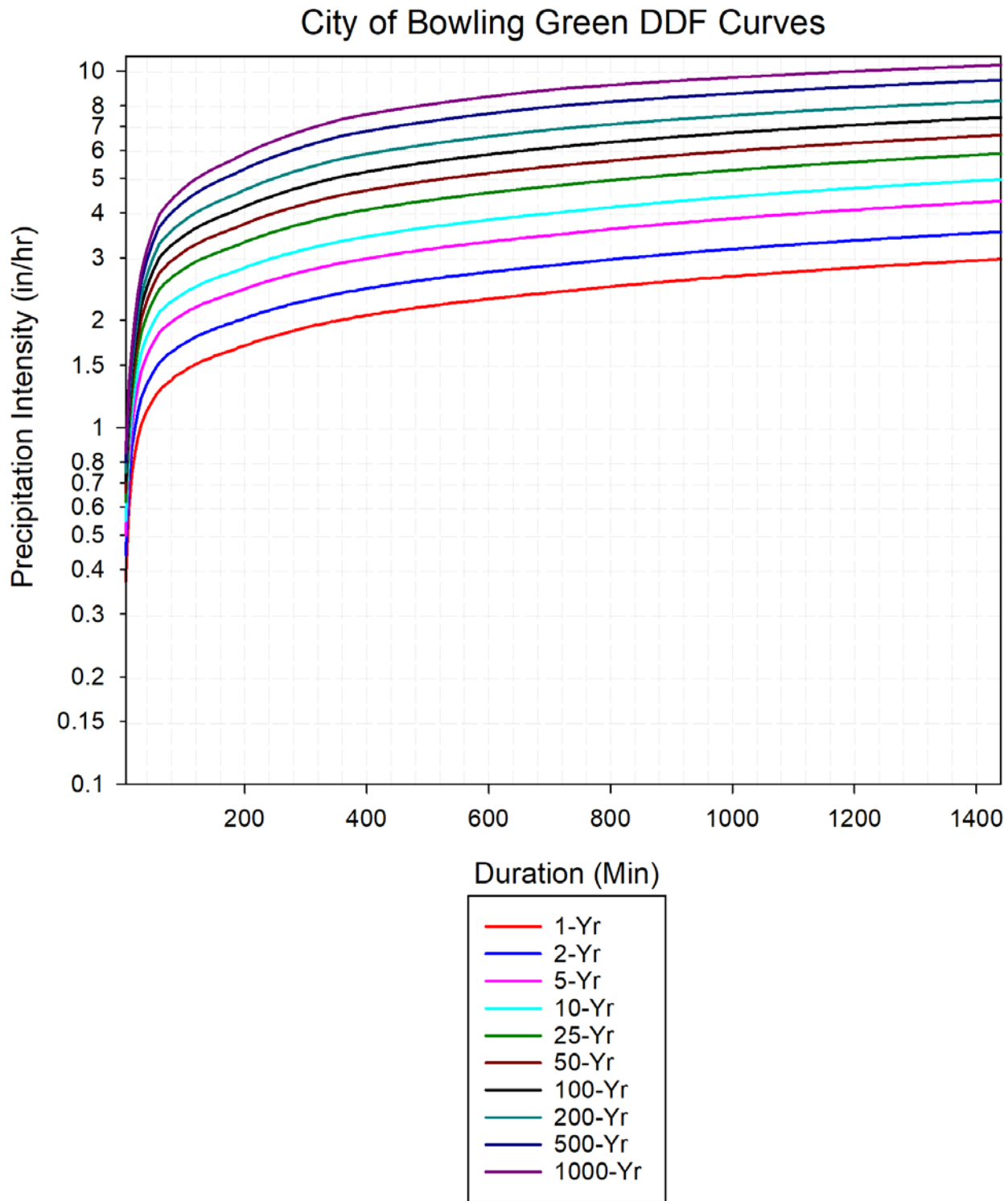


Figure 2.2: Depth-Duration-Frequency Curves for the City of Bowling Green

A fluctuating potentiometric surface map was produced with ArcGIS using water level data recorded by pressure transducers. The water level surface was generated for each time step using a Universal Kriging interpolation method. The Kriging maps made it possible to quickly identify problem areas as well as the depth and flood extent. The maximum groundwater elevation above the land-surface was regarded as the flood extent. Over the monitoring period the well and spring hydrographs were analyzed to determine basin recharge, discharge, and groundwater recession. Injection Well inflow was determined using an equation developed for the project. The equation calculates inflow based off water level changes within the Injection Well. The accuracy of was validated from field testing, and due to high resolution of the data, it is believed that the equation adequately captures the flashy nature of the karst system.

$$F_n = [n_{t+1} - n_t] \left( \frac{\left( \frac{\pi}{4} \right) (\phi)^2 h}{t} \right) \quad (3)$$

Where,

$F_n$  = Inflow at time step  $t$  (ft<sup>3</sup>/s)

$n$  = water level at time  $t$  (ft)

$\phi$  = well borehole diameter (ft)

To make it possible to create a water balance for the basin, daily evapotranspiration calculations were made using the Penman-Montieth equation, and soil infiltration was calculated using the Green and Ampt method.

$$ET_o = \frac{(0.408\Delta)(R_n - G) + \Upsilon \left( \frac{900}{T + 273} \right) (u_2)(e_s - e_a)}{\Delta + \Upsilon(1 + 0.34(u_2))} \quad (4)$$

Where,

$ET_o$  = Evapotranspiration Rate (mm/day)

$T$  = Mean Air Temperature ( $^{\circ}C$ )

$u_2$  = Wind Speed (m/s)

$R_n$  = Net Radiation ( $MJ/m^2$ )

$G$  = Soil Heat Flux Density ( $MJ/m^2$ )

$e_s$  = Saturation Vapor Pressure (kPa)

$e_a$  = Actual Bapor Pressure (kPa)

$\Delta$  = Slope of the Vapor Pressure Curve (kPa/ $^{\circ}C$ )

$\gamma$  = Psychrometric Constant (kPa/ $^{\circ}C$ )

$$\int_0^{F(t)} \frac{F}{F + \psi\Delta\theta} dF \quad (5)$$

Where,

$F(t)$  = Cumulative Depth of Infiltration (L)

$K$  = Hydraulic Conductivity (L/T)

$\psi$  = Wetting Front Suction Head (L)

$\Theta$  = Water Content (L)

Monthly water budgets were created for the monitoring period to examine seasonal trends, and the influence of Injection Wells on the aquifer's hydrologic functioning. The water balance equation developed by Gupta (1995) was used:

$$P + Q_{SI} - Q_{GI} - E - Q_{SO} - Q_{GO} = 0 \quad (6)$$

Where,

P = Precipitation

Q<sub>SI</sub>, Q<sub>GI</sub> = Surface and Groundwater Inflow

E = Evapotranspiration

Q<sub>so</sub>, Q<sub>go</sub> = Surface and Groundwater outflow

Finally, correlation analysis and some basic descriptive statistics were performed for each well to further evaluate injection well performance and to begin the initial stages of developing an Artificial Neural Network (ANN) model for forecasting potentiometric response to precipitation events.

### **Principal Findings and Significance**

The monitoring period for the study started on September 2017, and ended on February 2018. Over this period over 23,000,000 data points were collected, and twenty-one storm events were evaluated using the methodologies described above. Unfortunately, as a result of shipping issues with the monitoring equipment and delays in funding; the original timeline had to be altered, and the overall monitoring period had to be shortened. The alteration to the timeline makes it impossible to assess the seasonality shifts within the aquifer. However, it was possible to capture the Fall to Winter transition. Nevertheless, the brief monitoring period did provide valuable insight that made it possible to better understand how Class V Injection Wells influence urban karst hydrology and affect flooding in UKAs.



The most insightful method utilized in this study was the hydrograph analysis. From an observational standpoint it is evident that the karst aquifer responds much quicker than expected. Figures 3.0, and 3.1 displays some preliminary storm data that was collected in the initial phases of the study. When examining Figures 3.0 and 3.1, it is possible to ascertain that the choice of a one-minute sample resolution was appropriate for this study.

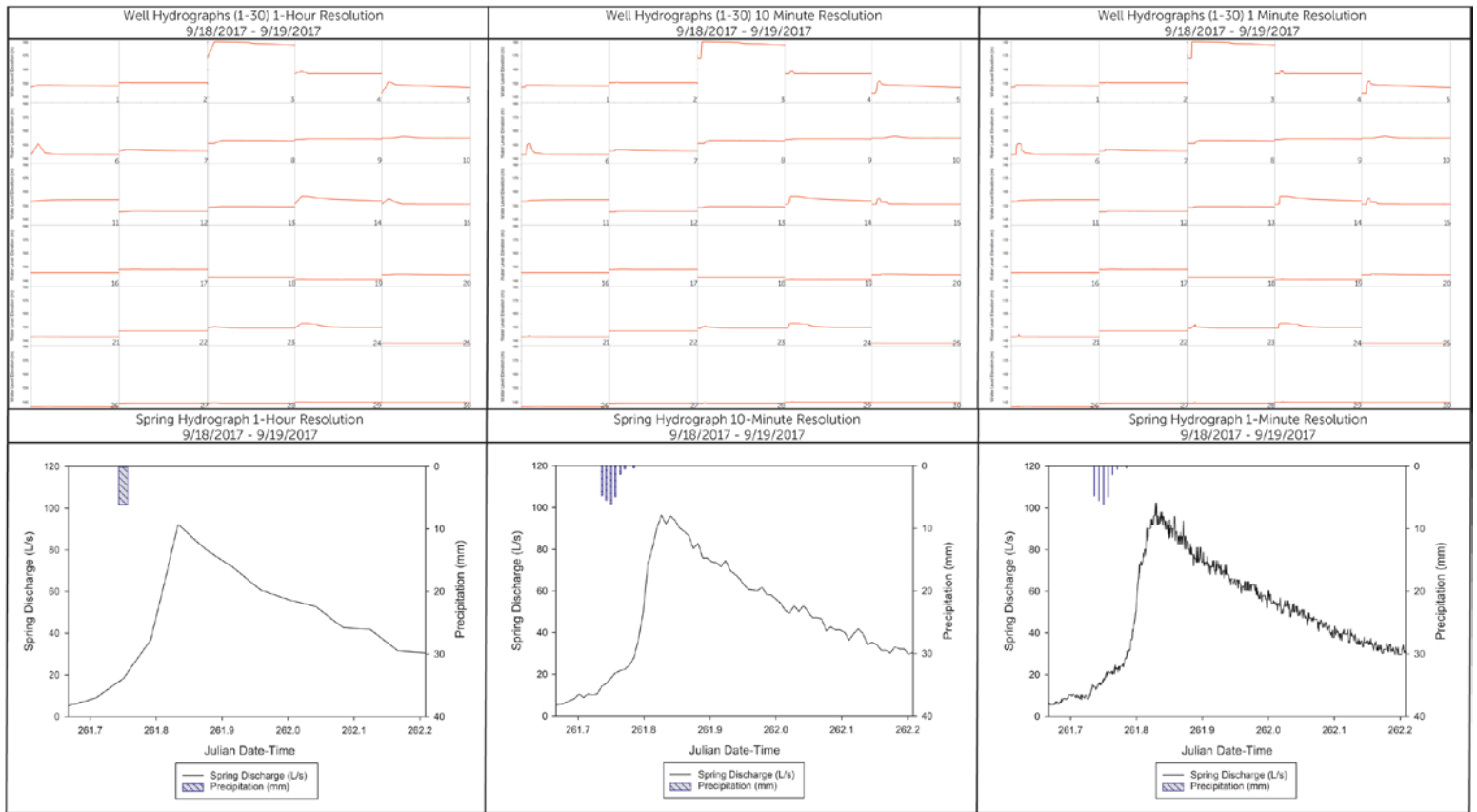


Figure 3.0: New Spring Groundwater Basin - Class V Injection Well and Outlet Spring Hydrographs at Multiple Resolutions During Storm Event (9/18/2017-9/19/2017).

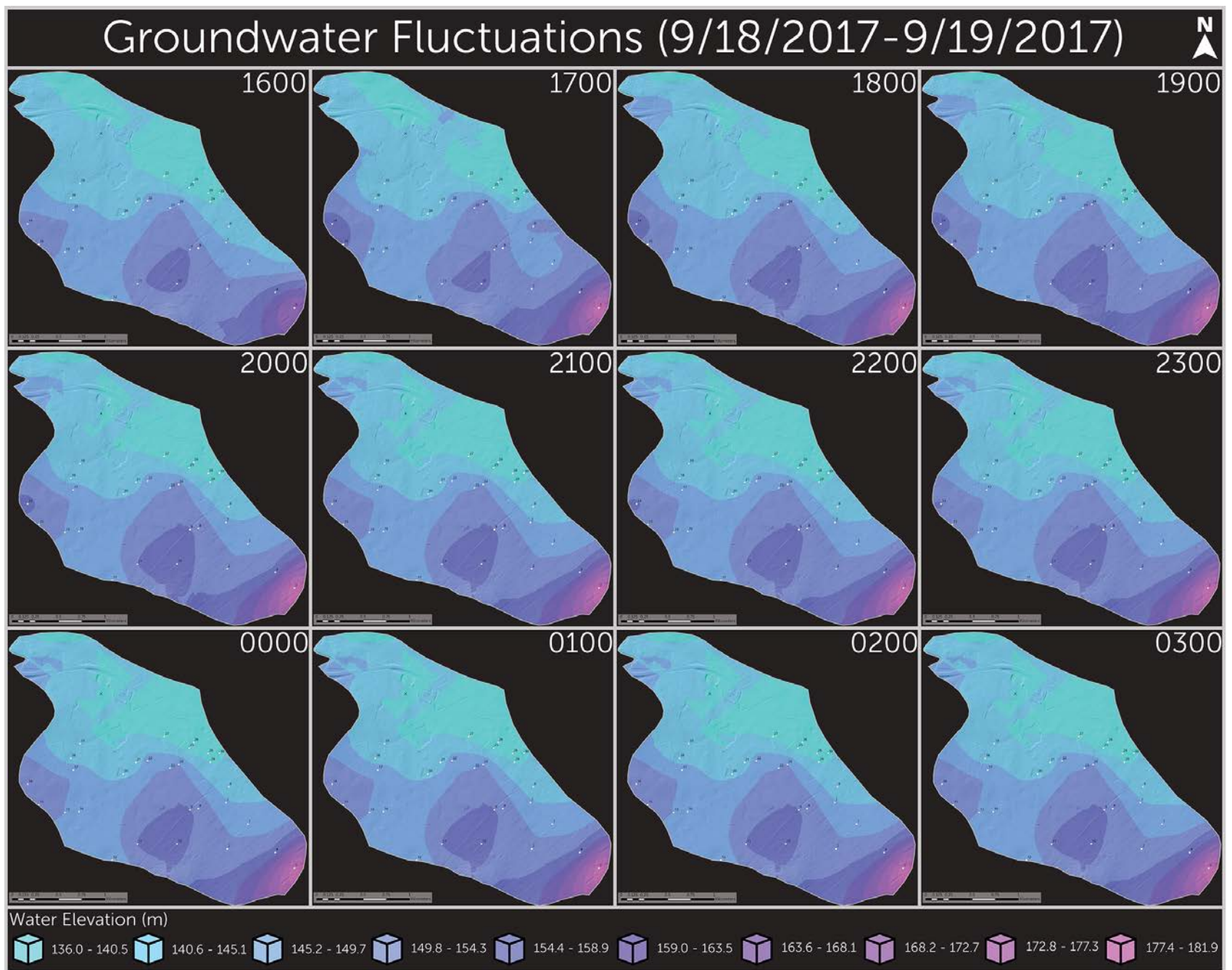


Figure 3.1: New Spring Groundwater Basin. Potentiometric surface fluctuations during storm event (9/18/2017-9/19/2017).

It is evident from the figures above that a lower monitoring resolution would have resulted in data loss and misinterpretation of peak levels and recession rates. Additionally, the hydrograph analysis in combination with water budget calculations reveals that most of the monitored Injection Wells exceed their grate elevation under low intensity storm conditions, and have a low contribution to the overall recharge for the basin. However, analysis of well and spring hydrographs contained in Figure 3.2 indicates that the Injection Well flooding is largely controlled by storm intensity. Moreover, high intensity short duration events result in flooding more often than low intensity long duration events. It should be noted that aquifer response to Injection Well recharge is highly variable and wholly dependent on antecedent conditions. Differences in well response may be attributable karst aquifer heterogeneity. Another important finding can be shown empirically, and validated using the Mann-Kendall trend test. Through examining Figure 3.2, many of the monitored wells are influenced by the hydraulic connectivity of upgradient Injection Wells. The interconnectivity of wells is prevalent across the basin.

Throughout the study numerous Injection Well maintenance and siting issues were discovered. A significant number of Injection Wells in Bowling Green are obstructed with sediment and debris. Proper BMP's, drainage design modifications and regular maintenance could improve longevity and reduce flooding. Also, to improve siting the City should implement a system that utilizes high-volume capacity testing under variable hydrologic conditions, and geophysical site investigations to eliminate the siting of low capacity Injection Wells. The groundwater exceedances from the minor one-year event shown in Figure 3.3 are primarily attributed to poorly sited Injection Wells that have limited connectivity to the aquifer, and thereby, only support borehole storage. Furthermore, it is imperative that guidelines and regulations for the siting, design, and maintenance of Class V Injection Wells are established to prevent flooding as the City continues to expand.

Originally, this project sought to develop a distributed physical model to predict groundwater response to precipitation events, but due to time constraints and lack of essential data, the model development was postponed. However, outside of this project, work is being conducted to develop a ANN model that would use the data collected in this project to predict groundwater response to precipitation events. It is believed that using an ANN model would be more cost-effective and accurate at forecasting groundwater levels than a physically based model because the flexibility and ease of the model architecture.

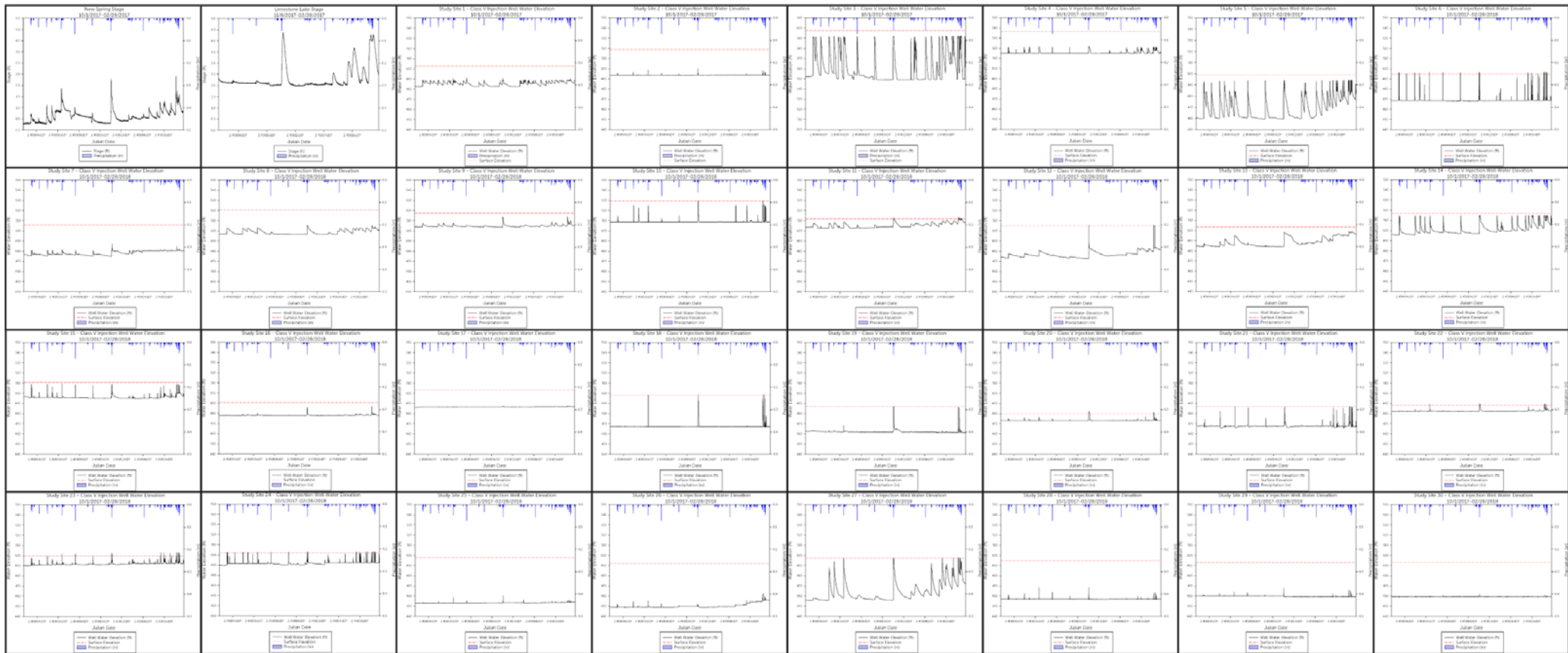


Figure 3.3: New Spring Groundwater Basin - Class V Injection Well and Surface Waterbody Hydrographs over the monitoring period

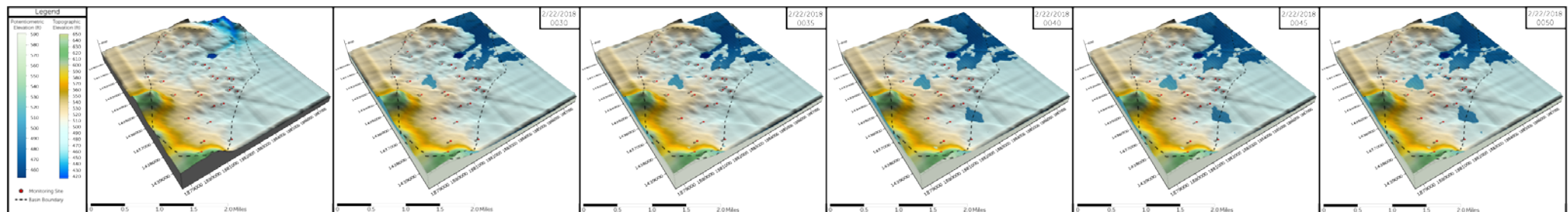


Figure 3.3: New Spring Groundwater Basin. Potentiometric surface fluctuations during storm event (2/22/2018)

## References

- Crawford, N.C., 1982. *Hydrogeologic problems resulting from development upon karst terrain, Bowling Green, KY*. Bowling Green, Kentucky: United States Environmental Protection Agency, 1-33.
- Crawford, N.C., Groves, C.G., Feeney, T.P. & Keller, B.J., 1987. *Hydrogeology of the Lost River karst groundwater basin, Warren County, Kentucky*. Bowling Green, Kentucky: Kentucky Division of Water and Barren River Area Development District, 1-124.
- Federal Emergency Management Agency, 2016. *Things You Can Do To Mitigate Against Flooding*. Available online at: <<https://www.fema.gov/blog/2012-03-14/things-you-can-do-mitigate-against-flooding>> [Accessed 11/25/2016].
- Nedvidek, D.C., 2014. *Evaluating the Effectiveness of Regulatory Stormwater Monitoring Protocols on Groundwater Quality in Urbanized Karst Regions*. M.S. Geoscience Thesis, Department of Geography and Geology, Western Kentucky University, Bowling Green, Kentucky. Available online at: <http://digitalcommons.wku.edu/theses/1407/>
- National Flood Insurance Program, 2016. *Flooding History*. Available online at: [https://www.floodsmart.gov/floodsmart/pages/media\\_resources/fact\\_floodfacts.jsp](https://www.floodsmart.gov/floodsmart/pages/media_resources/fact_floodfacts.jsp)
- Zhou, W., 2007. Drainage and flooding in karst terranes. *Environmental Geology* 51(6), 963–973.



# Optimizing yield and water use efficiency of soybean production in Kentucky - experimental and modeling approach

## Basic Information

<b>Title:</b>	Optimizing yield and water use efficiency of soybean production in Kentucky - experimental and modeling approach
<b>Project Number:</b>	2017KY270B
<b>Start Date:</b>	3/1/2017
<b>End Date:</b>	2/28/2018
<b>Funding Source:</b>	104B
<b>Congressional District:</b>	KY 1st
<b>Research Category:</b>	Climate and Hydrologic Processes
<b>Focus Categories:</b>	Agriculture, Irrigation, Water Use
<b>Descriptors:</b>	None
<b>Principal Investigators:</b>	Montserrat Salmeron

## Publication

1. Bernard, Maria Morrogh and Montserrat Salmeron Cortasa, 2018, Optimizing Yield and Water Use Efficiency of Soybean Production in Kentucky- Experimental and Modeling Approach, in Proceedings of the 2018 Kentucky Water Resources Annual Symposium, Kentucky Water Resources Research Institute, Lexington, Kentucky, p. 35.

# **Optimizing Yield and Water Use Efficiency of Soybean Production in Kentucky - Experimental and Modeling Approach**

## **Problem and Research Objectives**

We proposed the use of mechanistic crop simulation models in combination with field research trials to study soybean genotype x management x environment interactions that aim at increasing water productivity and sustainability. The specific objectives were:

Objective 1: (Mar 2017 - Nov 2017) Obtain the yield response to planting date for different MG cultivars at two locations in Kentucky under field conditions with no water limitation and under rainfed conditions. Six additional rainfed trials with one planting date were added. Note some modifications in the initial experimental design in section B below.

Objective 2: (Nov 2017 – Dec 2017) Evaluate the applicability of a calibrated crop simulation model to predict soybean development and the yield response across the treatments tested with a parametrization of soil properties based on soil texture.

Objective 3: (Jan 2018 – Mar 2018) Produce preliminary long term simulations for multiple combinations of soybean MG choices, planting dates, locations, and soil profiles that will allow investigating management options that optimize grain yield productivity and WUE.

Objective 4: (Mar 2018) Provide preliminary estimates of water use to the USGS for different climatic regions in Kentucky, different water management (irrigated vs. rainfed), and different soil types, that can be used as inputs for hydrological units (HUC12).

## **Methodology**

Field experiments were established at the two locations initially proposed located at the UK research farm facilities at Lexington and Princeton, KY. These trials had a main irrigation treatment with two levels (irrigated vs. rainfed). In addition, rainfed trials with one planting date were conducted at six other locations throughout the state (Calloway, Breckinridge, Hancock, Butler, Cumberland, and Pulaski county). These locations were added to further evaluate model predictions across rainfed environments in the state.

The experimental design at Lexington and Princeton included four cultivars randomized within each soybean maturity group (MG) from 2 to 5, making a total of 16 cultivars (instead of the 12 initially proposed). Two Lexington and one Princeton planting dates were established instead of the four proposed, due to low availability of planting machinery. Trials had a total of 256 plots (Lexington), 128 plots (Princeton), and 64 plots (Calloway, Breckinridge, Hancock, Butler, Cumberland, and Pulaski county). Additional data collection coordinated by Maria Morrogh at Lexington and Princeton included:

- Close monitoring of developmental stages
- Estimation of light interception from digital images
- Destructive samplings for estimation of crop growth rate and seed growth rate. A total of 1,536 destructive samples were collected at Lexington, and 600 samples at Princeton.
- Final yield and grain moisture, yield components.
- Node number and plant height.
- Lodging ratings.

In the irrigated treatments at Lexington and Princeton, KY, we installed a drip irrigation system. Irrigated treatments were watered when the crop evapotranspiration demand reached a 30 mm deficit. Flow meters were installed to quantify the amount of irrigation water supplied. To date, we applied 250 (May planting date) and 230 mm (June) of irrigation water in Lexington, and 300 mm in Princeton.

Crop modeling activities: Data from the irrigated treatments at Lexington and Princeton will be used for calibration of cultivar coefficients in the DSSAT-CROPGRO-Soybean model (Hoogenboom *et al.*, 2012) under conditions of no water limitations. The detailed phenological data, in-season data, and final yield and yield components will be used to calibrate the model to obtain good model predictions in the irrigated treatments. After cultivar coefficients are calibrated, the soil parameters in the model will be adjusted if necessary to improve predictions in the rainfed treatments. Soil parameters that influence the plant soil available water will be modified to resemble the observed in-season growth and final yield.

Prediction of evapotranspiration across sites and managements: Once the DSSAT-CROPGRO-Soybean model has been calibrated to predict timing of developmental stages, growth, yield and yield components across the three main experimental sites, it will be used to quantify evapotranspiration for each treatment. In addition, the model will be tested for yield prediction in the rainfed trials across sites in KY based on different levels of soil input data. This model evaluation can provide valuable information on the applicability of the model to predict yield differences across different sites and soil types in the state.

## **Principal Findings and Significance**

Objective 1: Quantify yield potential and yield gap due to water limitations across environments, genotypes and management options.

We quantified the yield potential across soybean MG cultivars at three different irrigated environments, and at 8 rainfed environments. The yield potential under irrigated conditions was highly dependent on the environment and MG choice, ranging from 56 to 87 bu/ac. The yield response to irrigation ranged from no response to a 30% yield increase. The effect of cultivar selection within a MG was relatively small relative to the effect of MG selection. MG 2 to 4 had the highest yield potential for the May planting date in Lexington (83 bu/ac), whereas MG 3 and 4 were best for the June planting date (71 bu/ac). At Princeton, MG 4 was the best choice (81 bu/ac), and selection of MG 3 cultivars reduced yields by 14%.

Yields under rainfed conditions showed higher variability in yields across sites and MG cultivars compared to the irrigated treatments (Figure 1 and 2). This is likely due to different soil water availability at each site, as well as different precipitation patterns.

These results evidence the need to optimize MG selection at each environment to maximize yield potential under irrigation. Data from more years combined with crop model simulations could help investigate MG choices that increase the probability of high yields under rainfed conditions.



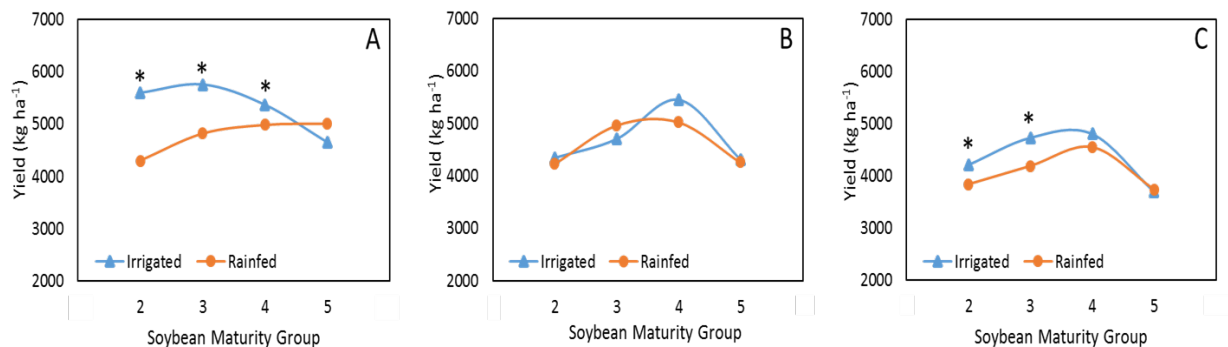


**Figure 1:** Soybean yield ( $\text{kg ha}^{-1}$ ) by maturity group (MG) under irrigated and rainfed condition at Lexington, planted May 16 (A), Princeton, planted May 15 (B), and Lexington, Planted June 15 (C). The asterisk (\*) represent a significant yield increase due to irrigation within a MG and environment. Least significant difference (LSD) of 567.04, 508.6 and 310.1  $\text{kg ha}^{-1}$  for environment 1, 2 and 3 respectively,  $p < 0.05$ .

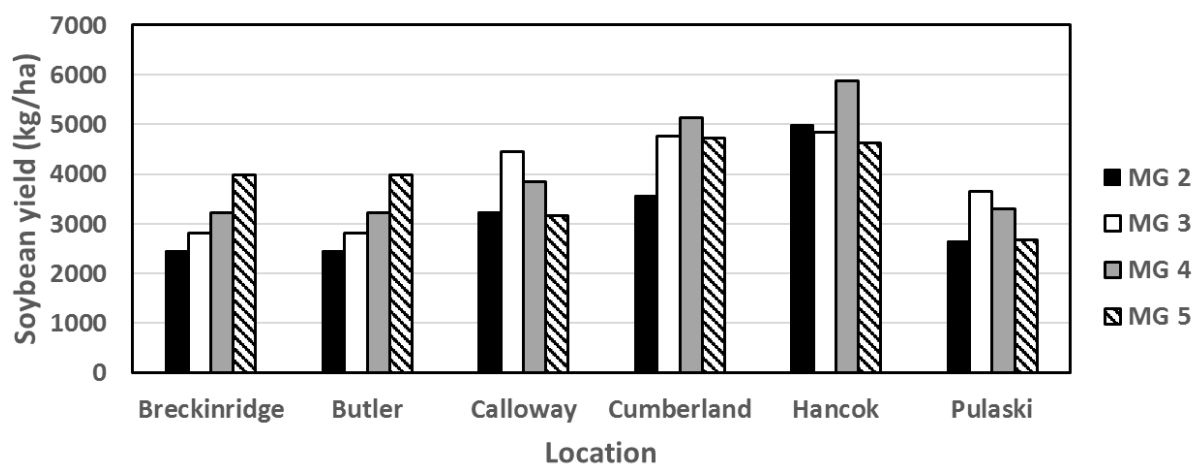


**Figure 2:** Soybean yield ( $\text{kg ha}^{-1}$ ) by maturity group (MG) under rainfed condition at five locations across Kentucky (Breckinridge, Butler, Calloway, Cumberland, Hancock, Pulaski).

Objective 2: Evaluate the applicability of a calibrated crop simulation model to predict soybean development and yield.

The model was efficient in the prediction of developmental stages after calibration with experimental data (Figure 3), with a root mean square error of 3.8 days in the total duration of the growing season. A preliminary evaluation of yield prediction with generic cultivar coefficients obtained for Midsouth conditions (Salmeron *et al.*, 2017) indicate the need to further calibrate crop coefficients for growth and partitioning (Figure 4). The model was more accurate in the prediction of yield under irrigated treatments (RMSE= 336  $\text{kg/ha}$ ) compared to rainfed conditions (RMSE=608  $\text{kg/ha}$ ). We will continue calibration activities to improve prediction of in-season biomass and yield potential under irrigated conditions. In a next step, we will calibrate soil properties to improve model predictions under rainfed conditions.

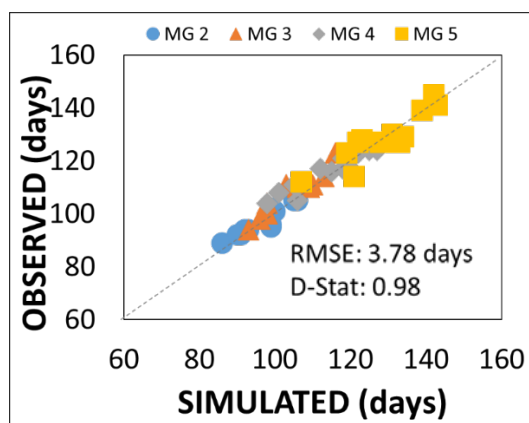


**Figure 3:** Observed and simulated duration of the crop growing cycle (emergence to physiological maturity). Data simulated with DSSAT-CROPGRO-Soybean after calibration with observed data.

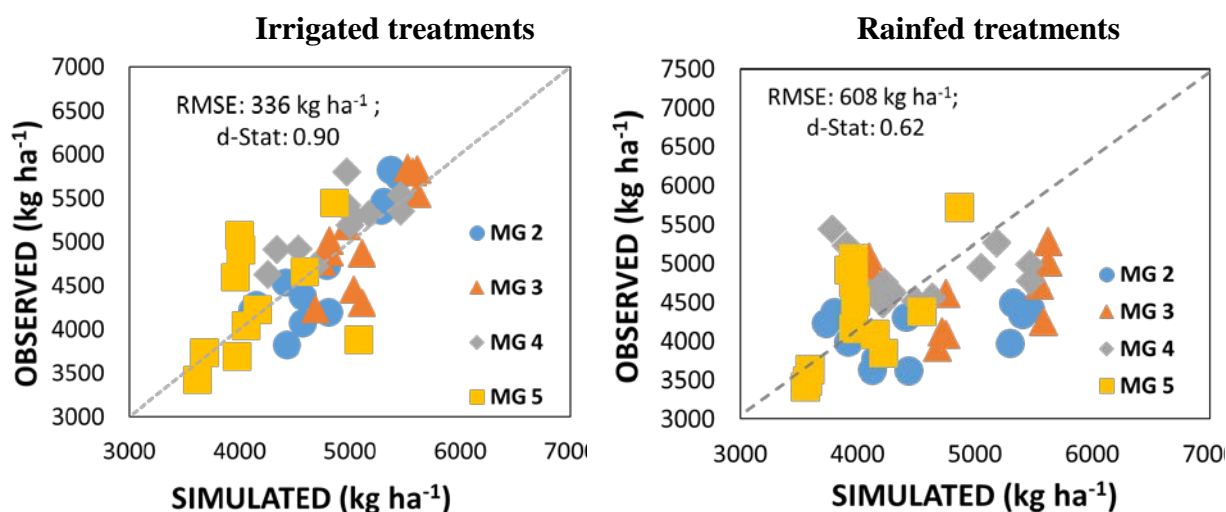


**Figure 4:** Observed and simulated yield for the irrigated treatments (left) and rainfed treatments (right) for the main trials at Princeton (planted in May), and Lexington (planted in May and June).

Objective 3: Produce a dataset with extensive genotype x management x environment combinations to investigate strategies to maximize crop productivity and water use efficiency.

Experiment and weather files at 8 of the 9 locations (Butler, Calloway, Cumberland, Hancock, Pulaski, Lexington, and Princeton) across the state have been prepared for generation of this dataset. We will finalize this dataset after model calibration has been completed.

Objective 4: Provide preliminary estimates of water use to the USGS for different environments, managements, and soil types in KY.

We will finalize this dataset once we have completed model calibrations.

Figure 5 shows a preliminary analysis of evapotranspiration estimation for irrigated treatments in the three main experimental sites. Preliminary results show a large potential to optimize both yield and water use efficiency with management decisions (Figure 4). Under irrigated conditions, early soybean maturities would allow to increase or maintain crop productivity and reduce water requirements compared to full-season and late soybean maturities.

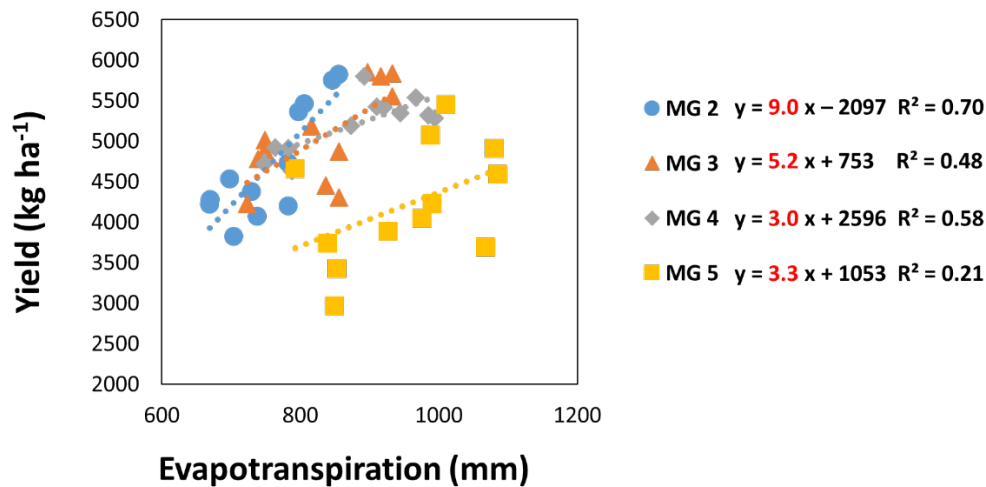


**Figure 5:** Relationship between observed yield and evapotranspiration estimated for each treatment with DSSAT-CROPGRO-Soybean. Data from irrigated treatments only. The slope of the relationship represents water use efficiency (kg ha<sup>-1</sup> mm<sup>-1</sup>) and is indicated in red.

## References

Hoogenboom, G., Jones, J. W., Wilkens, P. W., Porter, C. H., Boote, K. J., Hunt, L. A., Singh, U., Lizaso, J. L., White, J. W., Uryasev, O., Royce, F. S., Ogoshi, R., Gijsman, A. J., Tsuji, G. Y., and Koo, J. (2012). "Decision Support System for Agroecology Transfer (DSSAT) Version 4.5.023.," University of Hawaii, Honolulu, Hawaii.

Salmerón, M., and Purcell, L. C., Vories, E.D., Shannon, G. (2017). Simulation of soybean genotype-by-environment interactions for yield under irrigation in the Midsouth with DSSAT-CROPGRO. *Agricultural systems* 150: 120-129

## Water quality analysis in municipal water supply system for Lexington, KY with a focus on corrosivity

### Basic Information

<b>Title:</b>	Water quality analysis in municipal water supply system for Lexington, KY with a focus on corrosivity
<b>Project Number:</b>	2017KY271B
<b>Start Date:</b>	3/1/2017
<b>End Date:</b>	2/28/2018
<b>Funding Source:</b>	104B
<b>Congressional District:</b>	KY 6th
<b>Research Category:</b>	Water Quality
<b>Focus Categories:</b>	Water Quality, Surface Water, Water Supply
<b>Descriptors:</b>	None
<b>Principal Investigators:</b>	Junfeng Zhu, Alan Fryar

### Publication

1. Sherman, Amanda R., Ronald J. Merrick, Junfeng Zhu, Alan E. Fryar, and Brian D. Lee, 2018, Water Quality Analysis in Municipal Water Supply System for Lexington, KY, with a Focus on Corrosivity, poster presentation at the 2018 Kentucky Water Resources Annual Symposium, Kentucky Water Resources Research Institute, Lexington, Kentucky.

# **Water Quality Analysis in Municipal Water Supply System for Lexington, KY with a Focus on Corrosivity**

## **Problem and Research Objectives**

Exposure to lead via ingestion poses human health risks (HHR), especially in small children exposed to lead paint (DeNoon, 2007). The 2016 water crisis in Flint, Michigan brought this fact back to the public eye (Sanburn, 2016) and reframed the term “ingestion” to include lead present in water (Hanna-Attisha et al., 2016). Water provided by public water supply systems is presumed to be free of HHRs and treated to government-established drinking water standards. Historically, lead releases from public water systems have been correlated to changes in water treatment processes or chemicals (Edwards and Triantafyllidou, 2007). The unique aspect of Flint was the release of lead due to a change in source water from Lake Huron, which has a low chloride-sulfate mass ratio (CSMR), to the Flint River with a high CSMR (Masten, 2016). CSMR values are used to establish water’s corrosivity (the potential or ability to corrode pipes and solder materials) and, if present, lead can be potentially released when CSMR values are above 0.58 (Edwards and Triantafyllidou, 2007).

$$CSMR = \text{Concentration of } Cl^- / \text{Concentration of } SO_4^{2-}$$

The Flint water crisis led many to question the safety of their own drinking water. In Spring 2016, University of Kentucky students from the hydrogeology class (EES 585) collected and analyzed eight water samples from their homes. The results were unexpected. While none of the samples exceeded the EPA’s drinking water maximum contaminant level (MCL) for lead (15 µg/L), the sampled water had a higher corrosivity than the drinking water in Flint based on the CSMR. The average CSMR from these samples was 2.9 whereas a CSMR of 1.6 (Masten, 2016) was reported for the drinking water in Flint.

Concerned with the observed high corrosivity, we conducted a follow-up study to evaluate Lexington’s public water supply (PWS) water corrosivity and its seasonal variation. We hypothesize: 1) the high corrosivity observed in Spring 2016 is a result from winter road salt application (Stranko et al., 2013) and the observed low level of lead in drinking water, despite a high CSMR value, is due to the addition of corrosion inhibitors (Edwards and McNeil, 2002) and 2) water quality changes in relation to approximate pipe travel distance and pipe material.

## **Methodology**

A GIS ArcMap model was developed to aide in the selection of 11 PWS sampling locations within New Circle Road by employing the Cost Distance tool in ArcGIS. The tool determines the risk for metals leaching into drinking water with an assigned pipe material relative risk rating that based upon associated HHRs for each type of pipe

construction material (Table 1), pipe diameter, and pipe distance from the PWS treatment plant.

$$\text{Corrosivity relative risk ranking} = \text{pipe material relative risk rating} \times \text{pipe diameter} \times \text{pipe distance}$$

The resulting model visually ranked the distribution network showing areas of calculated relative corrosivity risk ranking from low (value 1) to high (value 5) risk for the potential to leach metals from pipes under corrosive conditions. The 11 sample sites were then selected to cover areas with different risks (Figure 1). One additional site was a source water sample from the Kentucky River collected near the Lexington's PWS intake.

Pipe Material Relative Risk Rating	Pipe Construction Material
1	Lock Joint, Mechanical Joint, Asbestos Cement, Concrete, Polyethylene, Polyvinyl Chloride
2	Steel
3	Cast Iron-Concrete Lined, Ductile Iron-Concrete Lined, Ductile Iron-Steel Lined
4	Ductile Iron
5	Copper, Galvanized, Unknown

Table 1. Pipe material relative risk rating based on associated HHRs for each type of pipe construction material rated 1-5, low to high.

To assess seasonal variation and possible road salt contribution to corrosivity, the 12 selected sites were sampled in Spring and Fall 2017. The samples were collected in accordance with EPA protocols for monitoring requirements of lead and copper in tap water (EPA 2016 b, c). At the time of collection, standard water quality parameters (pH, temperature, DO, specific conductance), as well as, phosphate and silica, were measured. Phosphate and silica are commonly used corrosion inhibitors. The samples were analyzed for metals and major ions by inductively coupled plasma-optical emission spectroscopy (ICP-OES) at the Kentucky Geological Survey (KGS) laboratory in accordance with the KGS Laboratory Services Quality Assurance Plan (KGS, 2009). Sample results were compared to EPA drinking water standards (EPA 2016 a, d).

Correlation and statistical analysis were conducted with Kendall's Tau and Pearson correlation to evaluate relative risk rankings and distance with lead, copper, and iron concentrations and CSMR values.

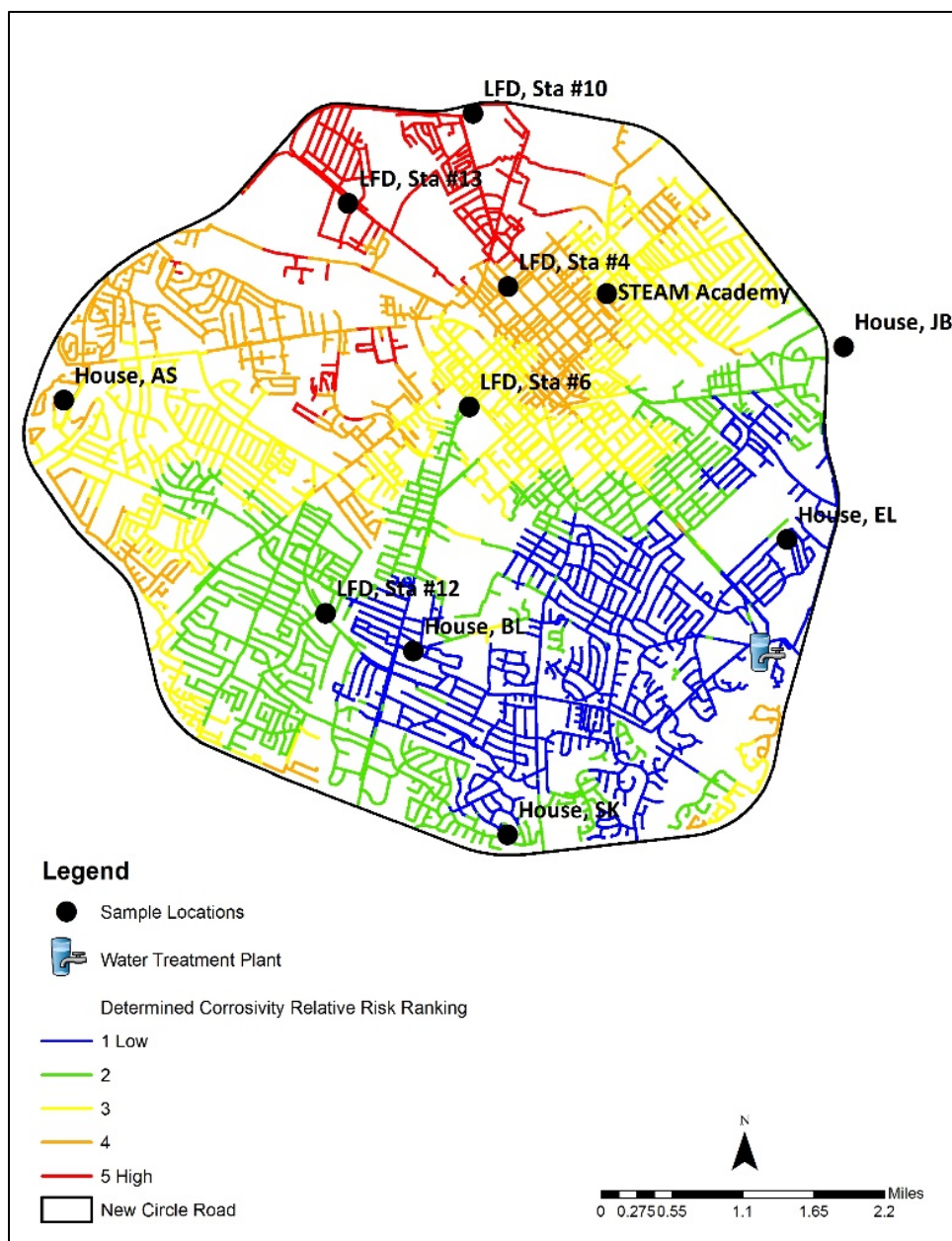


Figure 1. Eleven selected sampling locations inside New Circle Road, along with relative corrosivity risk rankings.

## Principal Findings and Significance

The chemical analysis showed one sample site exceeded the drinking water MCL for lead and four for iron. Iron is a secondary drinking water contaminant. The average CSMR value was 0.184 for Spring 2017 and 0.417 for Fall 2017 (Figure 1); both were much lower than that observed value of 2.9 in Spring 2016 (Table 2). From Pearson and Kendall's Tau correlations, the data indicated that the concentrations of dissolved metals

increased with pipe distance and were affected by pipe construction material. Also, indicated is that the ArcGIS model can identify potential areas of concern for metals leaching in Lexington's PWS system. The measured phosphate and silica concentrations suggested that corrosion inhibitors are used in treating Lexington's drinking water. The silica concentrations closely mirrored those in the KY River, while phosphate concentrations are present in samples post the PWS treatment.

			Spring 2017				Fall 2017			
Method Detection Limit (MDL)			0.005	0.002	0.010		0.005	0.002	0.010	
Maximum Contaminant Level (MCL)			1.3*	0.3	0.015*	≥ 0.58	1.3*	0.3	0.015*	≥ 0.58
<i>Site Id</i>	<i>Corrosivity Relative Risk Ranking</i>	<i>Linear Distance from PWS Plant (ft.)</i>	<i>Copper, Total by ICP</i>	<i>Iron, Total by ICP</i>	<i>Lead, Total by ICP</i>	<i>CSMR</i>	<i>Copper, Total by ICP</i>	<i>Iron, Total by ICP</i>	<i>Lead, Total by ICP</i>	<i>CSMR</i>
House, EL	1	4533	0.01	0.16	< 0.01	0.234	0.03	0.26	< 0.01	0.974
House, JB	2	12751	0.06	0.002	< 0.01	0.270	0.08	0.002	< 0.01	0.328
House, SK	2	13038	0.08	<b>0.5</b>	< 0.01	0.171	0.06	0.19	< 0.01	0.288
House, BL	1	14438	0.06	0.002	< 0.01	0.178	0.07	0.002	< 0.01	0.589
LFD, Sta #6	3	15666	0.05	0.002	< 0.01	0.186	0.06	0.02	< 0.01	0.863
STEAM	3	15907	0.76	0.002	< 0.01	0.181	0.64	0.002	< 0.01	0.460
LFD, Sta #4	4	18186	0.08	0.05	< 0.01	0.203	0.11	0.06	< 0.01	0.408
LFD, Sta #10	5	24960	0.34	<b>3.85</b>	<b>0.05</b>	0.179	0.29	<b>0.83</b>	<b>0.02</b>	0.328
LFD, Sta #13	5	24986	0.02	0.01	< 0.01	0.192	0.07	0.008	< 0.01	0.528
House, AS	4	30429	0.46	<b>0.49</b>	< 0.01	0.136	0.05	<b>0.97</b>	0.01	0.251
KY River	0	47743	0.006	<b>6.76</b>	0.01	0.065	0.03	<b>26.6</b>	<b>0.03</b>	0.081
Pearson Correlation Corrosivity Relative Risk Ranking			0.384	0.385	0.350	-0.632	0.214	0.408	0.471	-0.416
Kendall's Tau Correlation Corrosivity Relative Risk Ranking			0.241	0.279	0.422	-0.094	0.289	0.220	0.422	-0.262
Pearson Correlation Distance from PWS Treatment Plant			0.384	0.385	0.350	-0.632	0.082	0.595	0.350	-0.581
Kendall's Tau Correlation Distance from PWS Treatment Plant			0.341	0.215	0.248	-0.244	0.159	0.230	0.248	-0.315

Notes: \* indicates established action level and red, bold values exceed MCLs

Table 2. Spring and Fall 2017 sampling results with site associated corrosivity relative risk ranking and distance from PWS treatment plant. Includes Pearson and Kendall's Tau correlation with respect to distance and corrosivity relative risk ranking.



Our study provides a better understanding of tap water quality in Lexington, especially water's corrosivity and potential risks. Water corrosivity appears to be low in general, but can increase significantly during icy/snowy winters with high road salt application. The presence of phosphate-based and silica-based corrosion inhibitors likely lessen the leaching of metals under corrosive conditions, but risk remains. The increases in metal concentrations with pipe distance and the influence of pipe material on metal concentrations require the local drinking water agencies pay close attention to areas with high risk of metal leaching. The ArcGIS model developed in this study can be helpful in locating potential areas of concern for metals leaching in Lexington's water supply distribution system.

## References

Edwards, Marc and Laurie S. McNeil. 2002. "Effect of Phosphate Inhibitors on Lead Release from Pipes." *Journal AWWA* 94 (1): 79-90.

Edwards, Marc, and Triantafyllidou, Simoni. 2007. "Chloride-to-Sulfate Mass Ratio and Lead Leaching to Water." *Journal AWWA* 99 (7): 96-109.

Environmental Protection Agency (EPA). 2016a. "National Primary Drinking Water Regulations." *Code of Federal Regulations*, Title 40, Part 141, Subpart G National Primary Drinking Water Regulations.

Environmental Protection Agency (EPA). 2016b. "Monitoring requirements for lead and copper in tap water." *Code of Federal Regulations*, Title 40, Part 141, Subpart I Control of Lead & Copper, Section § 141.86 - Monitoring requirements for lead and copper in tap water.

Environmental Protection Agency (EPA). 2016c. "Monitoring requirements for water quality parameters." *Code of Federal Regulations*, Title 40, Part 141, Subpart I Control of Lead & Copper, Section § 141.87 - Monitoring requirements for water quality parameters.

Environmental Protection Agency (EPA). 2016d. "National Secondary Drinking Water Regulations." *Code of Federal Regulations*, Title 40, Part 143, Subpart G National Secondary Drinking Water Regulations.

DeNoon, Daniel J. 2007. "Lead Poisoning and Kids." *WebMD*. Accessed September 2016. <http://www.webmd.com/children/news/20070815/lead-poisoning-and-kids#1>

Hanna-Attisha, Mona; LaChance, Jenny; Sadler, Richard Casey; and Schneep, Allison. "Elevated Blood Levels in Children Associated with the Flint Drinking Water Crisis: A Spatial Analysis of Risk and Public Health Response." *AJPH Research* 106 (2): 283-290.

Kentucky Geological Survey (KGS). 2009. "Quality Assurance Plan." University of Kentucky, Kentucky Geological Survey, Laboratory Services.

Masten, Susan. 2016. "Flint Water System, How Could Things Go So Wrong?" Presented to Lyman Briggs College, January 2016. Accessed March 2016. <http://www.lymanbriggs.msu.edu/SpeakerSeries/Masten16.pdf>

Sanburn, Josh. 2016. "The Toxic Tap, How a Disastrous Chain of Events Corroded Flint's Water System - and the Public Trust." *Time*, February 1, 2016: 33-39.

Stranko, Scott; Bourquin, Rebecca; Zimmerman, Jenny; Kashiwagi, Michael; McGinty, Margaret; and Klauda, Ron. 2013. "Do Road Salts Cause Environmental Impacts?" Maryland Department of Natural Resources, Monitoring and Non-tidal Assessment Division. Manuscript: 1-33.

## Soil moisture conditions and yield across slope positions under western Kentucky irrigated management

### Basic Information

<b>Title:</b>	Soil moisture conditions and yield across slope positions under western Kentucky irrigated management
<b>Project Number:</b>	2017KY272B
<b>Start Date:</b>	3/1/2017
<b>End Date:</b>	2/28/2018
<b>Funding Source:</b>	104B
<b>Congressional District:</b>	KY 1st
<b>Research Category:</b>	Climate and Hydrologic Processes
<b>Focus Categories:</b>	Irrigation, Agriculture, Conservation
<b>Descriptors:</b>	None
<b>Principal Investigators:</b>	Brad Lee

### Publication

1. Bowling, Jessie, Brad Lee, E. Glynn Beck, Carrie Knott, John H. Grove, Edwin Ritchey, and Jerry McIntosh, 2018, Soil moisture conditions and yield across slope positions under western Kentucky irrigated management, poster presentation at the 2018 Kentucky Water Resources Annual Symposium, Kentucky Water Resources Research Institute, Lexington, Kentucky.

# Soil moisture conditions and yield across slope positions under western Kentucky irrigated management

## Problem and Research Objectives

There has been a significant increase (204 percent) in the number of high-yield (300 to 1,200 gal/min) agricultural irrigation wells installed in the northern portion of the Mississippi Embayment in western Kentucky since the drought of 2012. Because large scale irrigation is relatively new to Kentucky, little is known about irrigated row-crop management in the state.

The objective of this study was to demonstrate the utility of off-the-shelf water management technology including soil moisture sensors and discharge flowmeters to producers to a common soil in western Kentucky.

## Methodology

A 165 acre no-till, corn-soybean rotation field in eastern Hickman County was selected for this study (Fig. 1). Approximately 116 acres of this field have been irrigated since 2013. The field was planted in corn during the monitoring period of this study.

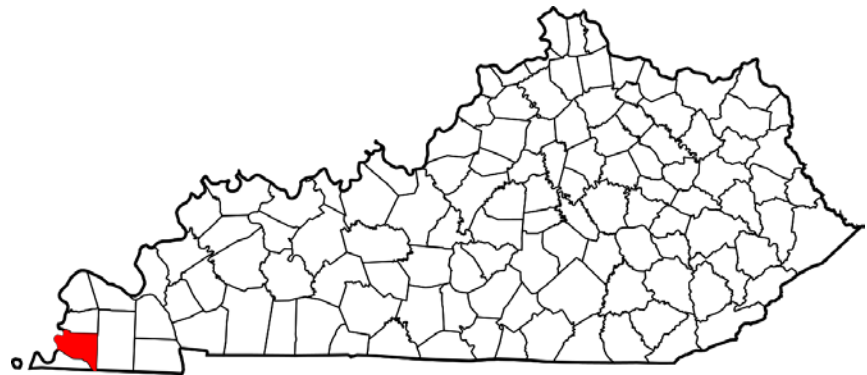
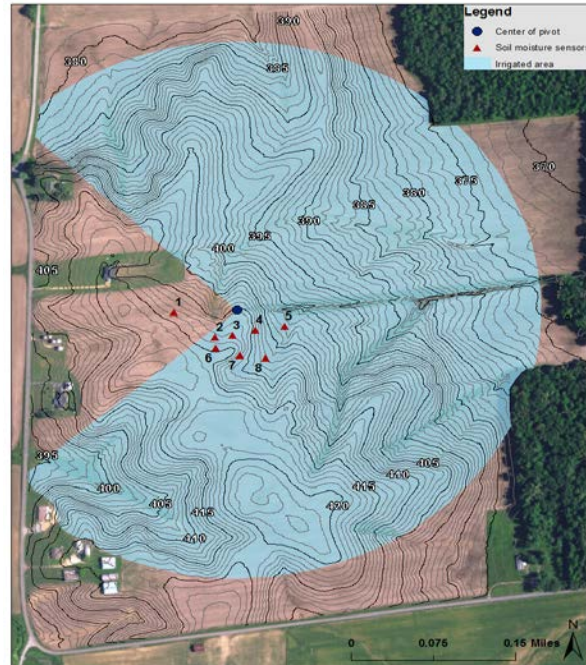


Figure 1. County map of Kentucky. Hickman County highlighted.

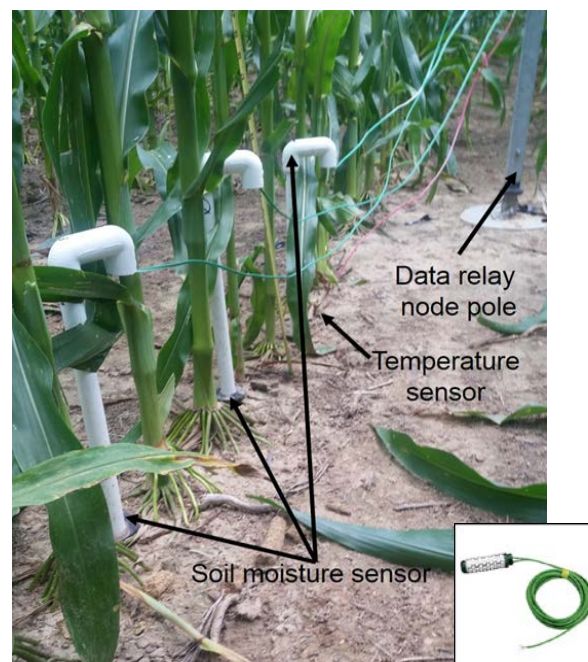
The predominant soil at the study site is a Loring silt loam (fine-silty, mixed, active, thermic Oxyaquic Fragiudalf). Multiple soil cores were collected from each landscape position represented in the field and described to confirm the presence and depth of the fragipan. Eight soil moisture sensor stations were installed in the row crop field. Seven sensor stations (stations 2 – 8) were located under the irrigation pivot and one station (station 1) was located outside of the pivot area (Fig. 2).

*Figure 2. Contour map of the study area with the irrigated area (shaded blue) and soil moisture sensor stations (red triangles). Contour interval is 1 ft.*



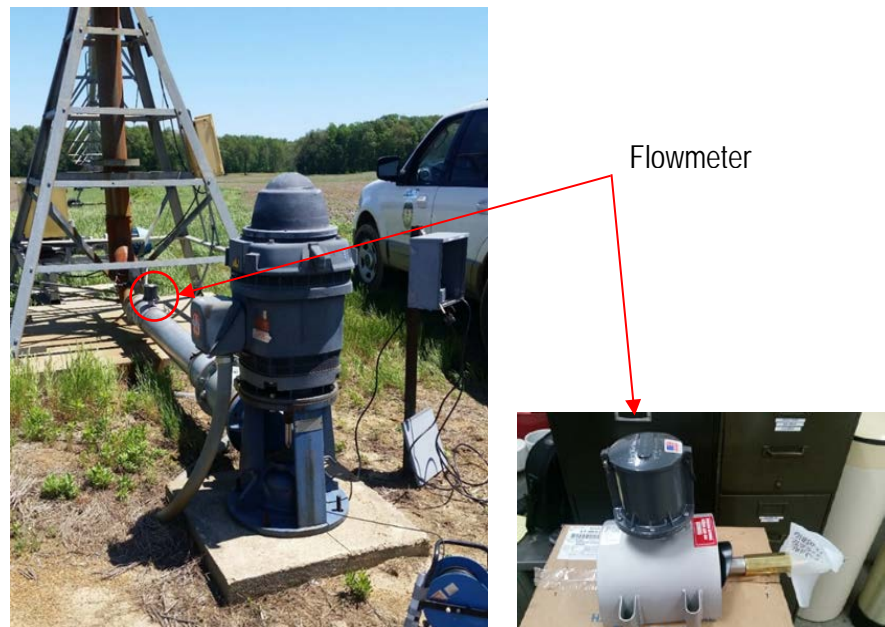
Three soil moisture sensors, a soil temperature sensor and a data relay node were installed at each station (Fig. 3). The soil moisture sensors were installed at a depth of 1ft, 2ft, and 3ft. Soil moisture and temperature data were recorded every 30 minutes, transmitted to a field base station and then transmitted to a web based data portal via cellular gateway every 4 hours.

*Figure 3. Soil moisture and temperature sensors adjacent to relay node at station. Inset image is soil moisture sensor.*



A flowmeter was installed in the production discharge pipe to record the volume of groundwater used during each irrigation event (Fig. 4). Also, a pressure transducer was installed in the production well to measure changes in groundwater elevations during the growing season.

*Figure 4. Flowmeter installed between wellhead and pivot.*



Wet weather delayed the application of nitrogen after planting, which needed to be completed prior to equipment installation. Additionally, technical difficulties with the soil moisture sensor data relay nodes caused us to miss one irrigation event and two rainfall events between May 10<sup>th</sup> and July 18<sup>th</sup> (Fig. 5).

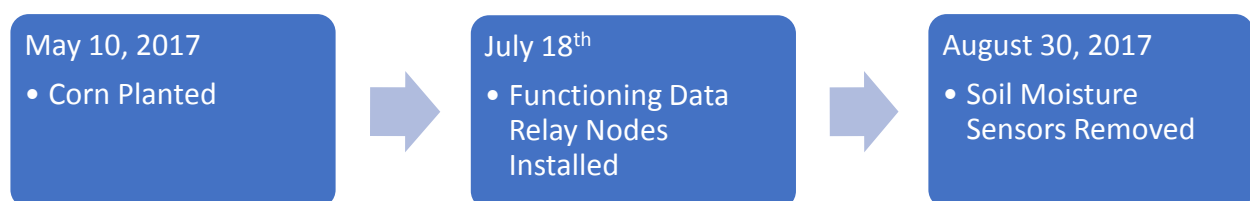


*Figure 5. Timeline of planting to soil moisture sensor removal.*

The soils monitored contained fragipans which are a common pedogenic feature of loess derived soils in western Kentucky. Fragipans are root impermeable layers formed from weak silica bonds between soil particles that slow water infiltration. Essentially the plant roots exist in the soil horizons above the fragipan but not below.



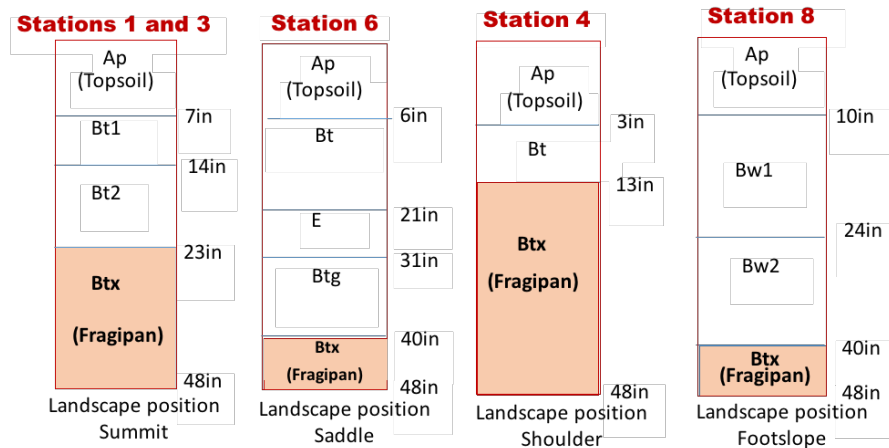


Figure 6. Soil descriptions for stations 1, 3, 4, 6 and 8 showing depth to fragipan and landscape position. Landscape position is moving downslope from left to right.

## Principal Findings and Significance

Soil moisture measurements for the non-irrigated station (station 1) and station 3 are very similar throughout the length of the study period (Fig. 7). However, station 1 showed an increase in soil moisture at the 1ft depth 3 days after a 0.6 in rain event on August 6<sup>th</sup>. Soil moisture at station 3 did not increase in any significantly observable manner after wetting events at Station 3. The lack of increased soil moisture with precipitation events at station 1 and 3 may be indicative summit landscape positions or other soil property (e.g. bulk density near surface, infiltration rate, surface crusting) that were not measured in this study.

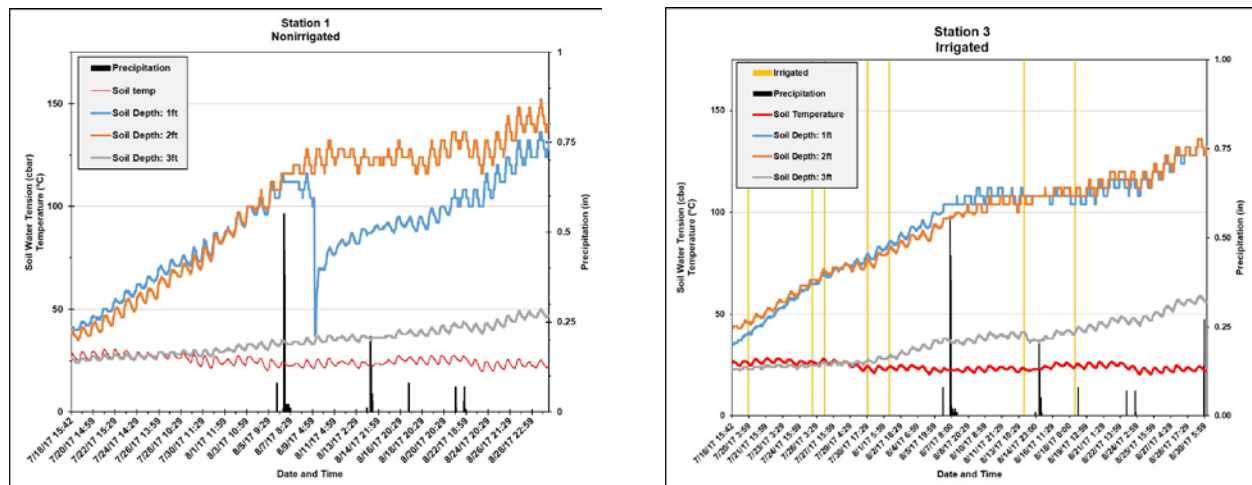
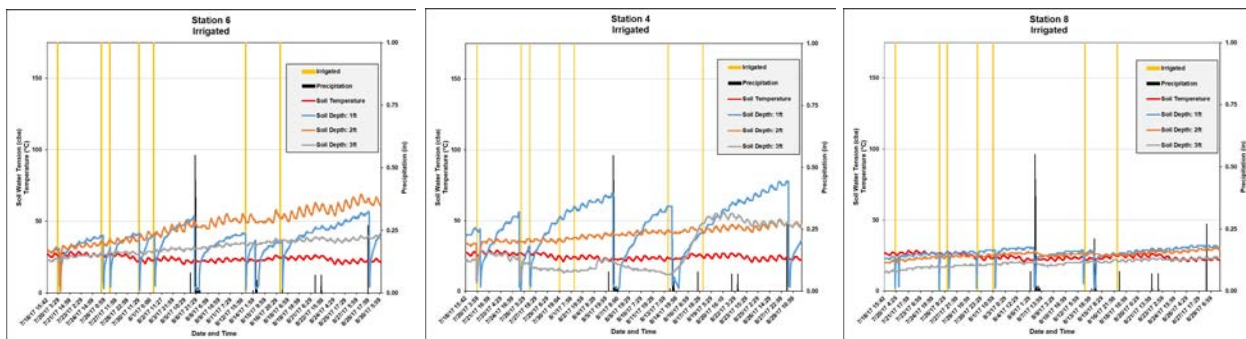


Figure 7. Soil moisture data for stations 1 and 3. Station 1 is a non-irrigated site and station 3 is an irrigated site.

Soil moisture measurements at the 1ft depth interval for stations 6, 4 and 8 are very similar in that soil moisture tends to increase shortly after a wetting event (irrigation or precipitation).

However, soil at the 1ft depth at station 4 tends to lose moisture quicker than at stations 6 and 8 (Fig. 8). This trend is most likely associated with the shallow depth (13in) of the fragipan at station 4, which causes the local soil to have less moisture holding capacity than the other sites. Soil moisture at station 6 for the 2ft and 3ft depth intervals does not increase after wetting events, but does gradually decrease over time (Fig. 8). Soil moisture at the 2ft depth interval at station 4 decreases slowly over time with no response associated with wetting events. However, soil moisture at the 3ft depth interval generally increases after wetting events, but sharply decreases around August 15<sup>th</sup> due to corn roots accessing this water late in the growing season. The increased soil moisture earlier in the growing season at 3ft depth is likely associated with preferential flow paths within the fragipan. The soil at all depths at station 8 contain more moisture throughout the study period than at any of the other stations (Fig. 8). Footslopes accumulate moisture from upslope and the thick solum above the 40in fragipan holds soil moisture.



*Figure 8. Soil moisture data for stations 6, 4, 8 (left to right). Landscape positions are moving downslope from left to right.*

Corn yield averages for the entire agricultural field where the study was conducted is divided into irrigated and non-irrigated acres (Fig. 9). Average bushels per acre for the irrigated and non-irrigated areas were 215 and 197 bushels/acre, respectively. Between May 1<sup>st</sup> and August 30<sup>th</sup> 11.4 in of precipitation fell within the study area. In addition, 2.6 in of water per acre were added via pivot irrigation. The similarity in yield between irrigated and non-irrigated locations is probably due in part to the adequate precipitation that occurred at critical reproductive growth stages, which is required to attain high yields.



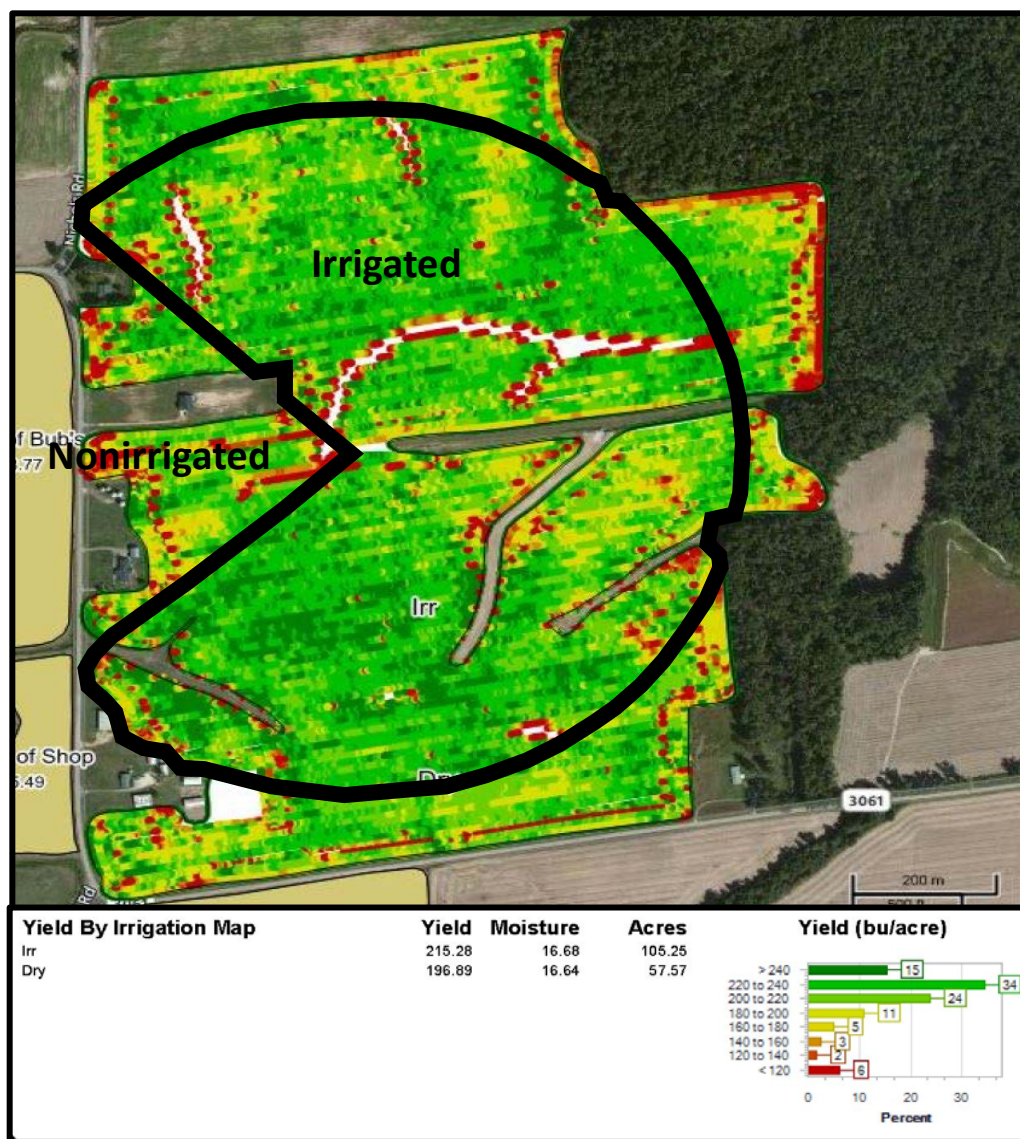
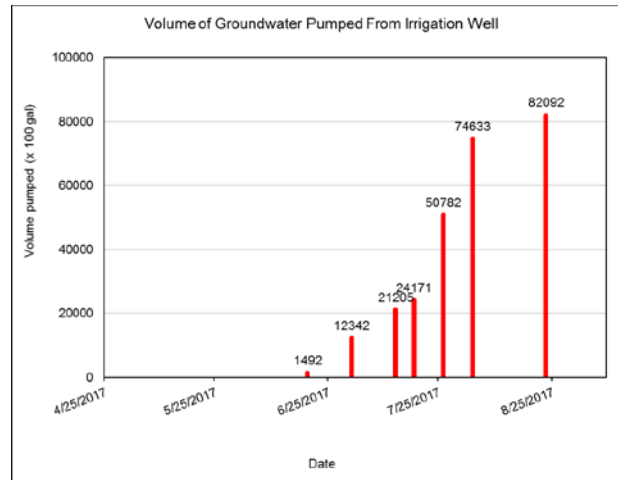


Figure 9. Corn yield map in study field.

Water use was monitored with the flow meter to record the volume of groundwater used per irrigation event and the total volume of groundwater used. Just over 8.2 million gallons of groundwater were used during nine irrigation events (Fig. 10).

*Figure 10. Volume of groundwater used for irrigation.*



The post-irrigation groundwater elevation was approximately 1ft lower than the pre-irrigation elevation and plateaued until January 2018 (Fig. 11).

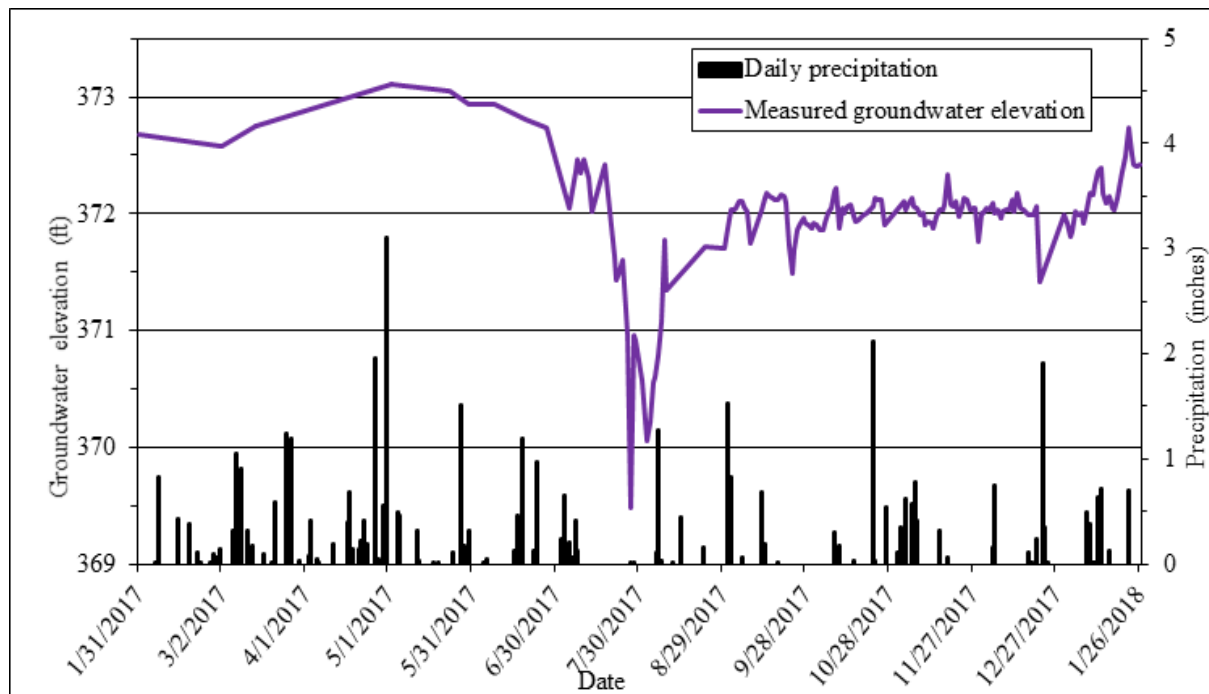


Figure 11. Groundwater elevation data collected at the irrigation well and precipitation data over the study year.

## Conclusions

Off-the-shelf flowmeters and soil moisture sensors that are used extensively in the western U.S. were successfully installed in western Kentucky and used by a corn producer. Soil moisture data indicate that the depth of fragipan and landscape position influence plant available soil moisture.

It appears that weather conditions, in 2017, were suitable for high yields in western Kentucky, with and without pivot irrigation.

Though the farmer appreciated the ability to monitor real-time soil moisture field conditions while away on a 7-day trip, the technical difficulties associated with setting up the system made him hesitant to employ this technology in the future. He instead prefers monitoring soil moisture conditions using a hand-held sensor, obtaining readings at select locations within the field. He was, however, pleased to see the relationship between data obtained with the hand-held sensor and that of the *in-situ* moisture sensors demonstrated with this study.

## **Information Transfer Program Introduction**

Information transfer activities are an important part of the overall program of the Kentucky Water Resources Research Institute. There are two main components, an annual symposium and the institute web sites. The institute also participates and supports numerous other technology transfer activities throughout the year.

## Kentucky information transfer project

### Basic Information

<b>Title:</b>	Kentucky information transfer project
<b>Project Number:</b>	2017KY273B
<b>Start Date:</b>	3/1/2017
<b>End Date:</b>	2/28/2018
<b>Funding Source:</b>	104B
<b>Congressional District:</b>	KY 1-6
<b>Research Category:</b>	Not Applicable
<b>Focus Categories:</b>	None, None, None
<b>Descriptors:</b>	None
<b>Principal Investigators:</b>	Lindell Ormsbee

### Publication

1. 2018 Kentucky Water Resources Annual Symposium Proceedings, Kentucky Water Resources Research Institute, Lexington, KY, 94 p.

## **Kentucky Information Transfer Project (2017KY273B)**

### **Problems and Objectives**

The Water Resources Research Act requires that Institutes or Centers shall:

- 1) plan, conduct, or otherwise arrange for competent applied and peer reviewed research that fosters -
  - (A) improvements in water supply reliability
  - (B) the exploration of new ideas that -
    - (i) address water problems; or
    - (ii) expand understanding of water and water-related phenomena;
  - (C) the entry of new research scientists, engineers, and technicians into water resources fields; and
  - (D) the dissemination of research results to water managers and the public.
- 2) cooperate closely with other colleges and universities in the State that have demonstrated capabilities for research, information dissemination, and graduate training in order to develop a statewide program designed to resolve State and regional water and water related land problems.

Each institute shall also cooperate closely with other institutes and other organizations in the region to increase the effectiveness of the institutes and for the purpose of promoting regional coordination.

Kentucky information transfer activities are conducted in support of these objectives.

### **Methodology**

Information transfer activities are an important part of the overall program of the Kentucky Water Resources Research Institute (KWRI). There are 2 main components, an annual symposium and the Institute's web sites. The Institute also participates in and supports other technology and information transfer activities throughout the year.

The Associate Director develops the program for the Annual Water Resources Symposium. Presentations in both platform and poster format allow researchers and practitioners to share progress on planned, ongoing, and completed water-related activities throughout the Commonwealth each year. Recipients of the 104(b) student research enhancement grants are required to present the results of their projects at the symposium.

The Research Analyst Principal assists with posting program announcements and providing symposium updates including registration information, award winners, pictures, and the final proceedings document on the web site. She develops and maintains content for several web sites

including the main Institute page at: [www.uky.edu/waterresources/](http://www.uky.edu/waterresources/). Links for additional sites describing projects and activities (for example, volunteer sampling results and watershed pages for the Kentucky River basin) are provided on the main web site. Research translation to make results accessible for a variety of audiences is a major goal of all technology transfer activities.

The Institute cooperates closely with other groups and agencies in planning additional technology transfer activities in the Commonwealth. These efforts included support for seminars/lectures, support for other web sites, an open house during Earth Science Week, and staffing an exhibit for the University's Engineering Day. Institute staff members serve a variety of support roles on technical committees and advisory panels for agencies and volunteer organizations to help disseminate relevant information about ongoing activities and research results.

### **Principal Accomplishments and Activities**

On October 5, 2017, KWRRI organized the Kentucky River Basin Team Meeting at the Floracliff Nature Preserve. This semi-annual meeting brings together watershed coordinators throughout the basin to discuss watershed project updates, discuss topics, and prioritize concerns. The discussion topic for the meeting focused on water quality education and outreach and how to reach the general public with messaging. On October 26, 2017, Dr. Ormsbee presented a half-day presentation on the Ten Key Management Areas at the Kentucky Water and Wastewater Operators Association's (KWWOA) Annual Fall Conference addressing almost 200 participants.

The University of Kentucky's Water Week, October 7-13, 2017, was a week-long series of events designed to inform faculty, staff, and students on the University of Kentucky campus of the environmental and economic importance of



water. This was the fourth year of this annual fall event. The project is a collaborative between the College of Agriculture, Food, and the Environment, the College of Arts and Sciences, the College of Engineering, the Kentucky Geological Survey, the Tracy Farmer Institute for Sustainability and the Environment, and the Kentucky Water Resources Research Institute. Featured events for 2017 included: Ignite Talks and Panel Discussion on Monday, October 9<sup>th</sup>; *Chasing Ice* film screening and panel discussion on Tuesday, October 10<sup>th</sup>; lecture on climate change featuring guest speaker Randy Kolka on Wednesday, October 11<sup>th</sup>; career panel and networking opportunity and a seminar, *Coal Sourced Natural Gas Resources in the US and China*, on Thursday, October 12<sup>th</sup>; and CATCHment Cleanup, a stormwater basin maintenance service learning opportunity led by the Biosystems and Agricultural Engineering student chapter on Friday, October 13<sup>th</sup>. These events were organized by a multidisciplinary group of researchers

working toward the advancement of water-related research and education at the University of Kentucky.

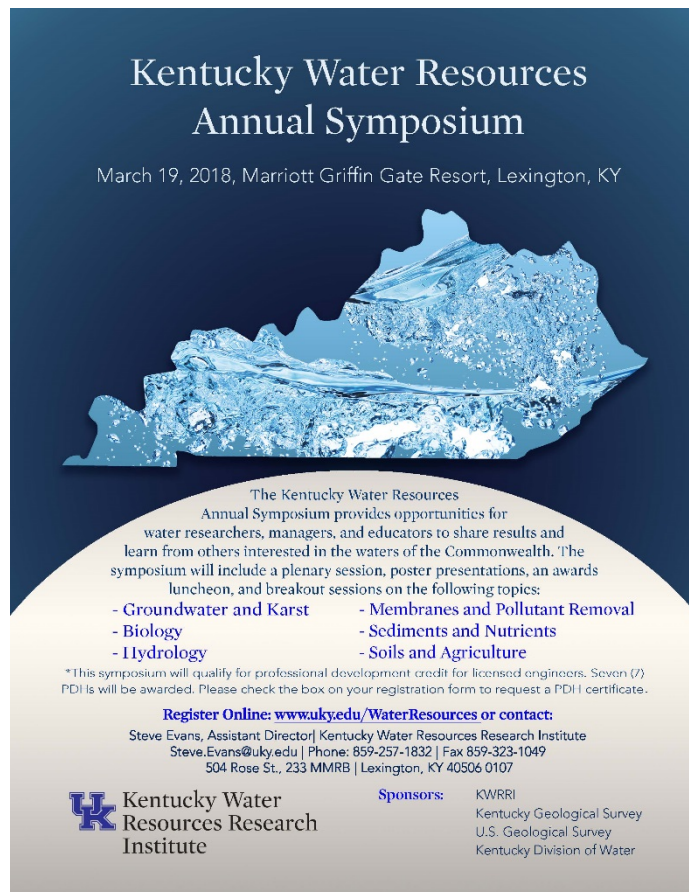
KWRRI participated in an open house on Wednesday, October 11, 2017, in association with Earth Science Week. This event was co-sponsored with the Kentucky Geological Survey. KWRRI staffed a water exhibit for the elementary, middle, and high school students and their parents who attended the event (approximately 200 people).

The Kentucky River Watershed Watch Annual Conference was held on November 11, 2017, in Lexington, Kentucky. This conference presented the results of citizen-led water quality monitoring efforts over the previous year. KWRRI developed the annual report and presented the results at this annual meeting as well as assisting in the monitoring events and data review throughout the year. KWRRI also served as representative of the Kentucky River Basin for the statewide Watershed Watch of Kentucky Science Advisors Committee. Over multiple sub-committee meetings, KWRRI helped streamline data entry techniques, systematize state-wide reporting, and develop water quality indices to help translate technical data results to public audiences.

On February 8, 2018, KWRRI chaired a reconvening of the Interagency Technical Advisory Committee (ITAC) on Groundwater. This state appointed committee evaluated trend analysis data for long-term ambient groundwater monitoring and discussed potential monitoring strategies and joint-agency collaboration in order to support groundwater research in the future.

The University of Kentucky's Engineers Day, or E-Day, is a celebration of everything engineering offers. E-Day brings together students, families and anyone interested in the field of engineering to learn more about what it's like to be an engineer or a UK engineering student or researcher. Approximately 150 demonstrations, exhibits and contests presented by UK students and departments, government organizations and industry are featured. The University of Kentucky's 2018 E-Day celebration was held on Saturday, February 24<sup>th</sup>, from 9 a.m. to 1 p.m. KWRRI staffed an Enviroscope exhibit demonstrating sources of nonpoint source pollution for participants at the event. E-Day comes at the end of Engineers Week, an annual event sponsored by a coalition of more than 100 professional societies, major corporations and government agencies dedicated to promoting math and science literacy and ensuring a diverse and well-educated future engineering workforce.





The 2018 Kentucky Water Resources Annual Symposium was held on March 19, 2018, at the Marriott Griffin Gate Resort in Lexington, Kentucky. Although the date of the symposium fell outside of FY2017, most of the planning and preparation for the event occurred during the fiscal year. Over 150 people attended the meeting, the highest attendance in many years. Attendees included researchers, personnel from local, state, and federal agencies, undergraduate and graduate students, participants from volunteer groups and NGOs, and members of the public. Conference registration fees are kept low through partial subsidy of symposium expenses (using 104(b) technology transfer and matching funds) to ensure accessibility to individuals from all potential audiences. The Symposium opened with a welcome address from

KWRRI's Director Dr. Lindell Ormsbee and a plenary session featuring three guest speakers. Following the plenary session, symposium attendees could choose from two tracks of breakout sessions that ran concurrently throughout the day. The topics of the breakout sessions included groundwater and karst, membranes and pollutant removal, biology, sediments and nutrients, hydrology, and soils and agriculture. In total, 20 oral presentations were made during the breakout sessions. There were also two poster presentation sessions during the day featuring 37 posters. An awards luncheon provided the opportunity for the presentation of KWRRI's annual awards acknowledging outstanding contributions in the areas of Water Resources Research, Water Resources Practice, and Water Quality. The Symposium closed at the end of the day with the presentation of student awards for Most Outstanding Undergraduate Poster Presentation, Most Outstanding Graduate Poster Presentation, and Most Outstanding Speaker Presentation. The presentation of student awards was a new addition to the symposium this year. The student presentations were evaluated by 14 volunteer judges using a scoring rubric developed by KWRRI. Judges included a USGS hydrologist and faculty and staff from the University of Kentucky, Eastern Kentucky University, Murray State University, Western Kentucky University. Abstracts for all oral and poster presentations were distributed to participants on the day of the symposium. The full proceedings document is also available online on the Institute's web site,

[www.uky.edu/waterresources/](http://www.uky.edu/waterresources/). All recipients of the 104(b) student research enhancement projects funded through the Institute during FY2017 presented their results at the symposium.

The 2018 KWRRI Annual Symposium was utilized again in 2018 to kickoff Water Week in Kentucky. Building off the theme for World Water Day, “Nature for Water,” Water Week in Kentucky was held March 18<sup>th</sup> through 24<sup>th</sup> and focused on natural solutions to water issues and water management policy and practice. Water Week in Kentucky included outreach events focused on water resources throughout the state.

Maintenance of the institute web site provides open access for those interested in the activities of the Institute. The site also provides additional links to related sites and information maintained by others. Creation and maintenance of the web site are ongoing throughout the year. Links on the site provide direct access to the Kentucky Center of Excellence for Watershed Management, the University of Kentucky Superfund Research Center, the Kentucky Research Consortium for Energy and Environment, the Kentucky River Watershed Watch, the Tracy Farmer Institute for Sustainability and the Environment, the Environmental Research and Training Laboratory, and the Kentucky Geological Survey.

# **USGS Summer Intern Program**

None.

<b>Student Support</b>					
<b>Category</b>	<b>Section 104 Base Grant</b>	<b>Section 104 NCGP Award</b>	<b>NIWR-USGS Internship</b>	<b>Supplemental Awards</b>	<b>Total</b>
<b>Undergraduate</b>	3	0	0	0	3
<b>Masters</b>	5	0	0	0	5
<b>Ph.D.</b>	2	0	0	0	2
<b>Post-Doc.</b>	0	0	0	0	0
<b>Total</b>	10	0	0	0	10

## Notable Awards and Achievements

2017KY269B (Modeling and Evaluating the Influences of Class V Injection Wells on Urban Karst Hydrology) - WKU Graduate student James Shelley received the John W. Hess Research Grant in Karst Research Studies at the 2017 Meeting of the Geological Society of America (GSA) in Seattle, Washington, on October 23, 2017. The John W. Hess Research Grant in Karst Research Studies supports student research involving any aspect of cave and karst studies aimed at providing improved understanding of how caves and karst work, including how these resources can be better managed. The recipient is determined by the Karst Division of Geological Society of America.

2017KY269B (Modeling and Evaluating the Influences of Class V Injection Wells on Urban Karst Hydrology) - WKU Graduate student James Shelley received the Kentucky Academy of Science Best Graduate Oral Presentation in the Geography section for his presentation, "Modeling and Evaluating the Influences of Class V Injection Wells on Urban Karst Hydrology," which he presented on November 4, 2017, at the 2017 Kentucky Academy of Science Annual Meeting.

2017KY268B (Using Anthropogenic Compounds in Sewage to Create New Fecal Source and Age Indicators) – On December 1, 2016, UK undergraduate civil engineering student Ashley Hall won Best Undergraduate Poster at the Tracey Farmer Institute for Sustainability and the Environment's 2016 Sustainability Forum for her poster, Using Anthropogenic Compounds in Sewage to Create New Fecal Source and Age Indicators.

2016KY260B (The Use of eDNA to Detect Bacterial Genetic Markers Associated with Fecal Contamination in the Triplett Creek Watershed, Rowan County, Kentucky)- On April 26, 2017, Morehead State University student Hannah Conley received a Merit Award for her poster presentation, The use of eDNA to detect bacterial molecular markers in the Triplett Creek Watershed, which she presented at the Celebration of Student Scholarship at Morehead State University in Morehead, KY.